



Universitat Autònoma de Barcelona

ADVERTIMENT. L'accés als continguts d'aquesta tesi queda condicionat a l'acceptació de les condicions d'ús establertes per la següent llicència Creative Commons:  http://cat.creativecommons.org/?page_id=184

ADVERTENCIA. El acceso a los contenidos de esta tesis queda condicionado a la aceptación de las condiciones de uso establecidas por la siguiente licencia Creative Commons:  <http://es.creativecommons.org/blog/licencias/>

WARNING. The access to the contents of this doctoral thesis it is limited to the acceptance of the use conditions set by the following Creative Commons license:  <https://creativecommons.org/licenses/?lang=en>

SELF-DEPLOYABLE POSITIONING
SYSTEMS FOR EMERGENCY SITUATIONS
EMPLOYING UWB RADIO TECHNOLOGY



Universitat Autònoma de Barcelona

PhD. Dissertation by
Abbas Al-baidhani

Thesis Advisers:

Prof. Antoni Morell Perez and Prof. Jose Lopez Vicario

Doctorate in Telecommunication and System Engineering

Department de Telecomunicacions i Enginyeria de Sistemes

Escola d'Enginyeria

Universitat Autònoma de Barcelona

March, 2019

To my beloved mother and family

Acronyms

AoA	Angle of Arrival.
ADS	Asymmetric Double Sided.
APIT	Approximate Point-in-triangulation Test.
AS	Anchor Selection.
CDF	Cumulative Density Function.
DoF	Degrees of Freedom.
DS-CMT	Distance Statistics Covariance Matrix Tunning.
ECDF	Cumulative Density Function.
FIU	Fuzzy Inference Unit.
FL	Fuzzy logic.
GDOP	Geometric Dilution Of Precision
GSM	Global System for Mobile communications.
IMU	Inertial Measurement Unit.
IoT	Internet of Things.
IPS	Indoor Positioning Systems.
LOS	Line Of Sight.
LS	Least Squares.
MEMS	Micro Electro Mechanical Systems.
ML	Machine Learning.
MLE	Maximum Likelihood Estimator.
MLSI	Modified Least Squares Iterated.

MSE	Mean squared Error
NLOS	Non Line Of Sight.
NN	Neural Network.
PDF	Probability Density Function.
PN	Personal Networks.
PRF	Pulse Repetition Frequency.
RFID	Radio Frequency Identification.
RMSE	Root Mean Square Error.
RSS	Received Signal Strength.
RT	Raising Time.
SDS	Symmetric Double Sided.
SLAM	Simultaneous Localization And Mapping.
SNR	Signal to Noise Ratio.
SVM	Support Vector Machine.
TDoA	Time Difference of Arrival.
ToA	Time of Arrival.
ToF	Time of Flight.
TWR	Two Way ranging.
UWB	Ultra Wide Band.
WLS	Weighted Least Squares.
WSN	Wireless Sensor Network.
ZUPT	Zero Velocity Update.

Notation

In general, boldface upper-case letters denote matrices (\mathbf{A}), boldface lower-case letters denote column vectors (\mathbf{a}), and italics denote scalars (a).

\log_a	Base a logarithm.
\ln_a	Natural logarithm.
$\exp(\cdot)$	Exponential function.
$a \ll b$	a is much less than b .
$a \approx b$	a is approximately equal to b .
\mathbf{A}^T	Transpose of matrix \mathbf{A} .
\mathbf{A}^{-1}	Inverse of matrix \mathbf{A} .
$\text{diag}(\mathbf{A})$	Main diagonal of matrix \mathbf{A} .
\mathbf{I}	Identity matrix.
$\hat{\mathbf{a}}$	Estimation of the vector \mathbf{a} .
$\bar{\mathbf{a}}$	Mean of the values of the vector \mathbf{a} .
$\ \mathbf{a}\ $	Euclidean norm of \mathbf{a} .
\mathbf{x}_k	Value of vector \mathbf{x} at the k_{th} time instant.
$\mathbf{x}_{0:k}$	Values of vector \mathbf{x} from time instant 0 to time instant k .
$N(\mu, \sigma^2)$	Gaussian distribution with mean μ and variance σ^2 .
$N(x; \mu, \sigma^2)$	Gaussian distribution of variable x with mean μ and variance σ^2 .
\sim	Distributed as. Used to make equivalences between random variables and the PDFs that generate them.
$E[\cdot]$	Statistical expectation.
$\text{Var}[\cdot]$	Statistical variance.

Abstract

Indoor positioning systems have been widely studied in the last decade due to the need of humans for them especially in the large building such as malls, airports, hospitals...etc. Still, there is no suitable precise indoor positioning system which can be implemented for different indoor environments and situations. We should mention military urban and emergency situations. In military urban and emergency response operations, the time is a crucial issue, and a precise positioning system with a clear indoor covering is a highly prerequisite tool to enhance safety. It should be seamless, low, frugal, power efficacious, low cost and supply less meter-level accuracy.

In emergency scenarios, we don't have enough flexibility and time to install all anchor nodes in a proper situation that may help to obtain an appropriate accuracy for locating a mobile station, but command centers require observing their operational forces, and rescuers demand to detect potential victims to perform proper care. The most common users for these situations are the firefighters, police, military, and civilians. The main goal of this Ph.D. dissertation is to create an accurate indoor positioning (IP) system that could be used in different indoor environments and situation, especially for the emergency situation. So, we create this system through different steps as explained below.

First, we have considered the study of different radio technologies to choose the suitable radio technology called Ultra wide band (UWB) radio technology. The reasons of selection the UWB and the commercial device that implements such technology are explained in details in chapters 3 and 4.

Afterward, due to some impacts of the UWB in indoor environments (see chapters 4 and 5), we continue the study of NLOS identification and mitigation methods. In these chapters, we create two different NLOS identification and mitigation methods

using a commercial UWB device experimentally. The first method used two parameters extracted from the UWB device to identify the propagation channel and map information of the building that the method is experimentally done in it to mitigate the NLOS channel. The second method of NLOS identification and mitigation used three parameters extracting from the UWB device to be an input set of the Fuzzy logic technique used to identify the propagation channels. In this identification method, it is not only to identify the propagation channel to NLOS and LOS but also to divide the NLOS channel into hard and soft channels. Then, we created a database that includes the three parameters and the distance Bias to mitigate the NLOS channel for obtaining an accurately estimated distance to be used for creating an accurate IP system.

Finally, with the aim of applying our designs to mass market applications, we move to create a novel IP system using the UWB technology called anchor selection (AS). In this technique, we focus on using fewer sensors (anchor nodes) to locate a mobile station under harsh circumstances such as scenarios where the installation area of the anchor nodes is narrow and/or the installation time should be very short. The proposed approach is based on grouping anchor nodes in different sets and evaluating the positioning error of each of these groups by means of a novel mean squared error (MSE)-based methodology. A virtual node approach is also proposed to consider the case where position must be computed with only two anchor nodes.

Acknowledgments

Now that I see near the end of my PhD I would like to thank those who have made this journey easier with their support over the years. First, I would like to thank my directors Prof. Antoni Morell Perez and Prof. Jose Lopez Vicario for their help, their constant support and, especially, for all the useful advice received during these years.

I would also like to thank the people in the ministry of transport of Iraq for their useful advice and for the kind treatment I received during the my study leave that I lived in Spain.

Finally, I would like to express my eternal gratitude to all my family, especially my mother and my wife, my brothers, and my sisters because without them this thesis would never have been possible.

Abbas Sabbar Ghali Al-baidhani

28/02/2019

Contents

1	Introduction	1
1.1	Motivation	1
1.2	Objectives	4
1.3	Outline	4
1.4	Research contributions	6
2	State of the art	8
2.1	Network based systems	9
2.1.1	Range-free localization	10
2.1.2	Range-based localization	13
2.2	Inertial based systems	22
2.3	Literature survey	25
2.3.1	NLOS identification and mitigation methods	26
2.3.2	Indoor positioning systems	28
3	An overview of UWB	31
3.1	UWB properties	32
3.2	FCC definition of ultra-wideband	32
3.3	UWB Compatibility with WSN	33
3.4	Strengths of UWB for wireless sensor networks	34
3.4.1	Energy efficient, economical and simple transceiver circuitry	36
3.4.2	Spatial capacity and transport mechanism	36
3.4.3	Multipath splitting ability	37
3.4.4	Interference resistance	38
3.5	Spectrum challenge	39
3.6	Conclusion	39

4 Ranging in UWB using commercial radio modules: experimental validation and NLOS mitigation	41
4.1 Introduction	42
4.2 Ranging protocols on IEEE 802.15.4a related with this work	44
4.2.1 Tow-way ranging (TWR) protocol with clock drift	44
4.2.2 SDS-TW-TOA protocol with clock drift	46
4.3 Hardware	48
4.3.1 Decawave 1000 (DW 1000)	48
4.3.2 EVK 1000	49
4.4 Experimental activities	49
4.4.1 LOS and NLOS measurements	50
4.4.2 NLOS identification and mitigation	51
a. NLOS identification	53
b. NLOS mitigation	55
4.5 Conclusion	58
5 NLOS identification and mitigation method for UWB technology in indoor environment using Fuzzy logic control	60
5.1 Introduction	60
5.2 Problem formulation	63
5.3 Proposed work	64
5.3.1 NLOS identification method	65
a. The main parameters	65
b. Fuzzy logic control	66
5.3.2 NLOS mitigation (ranging enhancement)	69
5.4 Fuzzy Logic-based NLOS identification and mitigation	70
5.4.1 NLOS identification	71
5.4.2 NLOS mitigation	77
5.5 Result and discussion	77
5.6 Conclusion	82

6	Anchor selection for UWB indoor positioning	83
6.1	Introduction	83
6.2	System model	85
6.2.1	LS linearization	87
6.2.2	Virtual distance	89
6.3	MSE computation in linearized LS	91
6.4	Anchor selection (AS)	97
6.5	Experimental and evaluation activities	100
6.5.1	Evaluation of the derived MSE and an overview of WLS, MLSI, and GDOP	100
6.5.2	Experimental activities	104
6.6	Results and discussion	107
6.7	Conclusion	111
7	Conclusion and future work	112
7.1	Conclusions	113
7.2	Future work	116
	Bibliography	117

1. Introduction

1.1 Motivation

To present location information of persons and devices, indoor positioning systems (IPS) have been designed. For user applications, the position information enables location-based protocols, and therefore, personal networks (PNs) are destined to reach the users' requirements and interconnect users devices equipped with different communications technologies in different places to form one network. Nowadays, the evolution of IPs enables the creation of indoor location-based services which build applications on top of the knowledge of the position. Different examples of this kind of services are the location of objects stored in a warehouse, the tracking of equipment inside a hospital, the guidance of people inside buildings with reduced visibility due to smoke, among others like the guidance of people inside airports or the development of assisted living systems for elderly care. IPs, obtaining a sufficient precisely indoor positioning method, robust with the changes in the environmental conditions, adequate for expanded areas, and simple as possible is a difficult task.

Several methods such as fingerprinting technique and geometric approaches (such as trilateration and triangulation) utilizing distinct technologies have been presented. Based on these methods, different IPs are on the market to present indoor location-based services (ILBS) [1]. However, none of these commercial IPs is adequate to overcome the problem of emergency responders location [2], as all solutions require in advance measurements, calibration, configuration, and deployment. In emergency scenarios, command centers require observing their operational forces, and rescuers demand to detect potential victims to perform a proper care. The most common users

for these situations are the firefighters, police, military, and civilians.

For 2020, the predicted market value of indoor location services is the US 10 billion [3]. Therefore, there is an interest need in developing IPs that can be easily scaled to mass market applications and deployed in millions of buildings in the world. The current way to minimize the cost of the systems is to implement the wireless infrastructures that are already deployed for communications as landmarks for positioning. Among the plenty of existing technologies for communications (WiFi, LTE Bluetooth, wireless sensor networks (WSN), the ultra-wideband (UWB), ...). UWB signal is considered one of the most precise approaches because it can provide location estimates with centimeter-level accuracy [4]. It is widely used for ranging estimation and creating an indoor positioning system. Although, WSNs are also commonly implemented due to its key role on the internet of the things (IoT) and the future of smart cities. In similar, the microelectromechanical systems (MEMS) provide low-cost inertial sensors that can also estimate the position of a pedestrian without the need for any infrastructure in the building.

There is a continuous increase in interest in positioning information in the last decades. A high number of applications has been found by the development of the Global Positioning System (GPS), first for military operations (e.g. in weapon guidance, target tracking, attitude determination, aircraft stabilization), then for civilian uses. The spectacular decrease in size and cost of the most modernistic GPS receivers has permitted this technology to enter in the consumer electronics market, and this system is currently widely implemented for personal navigation. However, while GPS is used in a satisfactory way in open space, it attends considerable problems inside buildings in which the true accuracy, typically about several tens or hundreds of meters, is significantly lower than that achievable in open space (in the order of about one meter or some centimeters). In fact, for the GPS system, Indoor environments pose singular challenges due to their particular properties. The existence of walls, heterogeneous ob-

stacles, and the complexity of the physical characteristics of these environments cause severe multipath propagation. Typically, due to reflection, scattering, and diffraction of the signals transmitted from the wireless sensors (WS) with the surrounding environment, the received signal is composed of tens or hundreds or relevant paths very closely spaced to each other. For civilian applications, the bandwidth of the GPS signal is only about 2 MHz, so the different multipath components are usually totally overlapping each other, and it appears highly problematic to precisely detect the Time of Arrival (TOA) of the direct path arriving from the sensors, which includes the beneficial information to determine the positioning, especially considering that the direct path often is not the strongest one. Furthermore, in indoor environments, it is particularly, that it would be possible to significantly gain by the availability of highly accurate position information. Higher accuracy is demanded in the smaller environment scale and also the larger number of possible applications which can profit from accurate indoor positioning information to motivate the interest towards this issue. In addition to the conventional seamless indoor-outdoor personal navigation, which has been the first application to demand solutions to the "indoor positioning bottleneck" experienced by GPS, several other emerging areas are currently exacting for sub-meter positioning. Localization in radio frequency (RF) communication network could be divided into range-free and range-based techniques [5]. The most common range-free method is a radio signal strength indication (RSSI). A theoretical or experimental model of the signal propagation in this method is translated into position or distance estimations [6], [7]. The range based methods are according to distances measurements between transceivers utilizing the time of arrival (TOA), time difference of arrival (TDOA) or two way ranging time of flight (TWR-TOF) [8]. In the following chapter, we briefly explain the two ranging approaches aforementioned above.

1.2 Objectives

This thesis concentrates on indoor positioning applications using UWB radio signals. It provides a contribution to the study of indoor positioning systems for pedestrians from an experimental perspective. We designed IPs based on the UWB radio signal from wireless networks that can be used with the current commercial technologies. Our study starts with the indoor positioning applications such as creating different methods of identification propagation channels based on UWB signal in the different indoor environment. Then, creating an indoor positioning system using a mean square error (MSE) evaluation method and weighted least squared method (WLS). Therefore, it is consumed that the reader of this manuscript is familiar with the general theory of wireless communications. However, despite the fact that the implementation of ultra-wideband signal (UWB) for indoor positioning system gains a considerable interest both from industry and from research, we think that not all the readers might have this specific background knowledge. For this reason, this chapter presents an overview of the main motivations, requirements, and challenges which arise when implementing UWB signals for indoor positioning applications, prior to introducing the main original contributions and outline of this thesis.

1.3 Outline

The design of indoor positioning systems and NLOS identification and mitigation algorithms and the metric implemented to measure the goodness of our system will be the error committed during a series of experimental tests are the objective of this Ph.D. dissertation.

Chapter 2 provides a review of the state of the art of indoor positioning systems with special concentration to the methods based on the UWB systems involving NLOS and LOS identification methods.

Chapter 3 presents a general overview of the UWB technology then focusing on the commercial device used in this work which is DW 1000 and presents all concepts and specification of this device.

Chapter 4 is devoted to the study of the NLOS identification and mitigation method. In this contribution, we created a novel technique to identify the propagation channel using a commercial UWB device called DW 1000. In this work, we evident that we can reach a ranging accuracy with estimated distance error less than 60 *cm* in a harsh environment.

Chapter 5 continues with the study of the NLOS and LOS identification and mitigation methods. In this work, a novel method to precisely obtain ranging accuracy with an error of the estimated distance less than 20 *cm* in hard NLOS environment is created. In this method, the Fuzzy logic control is implemented to identify the propagation channel not only for NLOS and LOS channel but also int hard NLOS and soft NLOS.

Chapter 6 presents a novel contribution of building an indoor positioning system in a harsh environment having an emergency situation. This system is named anchor selection (AS). The idea of this system is to install n anchor nodes in a small area then select ($\hat{n} < n$) only the nodes having better received power. Then, we will obtain different anchor nodes groups. The MSE in positioning accuracy is estimated for every possible subset in order to select the best possible combination. The AS algorithm can obtain less than 0.5 m^2 of MSE of positioning with less installation time and a number of wireless sensors in a harsh environment.

Chapter 7 concludes this Ph.D. dissertation with a summary and discussion of the obtained results. Some suggestions for future work in the field are also outlined.

1.4 Research contributions

The study of indoor positioning systems in emergency situations from an experimental point of view based on the use of all the systems designed with nowadays commercial technologies is the main contribution of this thesis. Next, the details of research contributions in each chapter are presented.

Chapter 4

This chapter addressing the design of a nonlinear of sight and line of sight identification and mitigation method created in an indoor environment when a walking human carrying an UWB device and moving inside a corridor facing different obstructions such as wall and office furniture. This work has been published in the IPIN 2016 conference.

- Abbas Albaidhani, Antoni Morell, Jose Lopez Vicario, "Ranging in UWB using commercial radio modules: experimental validation and NLOS mitigation", IEEE, IPIN conference, pp. 1-7, 2016.

Chapter 5

The main results of this chapter addressing the design of an NLOS identification and mitigation method using the Fuzzy logic control. In this work, it is not only to identify the propagation channel into NLOS or LOS but also is to identify which type of NLOS: hard NLOS or soft NLOS. This method is a robust method and presents a confident ranging accuracy.

- Abbas Albaidhani, Antoni Morell, Jose Lopez Vicario, "NLOS identification and mitigation method using Fuzzy logic", submitted to Transactions on Emerging Telecommunication Technologies, Wiley, pp 1-9, February 2019.

Chapter 6

A novel algorithm using UWB low cost commercial devices to create an indoor positioning (IP) system is the main result of this chapter. The IP system is named anchor selection (AS). In this system, we created and mathematically derived a novel MSE to evaluate the positioning accuracy computed by a different group of anchor nodes. Then, select the group having less MSE and relocate the tag position using the WLS algorithm.

- Abbas Albaidhani, Antoni Morell, Jose Lopez Vicario,” Anchor selection for UWB”, Transactions on Emerging Telecommunication Technologies, Wiley, 1-17, March 2019.

2. State of the art

For outdoor positioning, It is widely agreeable that GPS is the de facto standard and tracking application. However, while GPS is utilized in a pleasing way in open space, it attends considerable problems inside buildings in which the actual accuracy, typically between some tens meters is significantly lower than that achievable in open space (in the order of a few meters). Anyway, for indoor scenarios, there is no considerable and satisfied system.

Therefore, significant study effort has been concentrated on this topic. Indoor positioning systems have been intended for providing information about the position of a person or object inside a building. These systems could be characterized into three groups:

- * **Network based systems:** For wireless location finding, Wireless networking devices model the main infrastructure implemented. A location finding system should have the ability to seamlessly implement both cellular and WLANs for location finding by roaming between the networks. These systems use the information of the wireless signals to estimate the position of the user carrying a wireless device.

- * **Inertial navigation based systems:** Inertial navigation systems are self contained, non-radiating, non-jammed, dead-reckoning navigation systems which provide dynamic information through direct measurements They utilize self contained sensors that compute the motion of the user and estimate its position corresponding to the initial point without the necessity of a physical infrastructure deployed in the building.

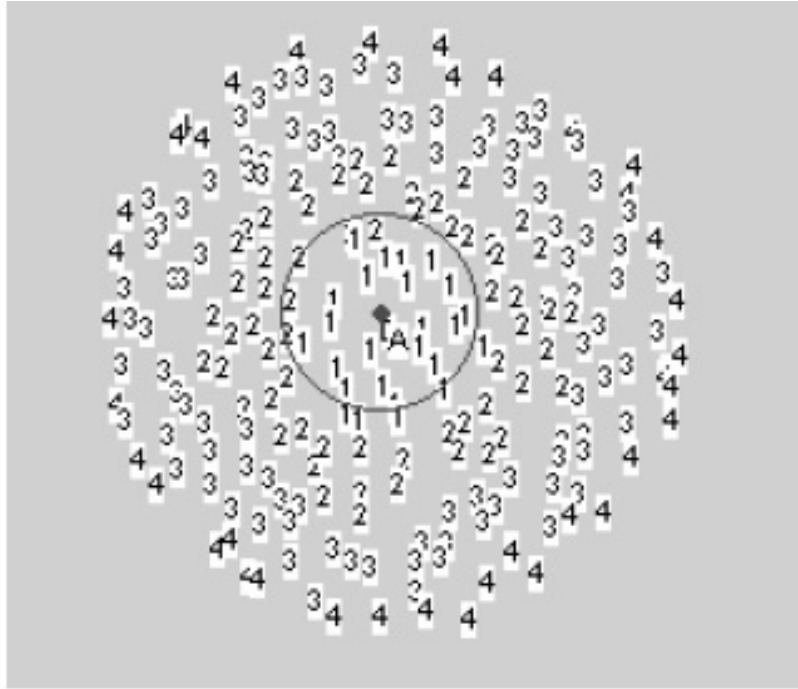


Figure 2.1: Anchor Beacon Propagation Phase [9].

* **Hybrid systems:** In order to improve the estimation of position, these systems combine two or more different methods. Figure 2.1 presents a complete classification of IPS containing references to noteworthy works.

Note: The hybrid systems are excluded from the classification because they have lots of possible combinations of IPs.

2.1 Network based systems

To determine the location of a mobile user by measuring its signal parameters when received at the network base stations (BSs), Network-based location technology depends on several existing networks (either cellular or WLAN). The BSs measure the signals transmitted from a mobile station (MS) and relay them to a central site for further processing and data fusion to provide an estimate of the MS location in this technology. A significant advantage of network-based techniques is that the MS is not involved in the location-finding process; thus, the technology does not require modification to

existing handsets. We can characterize the network based IPS systems depending on the information acquired from the wireless signals into two groups :

i) range-based localization and ii) Range-free localization methods.

Range-free localization technique is the cost effective technique because it does not require sensors to be equipped with any hardware, but uses less information than range based algorithm. One of the range free methods is a centroid algorithm, where the position information of the references sent out to neighbor nodes at periodic intervals. The position of the unknown node is then estimated to be the centroid of the reference nodes. Alternatively, Range-based localization assumes that the inter-node distances can be accurately measured by special ranging hardware. The location of a node is computed respectively to other nodes in its vicinity in range-based localization. Range based schemes utilize various algorithms to first determine distances between nodes (range) to (a number of) their neighbors and then compute location using geometric principles in range-based localization.

2.1.1 Range-free localization

Acknowledging that the cost of hardware required by range-based solutions may be inappropriate in relation to the required location precision. In sensor networks, researchers have researched alternate which is the range-free solutions to the localization problem. These range-free solutions implement only regular radio modules as basics for localization. In this subsection, we briefly explain the key characteristics of some state-of-the-art range free localization algorithms.

- **Centroid Localization:** N. Bulusu and J. Heidemann [10] proposed a range-free, proximity-based, coarse grained localization algorithm, that utilizes anchor beacons, containing location information (x_i, y_i) , for estimating node position. A node estimates its location after receiving these beacons using the following

centroid formula:

$$(\hat{x}, \hat{y}) = \left(\frac{x_1 + x_2 + \dots + x_N}{N}, \frac{y_1 + y_2 + \dots + y_N}{N} \right) \quad (2.1)$$

Where, \hat{x}, \hat{y} denote the estimated coordinated of the node and N denotes the total number of the anchor beacons. The distinguished advantage of this centroid localization scheme is its simplicity and ease of implementation. In a later publication [11], N. Bulusu raises his work by presenting a novel density adaptive algorithm (HEAP) to place additional anchors to minimize estimation error. Because HEAP requires additional data dissemination and incremental beacon deployment, other schemes, under consideration, only use ad hoc deployment.

Another algorithm of the range free localization explained in the next item is presented by [12] named DV-Hop localization.

- **DV-Hop localization:** DV-Hop localization utilizes a mechanism similar to classical distance vector routing. In this algorithm, one anchor sends a beacon to be submerged during the network containing the anchors' position with a hop-count parameter initialized to one. Each receiving node keeps the minimum counter value per anchor of all beacons it receives and disregards those beacons with higher hop-count values. Beacons are submerged outward with hop-count values increased at every intermediate hop. During this technique, all nodes in the network (including other anchors) obtain the shortest distance, in hops, to every anchor. For the purpose of converting hop count into the physical distance, the system estimates the average distance per hop without range-based techniques. Anchors apply this operation by obtaining location and hop count information for all other anchors inside the network. The average single hop distance is then estimated by anchor i implementing the equation 2.2 below.

$$Hopsize_i = \frac{\sum \sqrt{(x_i - x_j)^2 + (y_i - y_j)^2}}{sum(h_i)} \quad (2.2)$$

Where, $(x_j ; y_j)$ denotes the location of anchor j , and h_i is the distance, in hops, from anchor j to anchor i . Once computed, anchors send the estimated Hop Size information out to the nearby nodes. Once a node can compute the distance estimation to more than three anchors in the plane, it implements triangulation (multilateration) to estimate its location.

- **Geometric Grid Overlaying (GGO):** GGO algorithm consumes that a node is able to transmit a radio signal with a fixed range (r). Thus, it supposes that the anchor node transmits radio signal in two power levels, which associated with two radio range r_1 and r_2 respectively ($r_1 < r_2$). To represent the possible region that a normal node could reside in, GGO denotes a ring-belt region as $B(C_j, r_m, r_n)$, where C_j is the anchor position, and r_n and r_m are the outer and inner radii of the radio range. When a mobile node receives a message from an anchor, it will select the one with the minimum hop count. After recording the anchor's position information, the mobile node updates the hop count and re propagates the packet to its neighbors. With the anchor's information, the node can estimate its possible location region according to the following rules:

1. At both transmission power levels, the region of a mobile node is $B(C_j, 0, r_1)$ if it is reached by an anchor C_j .
2. A mobile node region is $B(C_j, r_1, r_2)$ when it can only be reached at the second power level.
3. If the mobile node n hops away from the anchors, then its region is $B(C_j, r_2, n \times r)$. The mobile node is able to estimate a region based on the rules aforementioned above for each received beacon packet. If a mobile node is reached by multiple anchors, the intersection area of all single estimates (from each anchor) is expressed as the final region of the normal node.

- **Approximate Point-in-triangulation Test (APIT)** The APIT method is based on the triangles created by reached anchors. It randomly selects three of them and examines if it (i.e., the normal node) is inside the triangle region created

by those three anchors when a mobile node is arrived by a set of anchor nodes. The node can have a set of possible triangles it may stay in when all combinations have been implemented. By intersecting these triangles, a possible smaller area will represent the final estimation. Because of the node has no knowledge of its own position, the one difficult aspect of this method is the Position in Triangle (PIT) test. To help the test, the authors of [13] implement neighborhood information. The algorithm assumes that if two nodes have the ability to receive signals from the same transmitter, the node obtaining the stronger signal (with higher energy) is closer to that transmitter. Based on this assumption, the authors in [13] point out that if no neighbors of the normal node are simultaneously farther from or closer to all three anchor nodes, the normal node can assume that it is inside the triangle. The PIT test is able to work in most situations except for some special cases, which would result in the following:

1. The edge effect: when the mobile node is close to the edge of the triangle.
2. The col-linear effect: when the mobile node and some of its neighbors reside on the same line.

An example from [13] is presented in Figure 3 below. Figure 2.2 (a) and (b) present two normal situations where mobile node (M) estimates its position with anchor nodes A, B and C. Figure 2.2 (c) presents the edge effect, where M wrongly considers it is outside of the triangle because one neighbor (node 3) is away from all the anchors. The collinear effect is shown in figure 2.2 (d) shows, where M estimates itself within the triangle because none of its neighbors is away from or closer to the anchors. Likely, it is found that this error is relatively small, and in worst cases, the occurrence is less than 14 %.

2.1.2 Range-based localization

Range-based methods depend on absolute distance from transmitting to receiving sensors. The accuracy of such estimation is subject to the communication through the

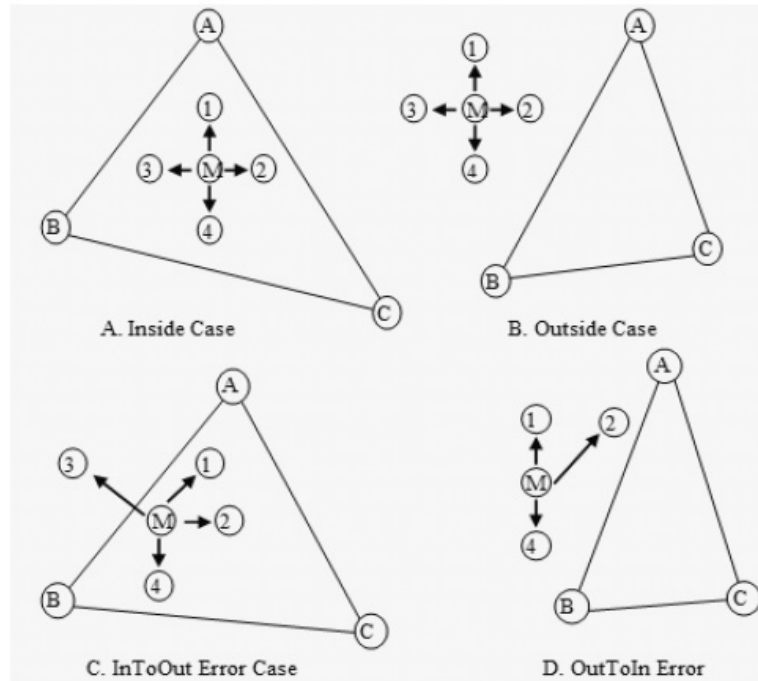


Figure 2.2: Eight APIT examples [13].

transmission media, embracing environment and supported hardware. From wireless signals, different ways exist to extract geometric information. The most common ways are the methods that rely on the propagation time of the signal between the transmitter and the receiver, the angle of arrival (AoA) or the received signal strength.

In the next items, we briefly explain the concepts of each class of the methods analyzing its advantages and disadvantages.

1. **Time based localization methods** In dynamic environments, Time-based localization methods can be useful, where the advantage of the Received Signal Strength (RSS) fingerprint based methods can be bounded. Time-based localization methods are not easily affected by such changes. Moreover, time-based methods do not require the construction of fingerprinting databases as RSS-based methods do. Moreover, the practical implementation of Real-Time Location Systems (RTLS) based on network packet time-based methods by using only off-the-shelf equipment is a challenging task. Typically, time-based localization methods can be divided into two main categories:

i) Hardware-based localization, ii) Software-based localization [14].

The first category refers to time-based methods implementing customized or modified hardware for localization purposes [15, 16, 17]. The second category is based on localization methods which are simply software based without using any specialized hardware or hardware amendment [18, 19, 20, 21, 22, 23].

Time-based localization algorithm is the travel time of a radio signal from a single transmitter to a remote single receiver. Also, it is known as a time of arrival (ToA) or time of flight (ToF). It measures the distance d between an anchor node and a mobile station. Equation 2.3 shows the one way ToA which requires highly accurate synchronization of sender and receiver clocks.

$$d_{ij} = \Delta\tau \times c \quad (2.3)$$

Where, $\Delta\tau = t_2 - t_1$ and c denote the ToA and the propagation speed respectively. To overcome the synchronization problem, two-way ranging (TWR) is applied when the sender sends a message to the receiver, the start of the ranging transaction commences. Then, the receiver waits for a known measure of time and sends a reply back to the sender. the distance is computed as presented in equation 2.4 below.

$$d_{ij} = \frac{(t_4 - t_2) - (t_3 - t_1)}{2} \times c \quad (2.4)$$

Figure 2.3 depicts the one way and two ways ToA.

Once the distances between the mobile node and reference nodes are computed, we use any localization methods such as lateration methods to compute the mobile position. Lateration methods compute the position of a user as the intersection of different circles with center the anchors position and radius the estimated distance as depicted in Figure 2.4. For a two dimensional position estimation, it is necessary to estimate the distance to at least three anchor nodes. Another technique that could overcome the synchronization problem is named the time

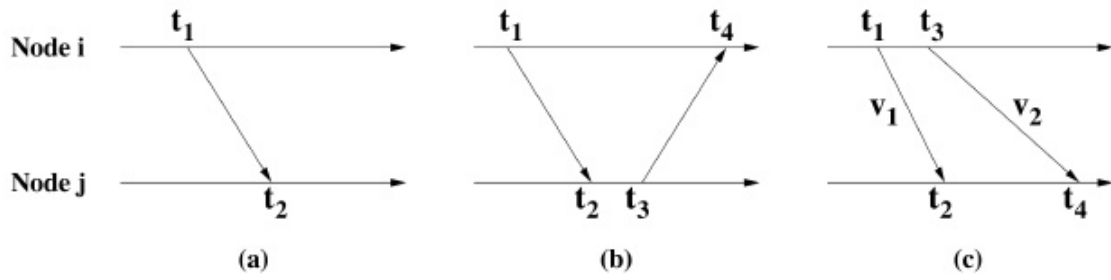


Figure 2.3: a- one way ToA, b and c Two way ToA (TWR).

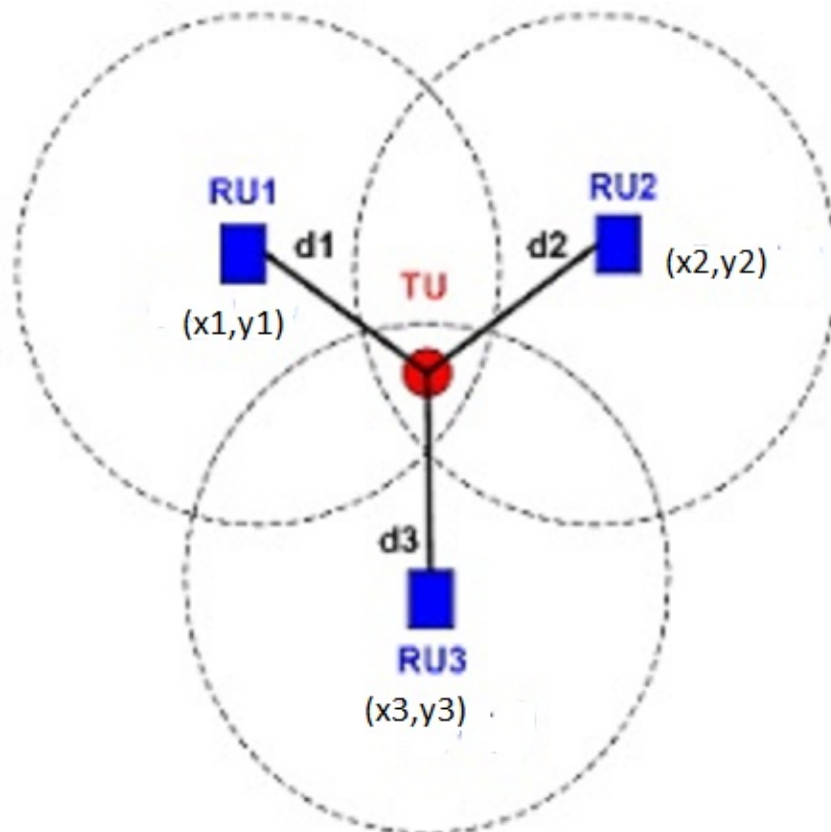


Figure 2.4: Lateralation method concept.

difference of arrival (TDoA). The TDoA of a signal can be estimated by two general methods.

- a. From two receivers, They produce a relative TDoA then Subtract ToA measurements or
- b. Employing cross-correlation techniques in which the received signal at one base station is correlated with the received signal at another base station.

To overcome the synchronization problem in ToA, arrival time difference of the signal at the receivers is required. The difference of arrival time of the signal removes some of the errors in ToA estimates commonly to all receivers. For additional improvement of the accuracy of the target position estimate, the cross-correlation algorithm can be implemented for the TDoA estimation techniques. In the following section, a general model for TDoA estimation is developed and the techniques for TDoA estimation are presented.

A conventional model for the two dimensional position location estimation of a target utilizing three fixed known positions of the target enabled receivers is developed. In this method, locating the target in two dimensions requires four reference receivers, when one of them should be near to the transmitter and assumed to be the first to receive the transmitted signal. The relationship between the range difference and the TDoA between receivers is given by equation 2.5.

$$R_{ij} = d_{ij} \times c = R_i - R_j \quad (2.5)$$

Where, $d_{i,j}$ is the TDoA between receivers i and j and c is the signal propagation speed.

The TDoA estimation, in the absence of noise and interference, restricts the pos-

sible source locations to a hyperboloid of revolution with the receivers at the foci. Fig.2.5 below presents a two dimensional representation of the target using Hyperbolic position location system. The main technology used for the time based localization techniques is the UWB signal. UWB is considered one of the most precise approaches because it can provide location estimates with centimeter-level accuracy [24]. It is widely used for ranging estimation and creating an indoor positioning system. In the indoor environment, the propagation channels could be divided into a line of sight (LOS) and a nonline of sight (NLOS). Also, the NLOS could be divided into soft NLOS and hard NLOS depending on the attenuation of the radio signal. In the UWB signals, it is possible to transmit and detect very short pulses permitting for high accuracy of positioning because of the accurate calculation of signal delays. In an indoor environment, the propagation path length is not always a good indicator of the ranging between a sender and receiver. Thus, these systems are predominately bounded to the LOS conditions [25]. It precisely measures the distance in the LOS channel but suffers in the NLOS channel, and the error in distance measurements is significantly high [26, 27] which impacts the positioning accuracy. In this Ph.D. dissertation, we focus on building a precise IP system using UWB technology with a concentration on the NLOS identification and mitigation techniques. Therefore, in the next section, we present a literature survey of the related works implemented in the last decade.

2. **Angle based localization methods** To compute the position of the receiver, Angle based localization methods utilize the angle of arrival (AoA) of a signal. As shown in figure 2.6, the sensors measure AoA by two common ways [28].
 - a. At the sensor nodes, a sensor array is implemented and array signal processing techniques are utilized. In this situation, each sensor node consists of two or more individual sensors (microphones for acoustic signals or antennas for RF signals). The locations of these sensors are known with respect to the node center. A four-element, Y-shaped, microphone array is shown

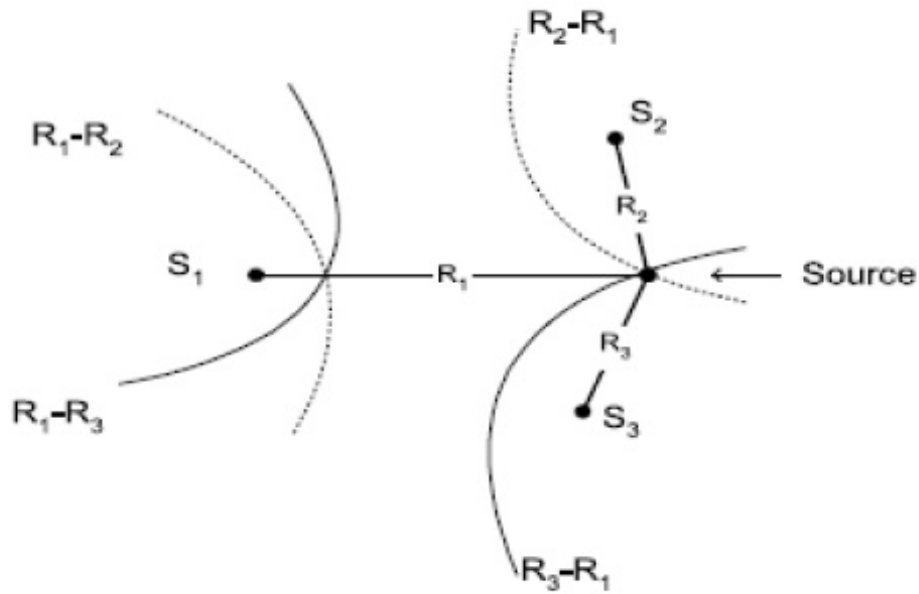


Figure 2.5: Intersection of Hyperboloid represents target in two dimensional plane [24].

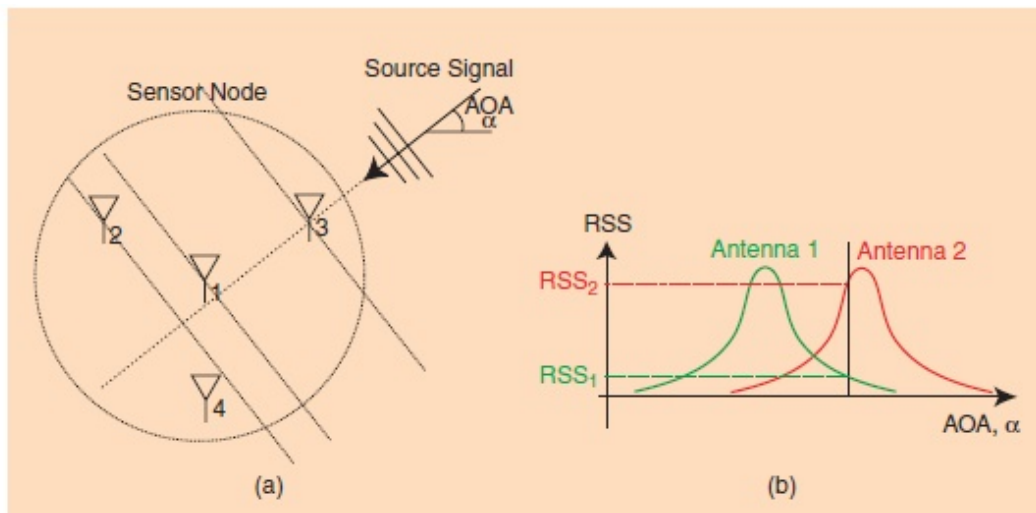


Figure 2.6: AoA estimation methods. (a) AoA is estimated from the ToA differences among sensor elements embedded in the node; a four-element Y-shaped array is shown. (b) AoA can also be estimated from the RSS ratio RSS_1/RSS_2 between directional antennas [28].

in figure 2.6 (a). From the differences in arrival times, the AoA is estimated for a transmitted signal at each of the sensor array elements. The estimation is similar to time-delay estimation discussed in the section on ToA measurements but generalized to the case of more than two array elements. When the impinging signal is narrow-band (the bandwidth is much less than its center frequency), then a time delay τ relates to a phase delay θ by $\theta = 2\pi f_c \tau$ where f_c is the center frequency. Narrow-band AoA estimators are often formulated based on phase delay [29, 30].

- b. The second approach implements the RSS ratio between two (or more) directional antennas located on the sensor [see Figure 2.6 (b)]. Two directional antennas pointed in different directions, such that their main beams overlap, can be used to estimate the AoA from the ratio of their individual RSS values.

Both AOA approaches need multiple antenna elements, which can contribute to sensor device cost and size. For more details, please refer to [31].

The main impact of AoA based approaches is the incremental in the cost of the system because of the additional hardware, as these systems need for arrays of sensors or antennas. Furthermore, if the AoA is computed based on the ToF of the wireless signals, inaccuracies in the clocks of the devices impinge in the accuracy of the position estimations.

3. **RSS based localization** localization based on the RSS doesn't require for specialized hardware. Thus, it is an interesting low-cost solution for the localization problem [31, 32]. Under the log-normal shadowing and log-distance path loss model (L), the path loss between the i th anchor node and the unknown mobile position, L_i , can be modeled depending on the following radio propagation path loss model (in dBm) [33, 34].

$$L_i = L_0 + 10\gamma \log_{10} \frac{\|x - a_i\|}{d_0} + v_i \quad (2.6)$$

$i=1,\dots,N$, where N denote the total number of the anchor nodes.

Where, L_0, γ, x, a, d_0 , and v denote the path loss value at a short reference distance, path loss exponent, mobile station, anchor node, reference distance, and the lognormal shadowing term modeled as a zero-mean Gaussian random variable with variance (σ^2) , ie., $v_i \sim N(0; \sigma^2)$. This model was validated by different measurement results [35, 36].

Depending on the relationship $L_i(dBm) = 10 \times \log_{10}(\frac{P_T}{P_i})$, where, P_i denotes the RSS measured by the i_{th} anchor, and P_T denotes the transmission power of the unknown position of a target, it is very simple to observe that the localization problem can be formulated by the path loss instead of the RSS [37, 38]. Based on equation 2.6, the ML estimator is found by solving the nonlinear and non convex LS problem.

$$\hat{x} = \underset{x}{\operatorname{argmin}} \sum_{i=1}^N (10 \times \gamma \log_{10} \frac{\|x - a_i\|}{d_0} - (L_i - L_0))^2 \quad (2.7)$$

As an example of the RSS, the author of [39] implemented an array of passive anchor nodes and collected the noisy RSS measurements from radiating source nodes in the WSN, which they use to estimate the target positions. They implemented the maximum likelihood (ML) estimator, since the ML-based solutions have particular importance due to their asymptotically optimum performance. However, the ML estimator needs the minimization of a non convex objective function which may have multiple local optima, thus making the search for the globally optimal solution hard. For solving this difficulty, they derived another non convex estimator, which approximates the ML one for small noise. Then, the new estimator is relaxed using efficient convex relaxations that are based on second order cone programming (SOCP) and semi definite programming (SDP) in the case of non cooperative and cooperative localization, respectively, for both cases of known and unknown source transmit power.

Another example of an RSS based localization system is proposed by [40], where authors implement the correlation between the RSS samples in nearby locations to fit several path loss models relying on the position of the user and therefore adapt to changes of the propagation model between areas of the same building.

As we mentioned in the time based localization methods, the TWR measurements have been simply obtained in wireless local area network (WLAN) systems using a simple device such as a printed circuit board [41]. Even though, TWR systems circumvent the problem of clock synchronization between nodes, the main drawback of this approach is the need for double signal transmission in order to perform a single measurement [42]. The drawback in the TWR was solved using a symmetric double sided algorithm (SDS-TWR) [43] used in the device implemented in this thesis. In chapter 3, We briefly explain the UWB technology and the device used in this thesis.

In the following section, we present concepts of inertial based systems and works related to them.

2.2 Inertial based systems

Inertial-based systems are systems based on sensors measuring angular velocity and linear accelerations. The measurements are performed using a combination of gyroscopes and accelerometers often referred to as an inertial measurement unit (IMU) [44]. To obtain the translation and rotation related to the last known position, the measurements are integrated. predominately, The inertia-based systems are combined with beacon-based systems such as GPS in research to transact with this drift. Other proposed systems taking advantage of geometrical features, resulting in an inertia-based system combined with map-based systems. the inertial sensors (i.e. gyroscopes and accelerometers), magnetometers and barometers are different from other technolo-

gies that acquired external reference signals. They are completely self-contained and can be seamlessly used in indoor/outdoor environments. The lack is that inertial sensors provide only short-term accuracy but experience from the accuracy degeneration with time [45]. The behavior of the vertical errors (i.e. the roll and pitch) can be controlled by the accelerometer measurements. However, the heading error will be increased when there is no additional useful information [46]. Magnetometers are able to support the heading estimation through sensing the Earth's magnetic field. However, the local magnetic field is liable to interference from man-made infrastructures when a subject moves into indoor or urban environments [47], which makes magnetometer measurements incorrect. When current sensors-based commercial products mounted on foot, The normal accuracy is 1 % of distance traveled [48] and 4 % - 8 % of distance traveled when there is no requirement of the location and attitude of the device on the human body [49]. The three main Inertial based systems are i) Simultaneous Location and Mapping (SLAM), ii) Strapdown systems, and iii) Step and heading systems (SHS). In the following statements, we present some contribution examples done in previous years. An approach of the SLAM technique is presented by [50] when they applied SLAM technique used in robotics to a mobile device, which is equipped with both inertial sensors and the IEEE 802.15.4 a Chirp Spread Spectrum (CSS) radio, to obtain locations of pedestrians in an indoor environment. They defined the state vector $[x_n, y_n, \beta_n]$ to represent the current state of the pedestrian \mathbf{q} at n times in two-dimensions, is calculated as shown in equation 2.8.

$$\mathbf{q}_n = \begin{bmatrix} x_{n-1} + \Delta D_{n-1} - \cos(\beta - 1) \\ y_{n-1} + \Delta D_{n-1} - \sin(\beta - 1) \\ \beta_n \end{bmatrix} \quad (2.8)$$

β_n denotes heading angle of the pedestrian and ΔD_{n-1} denotes the odometric distance which is measured from the magnetometer, and Δ is estimated from the three-axis accelerometer. Due to the accumulative errors, estimating the odometric distance from integration of sensing data is practically very hard. They, therefore, estimate the

odometric distance as shown in equation 2.9.

$$\Delta D_{n-1} = n_s \times l_s \quad (2.9)$$

Where, n_s and l_s denote the number of steps and side length respectively. The number of steps is computed using synthetic acceleration vector of a three axis accelerometer.

A peak detection algorithm [51] is implemented to state the candidate points of user stepping. The positions of a pedestrian are computed by equation 2.8 using the IMU sensor. The authors proofed that using only the IMU, the position error is about 13 m after moving a distance of 100 m. The new step of this algorithm is to locate a moving target using inertial sensors equipped in a mobile device. Since the obtained data from the inertial sensor has noise, the system keeps a number of particles to represent probable pedestrian position rather than a single position, as shown in Fig 8. A particle containing the pedestrian position in two-dimensional space at time t is represented as \mathbf{p}_t^i and estimated using equation 2.10.

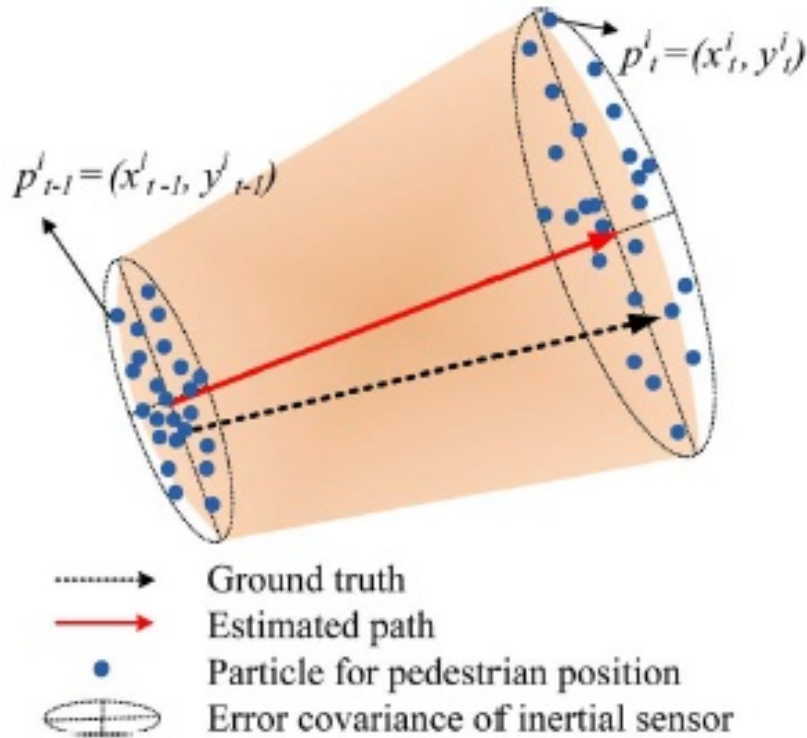


Figure 2.7: Particles of pedestrian position [50]

$$\mathbf{p}_t^i = \begin{bmatrix} x_{t-1}^i + (d_t + \delta^i)\cos(a_t + \vartheta^2) \\ y_{t-1}^i + (d_t + \delta^i)\sin(a_t + \vartheta^2) \end{bmatrix} \quad (2.10)$$

The error of the distance is Gaussian noise with mean and standard deviation of error distribution utilizing step counting. According to the characteristic of the magnetometer sensor noted in [52], the angle error is measured as presented by equation 2.11.

$$\vartheta = \vartheta_{bias} + \vartheta_{gaussian} \quad (2.11)$$

Where, ϑ_{bias} is the bias error and $\vartheta_{gaussian}$ is zero-mean Gaussian noise. It is observed from this experiment that the measured distance is rarely shorter than the actual distance, and the negative error is less than 1 *m*. Positive error, which is caused by multipath signal propagation, may reach to the maximum communication range.

The following section presents several works related to the works presented in this PhD dissertation.

2.3 Literature survey

As we mentioned in section 2 of this chapter about the two main Indoor positioning systems; the inertial based and network based systems. In this Ph.D. dissertation, we constraint on building an IP system in an indoor environment using network based, especially, the time based method based on (UWB) radio technology. UWB technology has been identified as an ideal candidate to provide positioning information in these environments in the last years. The implementation of sub-nanosecond duration UWB pulses with several *GHz* of bandwidth presents the unique possibility of distinguishing the different multipath components which compose the received signal and of accurately estimating its Time of Arrival (TOA), which includes the relevant information for positioning. In this way, centimeter level accuracy can be obtained, even in multipath rich indoor environments. The UWB technology will provide a good result of

positioning accuracy when we are able to identify the environments (propagation channels) and therefore, we can build our IP system accurately with very few centimeters error. So, the survey will be divided into NLOS identification methods and indoor positioning systems using UWB technology.

2.3.1 NLOS identification and mitigation methods

In 2018, Dae-Ho Kim [53] presented another method to identify the NLOS and LOS channels in a different indoor environment. The author enhanced the technique used in [86] by adding different types of the direct path of the UWB signal to experimentally evaluate it if it comes through a LOS or NLOS (hard and soft) channel. In this work, only an NLOS and LOS identification method is created.

The authors of [54] implemented an algorithm to identify the propagation channel and enhance the ranging accuracy. In this method, the received signal strength (RSS) measurements from the Wifi signal. The authors exploited several statistical features of the RSS time series and implemented two approaches based on machine learning and a third based on hypothesis testing to separate LOS-NLOS measurements. This algorithm of NLOS identification and mitigation are conducted implementing only RSS from real experiments with mobile devices. The authors' algorithm is able to distinguish between LOS and NLOS conditions with an accuracy of around 95 %. Furthermore, the presented techniques improve distance estimation accuracy by 60 % as compared to previous NLOS mitigation techniques and they obtained an improvement in distance estimation accuracy of 50 %.

The authors of [55] implemented measurements taken at more than one hundred points in the considered area. Points are placed randomly but are enforced to areas which are attainable by the carts. The measurement points are clustered into non-overlapping clusters, i.e., each point only corresponding to a single cluster. Typically, a cluster corresponds to a room or a region of a hallway. When two clusters were within

transmission range, every inter-cluster measurement was collected as well. Overall, more than one thousand unique point-to-point measurements were implemented. For each pair of points, different received waveforms and range estimates are recorded, along with the true range. Then, they create a database which includes 1024 measurements consisting of 512 waveforms captured in the LOS condition and 512 waveforms captured in the NLOS condition. Their algorithms are non-parametric, and rely on least-squares support-vector machines (LS-SVM). They describe the features for recognizing LOS and NLOS situations, followed by a brief introduction to LS-SVM. They describe how LS-SVM can be implemented for NLOS identification and mitigation in localization applications, without needing to determine parametric joint distributions of the features for both the LOS and NLOS conditions. To identify the LOS and NLOS, they extracted different features : (i) in NLOS conditions, signals are considerably more attenuated and have smaller energy and amplitude due to reflections or obstructions; (ii) in LOS conditions, the strongest path of the signal typically corresponds to the first path, while in NLOS conditions weak components typically precede the strongest path, resulting in a longer rise time; and (iii) the root mean-square (RMS) delay spread, which captures the temporal dispersion of the signals energy, is larger for NLOS signals. After the mitigation process, 60 % of the cases have accuracy with an error of less than 1 *m*.

In [56], Bo You offered an NLOS identification and mitigation method depending on the RSL and FSL. He stated two different thresholds (α and β) where α and β are 25 % and 10 % respectively. These thresholds are according to DW 1000 user manual [73]. Then he defined a ratio between the FSL and RSL. If the computed ratio is higher than the threshold α , the channel is probably to be a LOS. And if the ratio is lower than the threshold β , the channel is probably to be an NLOS. For an NLOS ranging error mitigation, they obtained the estimated ranging error experimentally and removed it from the estimated distance to obtain the mitigated distance. In this work, the authors did not mention what is the ranging accuracy after the proposed

method, but they only mentioned the localization accuracy had been increased 50 % when using the traditional least square localization method with the proposed method than without it.

The authors of [26] present an NLOS identification and mitigation method based on signal characteristic analysis and fuzzy theory. In this method, SNR, rais time (RT), RMS delay spread, kurtosis, and skewness are implemented to identify NLOS. This algorithm neither needs to build a statistical model nor to build and update a training database, so that it can be used conveniently for different application scenarios. Extensive experiments were conducted and the results show that the cumulative distribution function of the ranging error below 0.5 meter is over 90 % when using the proposed mitigation method, while that without implementing the mitigation method is below 70 %. Also, by using the proposed method, the root mean square error (RMSE) of the range measurements is reduced from 0.77 to 0.33 meter. However, the capability of this method is limited to the chosen representative propagation conditions.

2.3.2 Indoor positioning systems

In 2018, Imane Horiya Brahmi [57] presented an indoor positioning system based on a fuzzy logic approach called Fuzzy-LSE (FLSE). In this work, the authors used the fuzzy approach for only in the localization phase. Four parameters have been implemented to be elements of the input set of the fuzzy approach to create an indoor positioning system. These parameters are power, LOS value, Noise, and distance. The power element is an UWB signal power extracted from the Decawave (DW) 1000 device. The LOS element is identified using the LOS identification method created by Decawave company [73], which has enhanced by our work presented in IPIN international conference as shown in chapter 4. The authors claimed that the created system has demonstrated desirable accuracy improvement when compared to existing algorithms described in the literature.

In 2017, the authors of [58] presented a modified least squares iterated (MLSI) to

minimize errors and optimize the relationship of anchor nodes and a mobile station. The MLSI implements the iteration method to reduce the error of the conventional LS method. That means the MLSI can effectively improve position error rate. When using four anchor nodes system, the average error is 0.8 *m*. Moreover, increase anchor nodes from four to five; the error value is convergence to 0.48 *m*. The idea of this approach is to modify the vector of distance measurements used in the main equation of the conventional linearized LS method by involving the average distance error. Also, the positioning accuracy might be increased while implementing more number of the installed anchor nodes.

In 2016, Mathias Pelka [59] presented an iterative approach for anchors configuration of a positioning system. He used an anchor node randomly as the origin of the coordinate system. For the second anchor position, they presumed that the first two anchors are along one axis and the distance between both anchors is measured. An initial guess of the remaining anchor positions is generated according to a uniform distribution. The algorithm iterates for all anchor nodes in the positioning system. Then, the MSE is computed between the measured and Euclidean distance of the anchor nodes. The MSE is compared with a threshold which depends on the standard deviation of the distance estimation. If the MSE passes the MSE threshold, the algorithm dismisses the solution and starts the process again. The positioning problem with a Taylor expansion combined with a Monte Carlo approach is solved to avoid ambiguity flip. They obtained a mean positioning error of 0.62 *m*.

The authors of [60], presented a GDOP assisted nodes selection (GANS) algorithm for calculating the GDOP value of the current geometric distribution. As the evaluation criteria, sensor nodes contribution to the total GDOP value is adopted. When The contribution value of the node is higher than the threshold, it will be selected. The anchor nodes subset, which shares in the localization, will be real-time determined. By simulation, This approach shows that the GANS algorithm can minimize the energy

consumption of the system while the accuracy of the positioning system has no clear loss, and the computational complexity is decreased.

GDOP, Also, is presented by [61], where it is assumed that there is no mobile target but all anchor nodes will act as mobile units. In that work, 36 nodes are considered and a positioning accuracy around half meter is obtained.

In 2011, Paula Tarrío [62] presented two weighted least squares methods based on the standard hyperbolic, and circular positioning algorithms that consider the accuracy of the different measurements to obtain a better positioning estimation. With a limited overhead in term of computational cost, these methods present suitable positioning results and obtain greater robustness to an inaccuracy in channel modeling. The average errors of the positioning systems created by the proposed algorithms are 3.69 *m* and 2.56 *m*.

From the literature aforementioned above and other previous literature that used the received power of the UWB signal to create an indoor positioning system or NLOS identification method, we should mention the main drawback of these works which is the value of the received power when it is estimated by an UWB device. This value diverges from its true value when the received power is above -85 dBm, which results in a significant error in the positioning or ranging accuracy [73] (we will provide further details in Chapter 5). Since, in this dissertation especially chapter 5, we overcome the problem aforementioned above, so we can conclude that our Ph.D. dissertation will improve the positioning accuracy in different indoor environments and situations including the emergency situations when the positioning accuracy for pedestrians can be enhanced with less than 30 *cm* error.

3. An overview of UWB

During this Ph.D. dissertation, we designed two methods of NLOS identification and mitigation and one IP system using Ultra Wideband (UWB) technology, so having an overview of it will provide the reader with good comprehensive.

UWB technology has been identified as an ideal candidate to provide positioning information in these environments in the last years. The implementation of sub-nanosecond duration UWB pulses with several GHz of bandwidth presents the unique possibility of distinguishing the different multipath components which compose the received signal and of accurately estimating its Time of Arrival (TOA), which includes the relevant information for positioning. In this way, centimeter level accuracy can be obtained, even in multipath rich indoor environments. However, before being able to fully exploit the potentials of this technology, some issues need first to be addressed:

- UWB signals offer complex propagation phenomena. Due to the large bandwidth of these systems, different frequency components show significantly different interactions with the environment. For this reason, new propagation models describing and predicting the interaction of the traveling waves with the surrounding environment are of absolute importance, since the wireless channel is the first aspect which determines performance limits. However, available UWB channel models were developed with communications applications in mind, and they lack relevant information for positioning.
- Similar considerations hold for most of the suggested TOA estimation techniques, which are usually considered a simple expansion of well known channel impulse response estimation methods developed for communication applications, in which the TOA of the received signal comes as a byproduct. These approaches are

inherently sub-optimal since they do not address the unique UWB properties and do not concentrate on the relevant information which acquires to be retrieved; in addition, they can often be hardly utilized, since they have hardware or signal processing requirements far from what is currently available in the market.

3.1 UWB properties

Nowadays, there is not a union definition of UWB. Conversely, different countries have proposed, at different times, different definitions of UWB for civilian implementations. The first official document providing a regulatory body for UWB transmissions was released by the FCC, the US frequency regulator, in its first report and order dated February 2002 [63]. Some years later, similar definitions were started to be adopted in other continents. These rules present some variations among each other, especially with respect to the bandwidth in which UWB transmissions are permitted in several countries; however, the basic motivations and described principles of operation are similar. For this reason, only the FCC regulations will be discussed in the following; consequently, when in this dissertation, it is necessary to refer to regulatory issues, we will only consider these rules. The reason for this choice is twofold; first, FCC rules represent the regulatory body most often implemented and accepted in the scientific community; second and direct cause of the previous point, FCC provided regulations already in the early stage of UWB studies, while e.g. in Europe, the final documents provided by CEPT were issued only in April 2009. While the choice of some numerical values introduced in this thesis might require to be adapted to fit other regulatory bodies (e.g. the European ones [64]), the general validity of the proposed work continues to hold.

3.2 FCC definition of ultra-wideband

In reality, the original distinctive feature for the deployment of UWB radios was their potential ability to transmit in an unlicensed way very low power over an ultra wide

portion of the spectrum, allowing this technology to coexist with current and future licensed wireless systems. For this reason, the FCC does not directly specify any particular signal format or modulation technique for UWB; on the contrary, it strictly determines the spectral and emission properties for this technology.

UWB is defined as any wireless system with bandwidth (B), where $B \geq 500 \text{ MHz}$, or a fractional bandwidth $B_f \triangleq \frac{2B}{f_H - f_L} \geq 0.2$ where f_L and f_H are the lower and upper frequencies of the -10 dBm emission points respectively [63]. Also, the center frequency (f_c) can be derived as $f_c = \frac{f_H + f_L}{2}$. The operating band is limited in the portion of the spectrum between 3.1 and 10.6 GHz, provided that the emissions satisfy given limitations for communication and positioning applications. These limitations have been defined with the pulse based ultra-wideband approach in mind, and distinguish between peak and average power:

- $P_{meas}^{pk} \leq 0 \text{ dBm}$ in any 50 MHz signal bandwidth
- $P_{meas}^{av} \leq 41 \text{ dBm}$ in any 1 MHz signal bandwidth

where, P_{meas}^{av} and P_{meas}^{pk} are the average and peak measured EIRP power respectively.

Fig. 3.1 presents the FCC mask for the average measured power P_{meas}^{av} .

3.3 UWB Compatibility with WSN

Due to UWB properties, it is a solid candidate for the Wireless Sensor Network. Though narrow band transmission schemes under WSN, e.g., DSSS (direct sequence spread spectrum) are widely implemented and is very effective under 2.4 GHz band their performance matrix is lesser than the UWB. Major disadvantages of these transmission technologies are statistically explained in Table 3.1.

On the other hand, the UWB signal presents large bandwidth (e.g., 500 MHz plus) Figure 3.2. It works on a narrow pulse (width around Nano and Pico seconds) and a huge frequency spectrum ($\geq 500 \text{ MHz}$). By comparing the UWBs properties with the

sinusoidal carrier-based system, the following are the UWBs advantages.

- Cost: *Very Low*.
- Power Consumption: *Very Low*.
- Data Transmission Rate: *Very High*.
- Probability of Interception: *Very Low*.
- Space Frequency Spectrum: *Superb efficiency*.
- Implementation: *Easy/Moderate*

In the next section, UWB strengths are explained in more detail.

3.4 Strengths of UWB for wireless sensor networks

UWB is a lightweight platform, hence detection and interception of UWB signal (due to the low "T_x" power) are relatively complex Figure 3.3. UWB is less complex and more reliable that makes it very suitable for WSN.

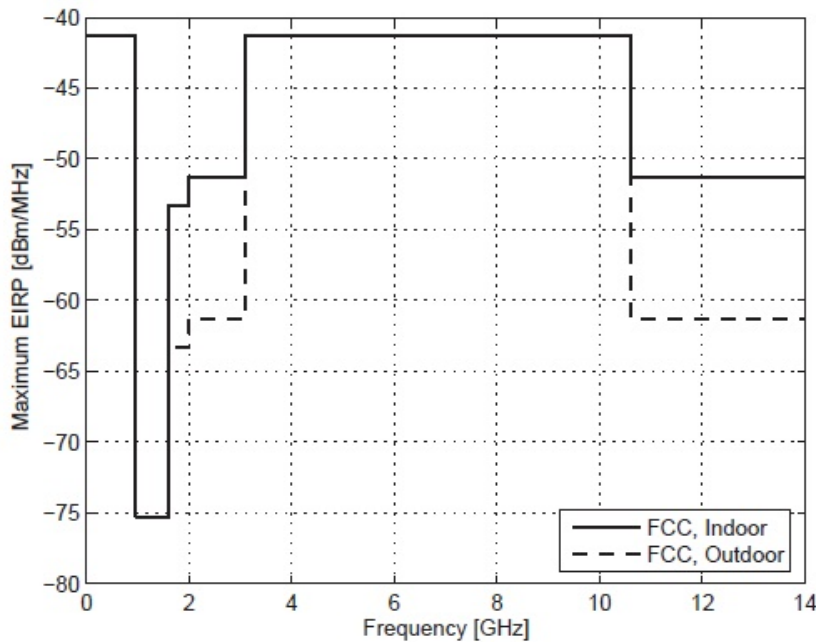


Figure 3.1: FCC mask for the average measured power, for UWB emissions in US [65].

Table 3.1: UWB vs. Existing Technology Solutions [66]

Technology	Standard/Spectrum	Frequency Band	Advantages	Hindrances
Zigbee	IEEE 802.15.4	2.4 GHz, 900 MHz	Low Power Efficient	Supports Limited No. of Nodes.
Wireless HART	IEEE 802.15.4	2.4 GHz	Widely recognized	Protocol Compatibility issue, Limited Nodes support
Wi-Fi	802.11 a/b/g/n/ac	2.4 GHz, 5 GHz	Higher Data rate	Power consumption
Bluetooth	IEEE 802.15.1	2.4 GHz	Low cost	Limited nodes support, Power consumption
UWB	IEEE 802.15.6,4a	3.1-10.6 GHz	Low energy, high bandwidth	Transceiver Design

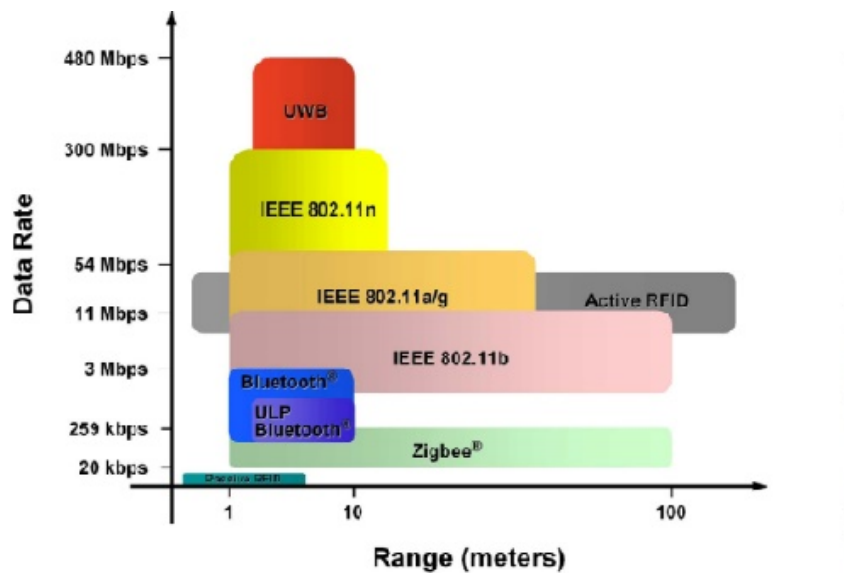


Figure 3.2: Different wireless standards in ISM Bands [66].

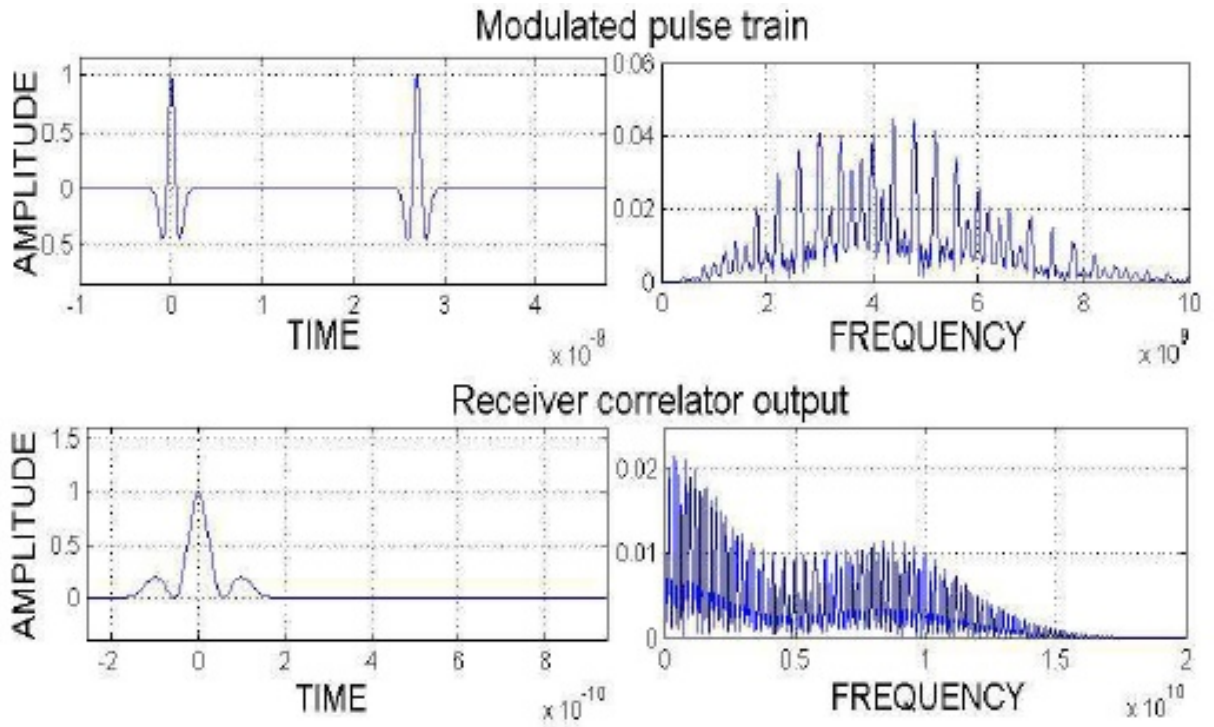


Figure 3.3: UWB pulses (modulated and at Correlator) [67].

3.4.1 Energy efficient, economical and simple transceiver circuitry

UWB implements narrow pulses and a wide frequency spectrum for the transmission. So the transceiver part of the node has no conventional circuitry which means no extra burden on the hardware. Also, simple transceiver architecture of UWB saves cost, power, and reduces the size of the hardware. Its capability of transmitting high data rate (for a short distance) makes it a superb choice for real-time multimedia applications. For example at the unit cost of power consumption of 1 bit under UWB, it is less than the conventional wireless communication model. Due to these qualities, UWB is an attractive scheme for modern sensor networks [68].

3.4.2 Spatial capacity and transport mechanism

Spatial capacity is the data intensity of a wireless channel and is crucial in wireless sensor networks, especially when the network environment is dense and large. When comparing UWB with the other short distance technologies, UWB provides better

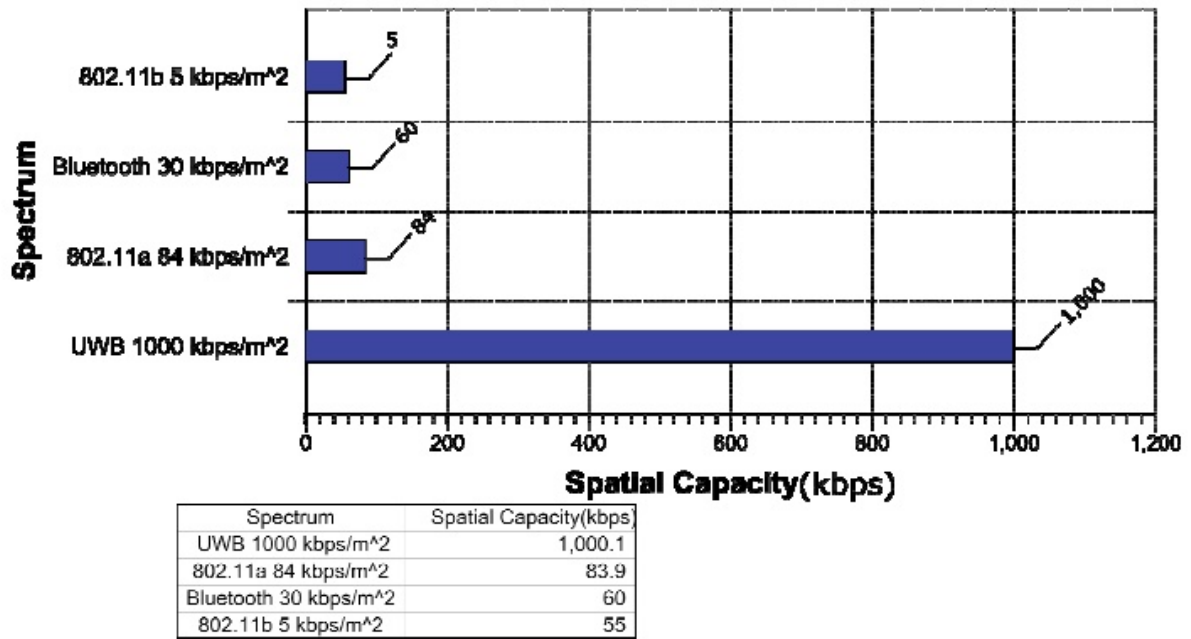


Figure 3.4: UWB spatial capacity [68].

transport mechanism and spatial capacity per unit area. That is one of the reasons UWB is considered for complex, dense environments shows the statistical comparison of UWB and the other related technologies in terms of spatial capacity. Figure 3.4 depicts the UWB spatial capacity.

3.4.3 Multipath splitting ability

For a wireless communication system, the transmission efficiency is a major concern. The RF (Radio Frequency) signals are continuous, in other words, take a longer period than the multipath transmission time in the conventional wireless systems which impacts the quality of transmission and data rate. Conversely, UWB radio signal has severely short maintaining time (due to single-period pulses) and very low duty cycle. For separating the multipath signals as per time, Low duty cycle and short maintaining time make it accessible. Figure 3.5 depicts three different scenarios of multipath that are considered. The upright values show a UWB pulse strength (in mV). The vertical vertices of each scenario are different, due to the different channel attenuation. The first graph is with LOS (line-of-sight) and the rest two with NLOS (non-line-of-sight). By viewing the experiments in various research, results show that the largest observed

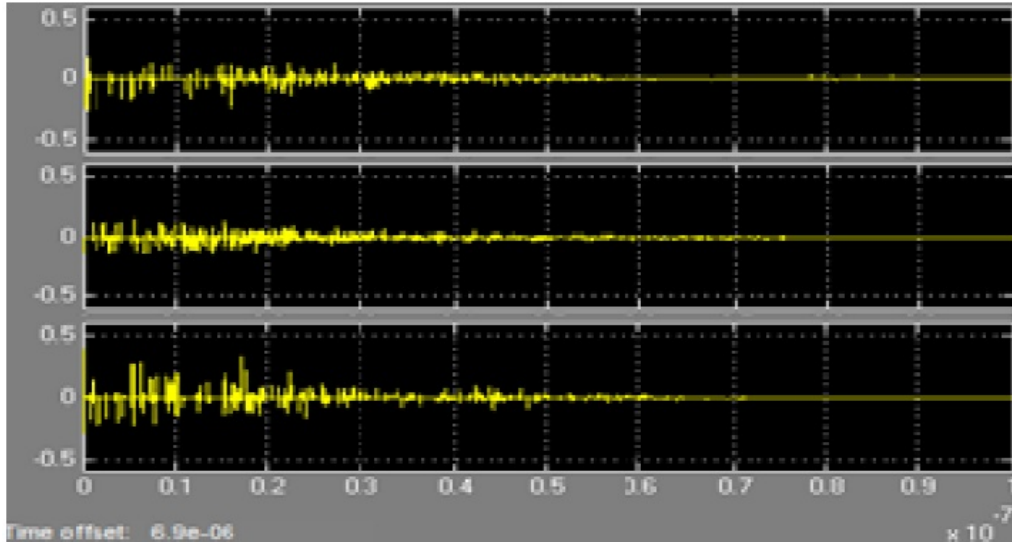


Figure 3.5: Multipath environment (UWB) [67].

fading of the UWB signal is only 5 dBm (in the multipath case). For the same multipath case, fading for narrowband radio signal exceeds 15 - 30 dBm.

WSN is usually deployed in complex (extreme) multipath environments in the real world,. Due to UWBs marvelous ability of "multipath separation", it works well with wireless sensor networks (Even in extreme conditions).

3.4.4 Interference resistance

In UWB, processing gain is observed high which can obtain interference immunity in UWB. The strength of the signal is almost equal to the white noise as the UWB signals energy is scattered in wide bands (for the other NB system). UWBs spectral density is very high, even lower than the usual environmental noise. Its probability of detection is also very low and almost impossible under pseudo random coding. That makes UWB an ultimate choice for high security (e.g., military) applications [69]. Besides this, it also allows band sharing. An excellent solution for the EMF (Electric and Magnetic Field) problem in severe dense environments.

3.5 Spectrum challenge

Data transmission by UWB is a striking solution for the wireless sensor network, but with various implications. Some core challenges in UWB radio technology. Spectrum Challenge is one of concern. Looking at the possible implementation of technology, the following are the three possible implementations of UWB.

- 1- UWB based connectivity to portable nodes (most common household devices like MP3 players, USB Drives, and digital sensors) is conceivable and under research for future SMART networks.
- 2- For the Wireless Universal Serial Bus connectivity with standard computing nodes (e.g., printers, and scanners), could be utilized.
- 3- UWB could be a suitable candidate for the next generation Bluetooth technology devices, such as smart-phones [70]. Spectrum is a major concern because of the absence of standardized spectrum for all three possible uses.

As UWB emission spreads over a huge frequency bandwidth with limited Giga-Hertz to operate. It is hard to adopt a solution that is compatible with all wireless systems. Another concern is compatibility with different services. UWB based service can create harmful interference to some of the other wireless services. So the challenge could be how to full fill spectrum demands. This issue needs to be worked out (especially for hybrid wireless sensor networks). Considering the SMART world, where spectrum utilization would be a major concern. UWB licensing is an open question.

3.6 Conclusion

According to the UWB overview aforementioned above, we can conclude that this Ph.D. dissertation implements a suitable and convenient technology (UWB radio technology)

for building a prices IP system using commercial existing low coast wireless sensors that could be implemented for different indoor environments and situations in real life.

4. Ranging in UWB using commercial radio modules: experimental validation and NLOS mitigation

In this chapter, we begin the study of NLOS identification and mitigation methods. We concentrate on the UWB radio technology especially low cost commercial devices. We intended to study the characteristics and specifications of such devices.

Ultra wideband (UWB) wireless transmission has received notable and considerable attention in the field of next generation location-aware wireless sensor networks (WSNs). This trend is due to the large bandwidth of UWB signals contributing many advantages for positioning, communication, and radar applications: penetration through obstacles, accurate position estimation, high-speed data transmission, and a low-cost, low power transceiver. Commercially available UWB radio modules were evaluated. Such modules have the ability to very precisely measure the time of arrival of RF signals, range, or localization. The physical layers specify the received signal strength indicator utilized in the localization technique.

The main impact in the UWB signal is the distance computed from the received signal due to this distance will absolutely have an error when the UWB signal travels in an indoor environment through obstacles such as wall and humans. Usually, this error is a positive Bias in the measured distance when the UWB signal travels through obstetrical. To identify the propagation channels that the UWB signal travels through is a confident solution to remove the error from the measured distance. We study a

device called decawave 1000 (DW 1000); how this it works, what ranging protocol it uses and etc.

4.1 Introduction

UWB 802.15.4a transceiver technology ideally meets the demands of next generation wireless sensor networks [71]. IEEE has realized the requirements to standardize UWB technology for use in personal area networks (PANs) and has committed the IEEE 802.15.4a standard specifying a new UWB physical layer for WSNs [72]. For some WSN applications, for example tracking a missing firefighter in the interior of a harsh smoky environment, sensing data without recognizing the sensor location is useless. Localization is a crucial technique in acquiring the location of data sources within WSNs. WSNs consist of small so-called sensors armed with environmental power sources, sensing devices, radio, and processor units. The mobile stations can communicate with each other or with the bay-station. In most situations, the mobile stations are randomly deployed within fields where the location information is missing. Some localization systems should be performed on mobile station fields for the location each mobile.

Four signal parameters are taken in the localization technique: received signal strength (RSS), time of arrival (TOA), time difference of arrival (TDOA), and angle of arrival (AOA)[43]. To attain precise positioning accuracy, IEEE 80215.4a-2007 specifies additional PHYs using impulse radio (IR)-UWB. UWB provides accuracy with a very small margin of error because it uses a center frequency equal to or greater than 3.5 GHz and a bandwidth of 500 MHz or more. Recent developments in UWB enable the acquirer of low-cost chips equipped with UWB to very precisely measure distance.

One low-cost commercial UWB module that provides a very precise time of arrival RF signal with valuable information that may assist in identifying NLOS channels is Decawave 1000 (DW 1000), Evaluation Kit 1000 (EVK 1000) [73] [74]. Some literature has already evaluated the performance of such devices but only with fixed stations.

DW 1000 implements an SDS-TWR-TOA ranging protocol[75] which is explained in detail in the next section. This protocol is accompanied by some disadvantages because a device has to wait for a time (replay time). Thus, when the devices move while the ranging measurements are proceeding, the distance changes over time, and then the longer ranging delay results in a larger ranging error. An asymmetric double sided two-way ranging for crystal offset (ADS-TWR) was presented by [76] to reduce ranging delay.

A novel evaluation is presented in this chapter to examine the DW 1000, EVK 1000, mounted on a moving human, and how the movement of a human body may affect its measurements. It also evaluates a novel technique for identifying and mitigating NLOS claimed from [73] [27] in a harsh environment, which has not yet been evaluated. As we showed in a later subsection(NLOS identification and mitigation), the technique committed by [73] does not satisfy all LOS and NLOS probabilities, so we expanded the NLOS identification technique to add two new conditions to cover all NLOS and LOS channels probabilities to determine a precise ranging measurement. Our goal will assist us in ascertaining whether we can utilize DW 1000 to design an indoor localization system.

The main contributions of this chapter follow:

- To identify the propagation channel to LOS and NLOS using two parameters extracted from the DW 1000.
- To mitigate the NLOS Channel using map information and apply distance enhancement by removing the error from the measured distance.

The ranging protocols on IEEE 802.15.4a related to this work are described in detail in Section 4.2 . Section 4.3 represents the properties of the hardware applied in this work. In Section 4.4, experiment activities involving moving humans are implemented in LOS and hard-NLOS environments with different materials, such as different types

of walls, doors, and chairs. Relevant UWB signals, the signal power in the first path and the received signal power, are estimated, and NLOS channels are identified and mitigated. Finally, a conclusion is offered in Section 4.5.

4.2 Ranging protocols on IEEE 802.15.4a related with this work

Three different ranging protocols have been realized by IEEE 802.15.4a. The first mandatory protocol is a two-way time of arrival (TW-TOA). The second one, symmetric double sided (SDS) TW-TOA, is much more precise and preferred. The last protocol, private ranging, is designed for systems in which positioning information is sensitive and has to be secure [27]. The description of the first and second protocols with the clock drift is explained in the next subsections, respectively.

4.2.1 Tow-way ranging (TWR) protocol with clock drift

In this protocol, shown in Fig 4.1, when device A sends a message to device B, the start of the ranging transaction commences. Then, device B waits for a known measure of time and sends a reply back to device A [27]. One of the error sources in the TW-TOA approach is the clock set off. The crystal oscillators employed in sensor devices (source or target) are not processed at the exact optimal frequency, resulting in a small positive or negative offset in the time measurements. With the high speed of light, this small offset may cause a significant error in ranging [75]. The target node computes the TOF as

$$2TOF = t_{rd}^A - t_{rep}^B \quad (4.1)$$

Due to clock drift, device A estimates TOF by

$$2\widehat{TOF} = (1 + e_A)t_{rd}^A - (1 + e_B)t_{rep}^B \quad (4.2)$$

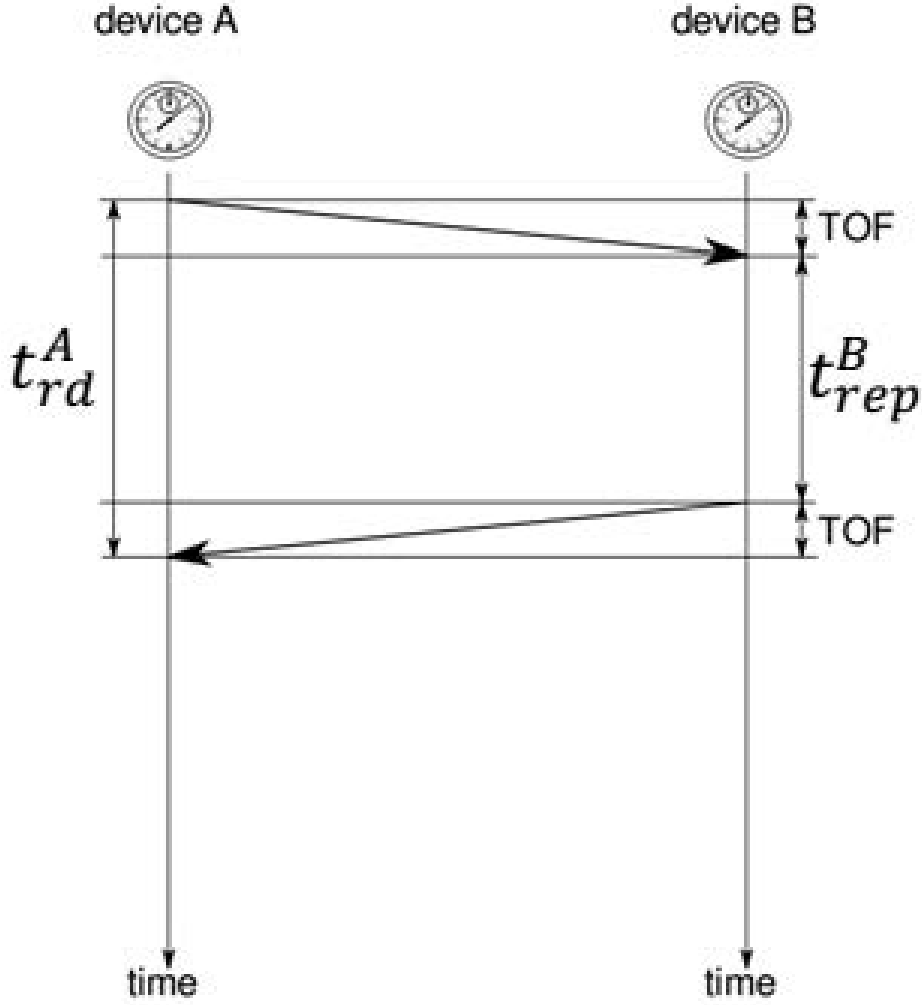


Figure 4.1: Tow-way ranging (TWR) [75].

Subtracting Eq 4.2 and Eq 4.1 and then dividing the resultant equation by 2, we obtain

$$\widehat{TOF} - TOF = e_A TOF + \frac{1}{2} t_{rep}^B (e_A - e_B) \quad (4.3)$$

Practically, the $t_{rep} \gg TOF$, so the dominant error is

$$\frac{1}{2} t_{rep}^B (e_A - e_B)$$

For the practical value of t_{rep}^B and frequency offset, the error in the accuracy of the range is large. Please see Table 4.1.

The more precise algorithm has been implemented in DW 1000 and is explained in

the following subsection.

Table 4.1: Frequency Offset error using the TWR-TOA protocol [27]

	$e_A - e_B$			
t_{rep}^B	2 ppm	20 ppm	40 ppm	80 ppm
100 μs	0.1 ns	1 ns	2 ns	4 ns
5 ms	5 ns	50 ns	100 ns	200 ns

4.2.2 SDS-TW-TOA protocol with clock drift

In this protocol, shown in Fig 4.2, the target node sends a second $RFRAME_{req}$ to the source node after receiving the $RFRAME_{rep}$. Consequently, each node has an estimate of the round trip time, T_{rd} , and replay time, T_{rep} . At the final stage, the source node sends a time stamp, including measured T_{red} and T_{rep} , to the target node [27] [75] [76]. Thus, the target node computes TOF as

$$2TOF = t_{rd}^B - t_{rd}^A \quad (4.4)$$

The TOF can be constructed by adding equations (4.1) and (4.4)

$$4TOF = t_{rd}^A + t_{rd}^B - t_{rep}^A - t_{rep}^B \quad (4.5)$$

As we explained in subsection A, due to clock drift, device A estimates TOF by

$$4\widehat{TOF} = (1 + e_A)(t_{rd} - t_{rep}^A) + (1 + e_B)(t_{rd}^B - t_{rep}^A) \quad (4.6)$$

$$\Delta = t_{rep}^B - t_{rep}^A$$

Subtracting Eq 4.6 and Eq 4.5, and then dividing the resultant equation by 4, we obtain

$$\widehat{TOF} - TOF = \frac{1}{2}(TOF(e_A - e_B)) + \frac{1}{4}(\Delta(e_A - e_B)) \quad (4.7)$$

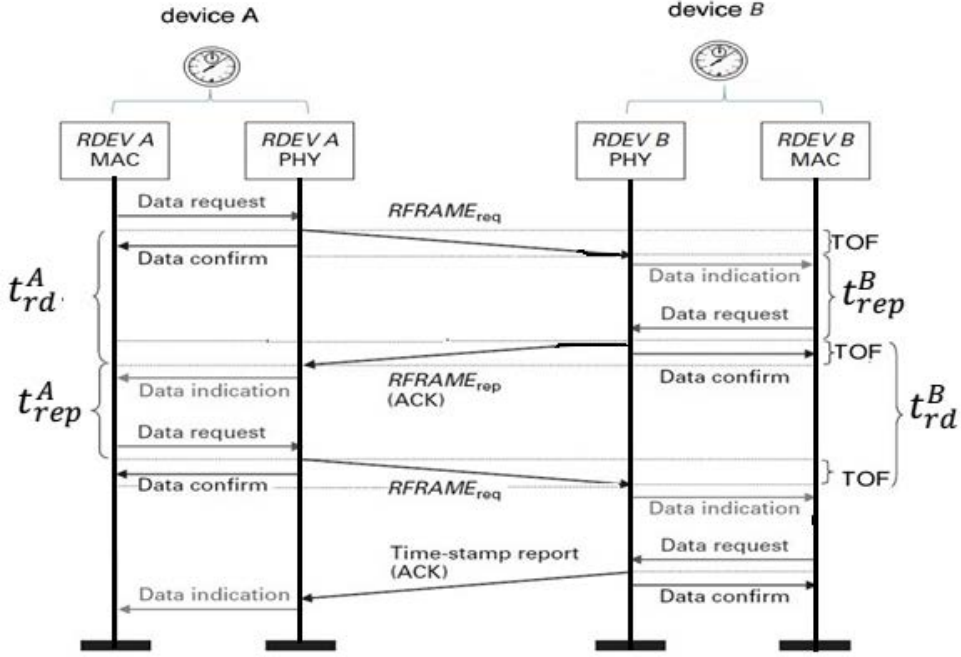


Figure 4.2: SDS ranging protocol [27]

Practically, $\Delta \gg TOF$, so the dominant error is

$$\frac{1}{4}\Delta(e_A - e_B) \quad (4.8)$$

Clearly, as we can ascertain in SDS-TWR, the clock offset is reduced to half that of TWR. Table 4.1 and Table 4.2 illustrate the clock offset of TWR-TOA and SDS-TWR, respectively.

Table 4.2: Frequency offset error using the SDS protocol [27]

$t_{rep}^B - t_{rep}^A$	$e_A - e_B$			
	2 ppm	20 ppm	40 ppm	80 ppm
1 μs	0.0005 ns	0.005 ns	0.01 ns	0.02 ns
10 μs	0.005 ns	0.05 ns	0.1 ns	0.2 ns
100 μs	0.05 ns	0.5 ns	1 ns	2 ns

The features of DW 1000 and EVK 1000 are explained in detail in the next section.

4.3 Hardware

4.3.1 Decawave 1000 (DW 1000)

The DW 1000 is a fully integrated low-power, multichannel single-chip CMOS radio transceiver that meets the IEEE 802.15.4-2011 UWB standard [73].

- Its ranging accuracy is ∓ 10 *cm* error using TW-TOA.
- It spans 6 RF bands from 3.5 *GHz* to 6.5 *GHz* with a bandwidth ranging from 500 to 900 *MHz*.
- It supports data rates of 110 *kbps* and 6.8 *Mbps*.
- It saves power and extends battery life.
- It has the ability to deal with severe multi-path environments, so it is ideal for highly reflective RF.

Also, the DW 1000 has features [27] necessary in the localization technique as written below:

1. Detect the signal from below the noise floor,
2. Extract the direct path signal and any multi-path signals that follow it, and
3. Process the impulse response and timestamp of the first peak in this response that exceeds a dynamically adjusted detection threshold.

The timestamp of the first peak is reported by the DW 1000 in the impulse response via registers to which the application software has access. This value can then be utilized in a variety of different ways to implement location and ranging schemes [77]. The EVK 1000 specifications are explained in the next subsection.

4.3.2 EVK 1000

EVK1000 consists of a pair of evaluation boards (EVB 1000). Each pair of EVK 1000 boards is configured to run a pre-programmed two-way ranging demonstration application. In addition to the features of DW 1000, the EVK 1000 [74] is programmed to possess the following:

1. It gives the estimated distance after calibration,
2. It estimates the signal power in the first path(FSL)[73], and
3. It estimates the received signal power (RSL)[73]

In this work, two EVK 1000 boards have been implemented to estimate the distance between a mobile station (walking man) and an anchor node and to extract information such as RSL and FSL to ascertain whether it can be utilized in NLOS channel identification, as described in the next section.

4.4 Experimental activities

This experiment seeks to examine and validate the estimation ranging accuracy of the commercial module of an UWB transceiver (EVK 1000) mounted on a walking human for LOS and NLOS channels with distances from 2 *m* to 45 *m* in LOS channel and 4 *m* to 26 *m* in hard-NLOS in an indoor environment. It also focuses on evaluating the technique used to identify and mitigate NLOS channels committed by DW 1000 [73], which has not yet been evaluated.

Also, we expanded the NLOS identification technique by adding two additional obtained conditions by this experimentation to overcome all LOS and NLOS channel probabilities. This experiment will assist our future work to sustain a precise positioning system in a harsh environment. We implemented two different channel modes, ch2 (4 *GHz*) and ch3 (4.5 *GHz*). See Table 4.3 for specifications.

Table 4.3: channel modes details [74]

ch	fc (GHz)	Band width(MHz)	Data Rate	PRF	Preamble length	Preamble code
2	4 GHz	500 MHz	110 kbps	64	1024	9
3	4.5 GHz	500 MHz	110 kbps	64	1024	9

4.4.1 LOS and NLOS measurements

The measurements were obtained using two FCC-compliant UWB radios obtained from Decawave. The experiment took place in a 52 m length by 3 m width corridor on the second floor of the engineering faculty building of the UAB. Two transceivers (EVK 1000) were used, one placed on a 1.6 meter high tripod and the other transceiver carried by a moving person. Also, the transceivers should be placed in the Fresnel zone (FZ) [27]. In the equation 4.9 below, rf is denoted for radius of the first Fresnel zone, λ is denoted for the wavelength of the radio signal, and the distance between sites is denoted by d .

$$rf = \frac{1}{2}\sqrt{\lambda \cdot d} \quad (4.9)$$

To ensure no NLOS effects in the two channels, we placed the device within a radius of 1.5 m around the straight line optical path between the devices, Table 4.4 depicts the FZ.

Table 4.4: Fresnel Zone(FZ) for ch 2 and ch 3 [27]

ch	fc (MHz)	Band width (MHz)	FZ radius bottom cm	FZ radius top cm
2	3993.6	3774-4243.2	44.6	42
3	4992.8	4243.2-4742.4	42	39

The experiment is don in an indoor environment. First, between transceivers, was a LOS channel. Range, FSL, and RSL were measured 20 times per distance. Twenty-

three distances were estimated and compared with known distances from 2 m to 45 m. One transceiver (anchor node) was placed on a 1.6 m high tripod, and the other (moving target node) was carried by a human while moving. Fig 4.3 illustrates this scenario.

Second, between transceivers, were NLOS channels (through the concert and different types of walls and furniture). The same scenario of LOS was implemented in a 26 m corridor. A different number and types of walls were involved with different distances. Fig 4.4 illustrates this scenario.

We calculated the mean, root mean square error, and standard deviation (STD) of 20 estimated distance of a walking human for each physical distances in LOS and NLOS channels. Fig 4.5 depicts the standard deviation in LOS and NLOS channels for the two channel modes (ch2 and ch3). Clearly, we determined that the standard deviation for both channels (ch2 and ch3) in LOS does not exceed 16 cm. In the NLOS channel, we observe the standard deviation increased to touch 40 cm for ch3 and less than 35 cm for ch2.

4.4.2 NLOS identification and mitigation

UWB-decawave 1000 has a very important specification, the ability to distinguish the direct path of a signal in between other reflective paths, using a receiver detection threshold. This threshold functions to not only avoid false path detection, due to the presence of noise, but also to allow optimum direct path detection [78].

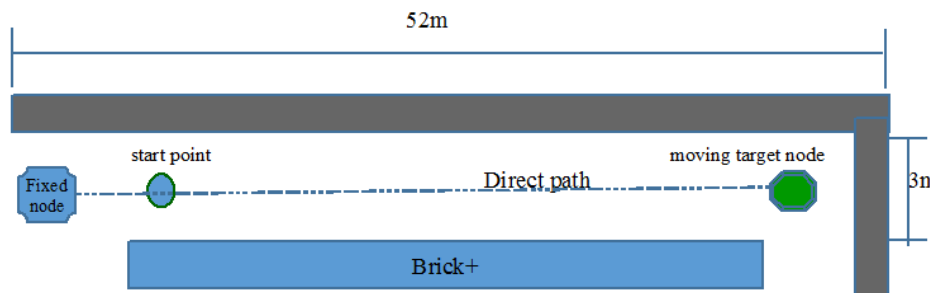


Figure 4.3: Direct path through air with no obstruction (LOS).

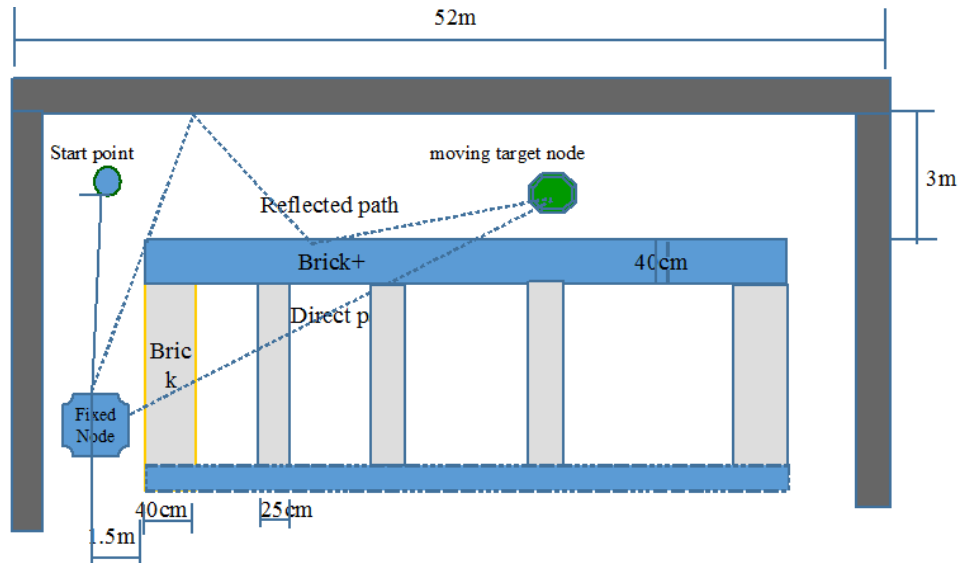


Figure 4.4: NLOS through solid cement and brick and concrete walls with reflection.

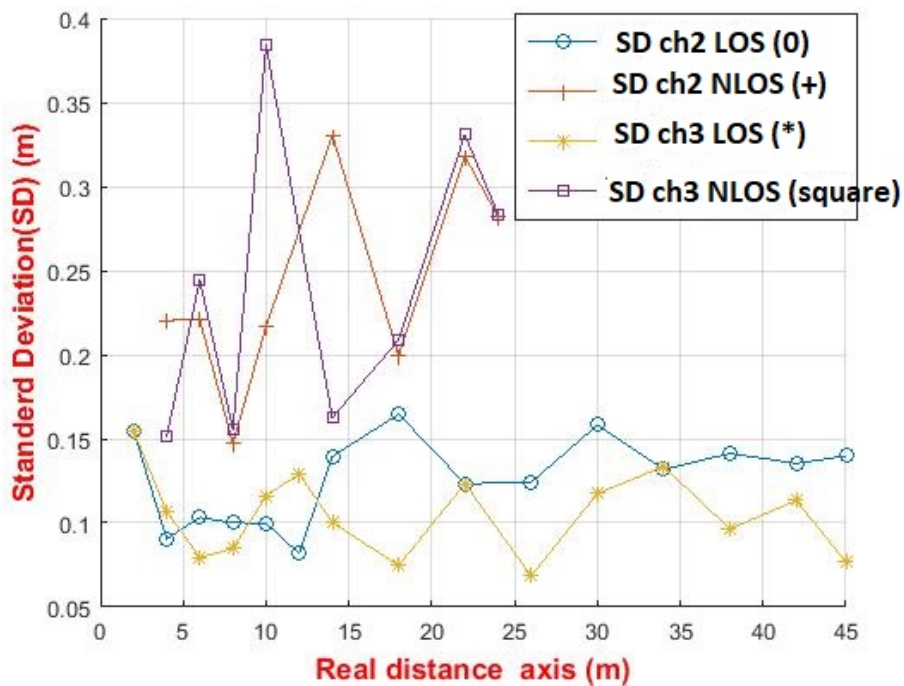


Figure 4.5: STD for ch2 and ch3 in LOS and NLOS.

Three important aspects should be considered when examining NLOS operation:

- Reduction in direct path detection range due to attenuation of the direct path signal,
- Reduction in communication range due to overall signal attenuation, and

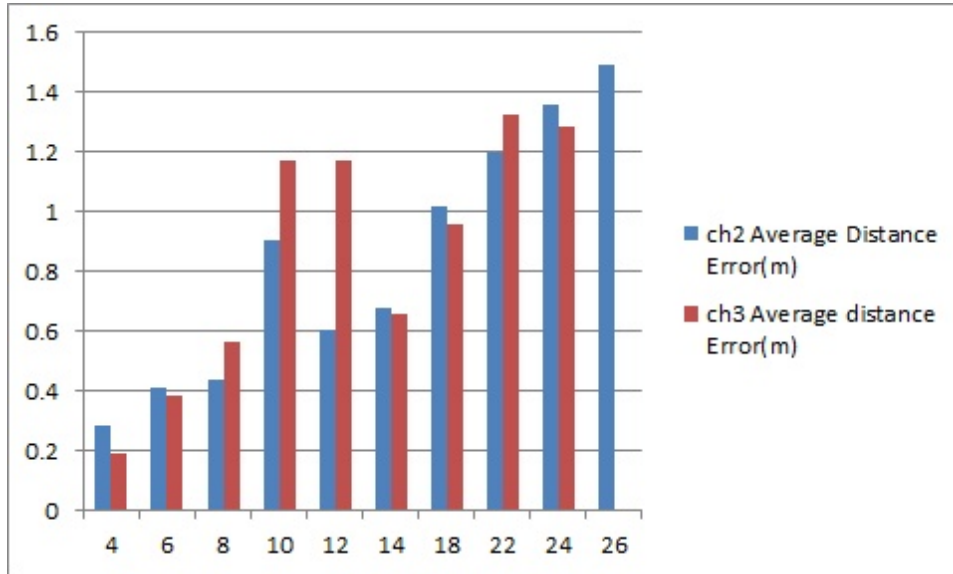


Figure 4.6: Average error of each distance in hard-NLOS.

- Time of Flight errors due to differences in the refractive index of the obstructing material.

a. NLOS identification

Some NLOS channels are implemented in this experiment: different numbers and types of walls for each distance and different types of office and lab furniture.

We assume to identify NLOS channels given by EVK 1000 as FSL and RSL. These two parameters are rolling as follows:

1. $RSL - FSL \geq 11$ dB considered an NLOS channel.
2. $RSL - FSL \leq 5$ dB considered an LOS channel.

The two conditions above committed by [73] were evaluated through our experiment, and we implemented the sensitivity and specificity algorithm to assess the accuracy of the above conditions, as shown in Table 4.5. The two equations below express the true position rate (TPR), sensitivity, recall, and true negative rate

(TNR) and specificity, respectively.

$$TPR = \frac{\sum TP}{\sum CP} \quad (4.10)$$

Where, TP and CP denote true positive and condition positive values respectively.

$$TNR = \frac{\sum TN}{\sum CN} \quad (4.11)$$

Where, TN and CN denote true negative and condition negative values respectively.

And the accuracy equation (ACC)

$$ACC = \frac{\sum TP + \sum TN}{\sum ToTP} \quad (4.12)$$

Where, $ToTP$ denotes the total population.

The accuracy of the NLOS identification technique is 74 % for ch2 (4 - 26 m) and 74 % ch3 (4 - 24 m), as shown in Table 4.5 because the two conditions above do not fully satisfy all LOS and NLOS probabilities (RSL - FSL = 10, 9,8,6). In this experiment, we made 1000 RSL and FSL measurements of different distances from 4 m to 26 m in LOS and NLOS (Table 4.7 depicts the FSL and RSL in LOS and NLOS channels), and then compared with the RSL in the free space (please see appendix 1: table of receiving signal power from [79]) to add new two conditions to decide whether LOS or NLOS channel as shown below. In the new conditions, and because we already have the RSL table in free space, we estimated the average RSL = -87 dBm, which was taken from EVK 1000 measurements in LOS and NLOS channel, as a reference to identify NLOS and LOS channel. As stated below:

3. If RSL - FSL = 6,7,8,9,10 dB and RSL \leq -87 dBm is considered an NLOS channel
4. If RSL - FSL = 6,7,8,9,10 dB and RSL $>$ -87 dBm is considered an LOS channel

The two above-created conditions and the selected value of RSL = -87 dBm were also evaluated by implementing the same algorithm of accuracy used in the first two conditions. By enforcing the new conditions, we increased the accuracy to 93 % for ch2 and 97 % for ch3, as shown in Table 4.5. By the four conditions, we covered all LOS and NLOS channel probabilities.

Table 4.5: Accuracy of NLOS identification algorithm

Channel mode	distances (m)	<i>TPR</i>	<i>TNR</i>	<i>ACC</i>	Note
2	4-26	0.636	0.859	0.747	First two conditions
2	4-26	0.261	0.124	0.182	Created two conditions
2	4-26			0.929	Total Accuracy
3	4-24	0.868	0.644	0.748	First two conditions
3	4-24	0.1074	0.341	0.223	Created two conditions
3	4-24			0.971	Total Accuracy

b. NLOS mitigation

To implement the NLOS mitigation, we should recognize the area of the experiment. All information related to this area is important, such as walls, furniture, and human, and may be interfered to this area. Then, after obtaining all relative information, we applied a simple equation 4.13 [27], written below, to mitigate the NLOS channels. The NLOS channels in this experiment are different from each other ranging from two walls between sites (walking human, and tripod) to four walls, and office furniture was always involved. The width of walls was between 50 cm and 2.2 m. Each object has a refractive index. This index reduces the power of the received signal according to the type of jamming object (wall, human, or water) [27].

$$d = \hat{d} - w(ri_i - 1) \quad (4.13)$$

d = obtained distance, \hat{d} = estimated distance given by EVK 1000, w = width of the

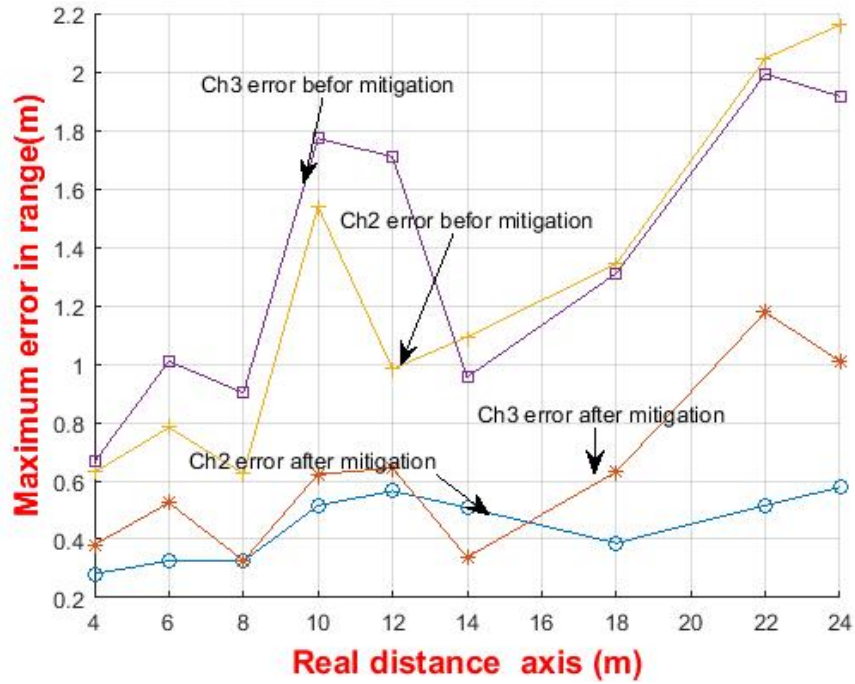


Figure 4.7: The maximum error in measured distances for ch2 and ch3 in NLOS before and after mitigation.

total effected walls, and ri_i = Refractive index is obtained from Table 4.6.

We applied the refractive index (ri_i) of concrete hollow as an average of the different type of walls used in the experiment. Table 4.6 is only for ch2, so we applied $ri_i = 1.73$. For ch3, we applied $ri_i = 1.82$ as an average obtained from our 1000 measurements of nine different ranges in different NLOS environments.

Table 4.6: The refractive index of each object [27]

Material	Dielectric constant	Refractive index	Notes
Concrete solid	7.5	2.73	
Concrete hollow	3	1.73	
Drywall	2	1.41	
Human-body	51	7.14	
Plywood	2	1.41	
water	80	8.96	at 4 GHz

Table 4.7: (RSL) and (FSL) average in LOS and NLOS for ch2 and ch3, 20 measurements of each distance of a walking human

D	LOS				NLOS			
	ch2		ch3		ch2		ch3	
	RSL	FSL	RSL	FSL	RSL	FSL	RSL	FSL
2	-79	-82	-79	-82	-	-	-	-
4	-79	-83	-79	-82	-80	-92	-80	-96
6	-80	-84	-79	-82	-82	-100	-83	-101
8	-82	-88	-80	-83	-87	-107	-86	-99
10	-81	-86	-81	-88	-90	-106	-89	-102
12	-83	-89	-81	-85	-92	-111	-90	-99
14	-81	-84	-80	-83	-92	-110	-94	-109
18	-84	-91	-80	-83	-94	-112	-95	-107
22	-81	-83	-81	-83	-97	-112	-99	-112
24	-82	-84	-83	-86	-99	-113	-99	-109
26	-82	-85	-83	-87	-101	-111	-	-
30	-87	-97	-85	-90	-	-	-	-
34	-84	-87	-82	-84	-	-	-	-
38	-86	-92	-82	-84	-	-	-	-
42	-87	-92	-84	-87	-	-	-	-
45	-87	-95	-89	-94	-	-	-	-

With this experiment, we evaluated and attempted to validate a commercial low-cost UWB module in a ranging system for a walking human and evaluated the NLOS and LOS identification and mitigation technique committed by [27][73] and us. In an indoor LOS channel, both channels (2 and 3) are able to obtain ranging even further than 45 *m* with an error less than 20 *cm*. In a hard-NLOS channels with multipath concrete walls or multi-obstructions that severely attenuate the UWB signal propagation and generate large positive bias in the range estimates, the average distance error varies from 20 *cm* to 1.5 *m* according to how the number and type of walls in each distance obstructed the UWB signal.

From this experiment, we observed that ch3 cannot read farther than 24 *m*, while ch2 can read up to 26 *m* in hard-NLOS channels; Fig 4.6 and Table 4.8 depict the hard-NLOS condition. Higher frequencies exhibit better performance than lower frequencies in LOS, while lower frequencies are better than higher frequencies in an NLOS

Table 4.8: Type and thickness of walls for each distance

D(m)	Wall Number	Wall type	Total thickness(m)	Note
4	2	Concrete hol- low+Brick	0.5	
6	2	=	0.65	Extension in second wall
8	2	=	0.65	Extension in second wall
10	3	=	1.4	Extension in second wood+wood wall
12	3	=	1.3	Extension in second wall
14	2	=	0.8	Extension in second wall+door
18	3	=	1.4	Extension in second wall+door
22-26	4	=	2.2	Extension in second and forth wall + wood wall

environment. Fortunately, the identification and mitigation technique we implemented performed very well and reduced the maximum error to less than 60 *cm* in ch2 and 1 *m* in ch3; Fig 4.7 illustrates the NLOS mitigation. Also, in this experiment, we observed that the readings from the transceivers demand a long time (approximately more than 0.15 second) due to the ranging delay for distances farther than 26 *m* in a hard-NLOS channel. We compared the obtained results with the results of work presented by [79] based on inertial measurement units (IMU) and we clearly observed that UWB device (DW 1000) provides more precisely results than IMU for the same application.

4.5 Conclusion

In this chapter, we practically and realistically evaluated and validated low-coast UWB module; the EVK 1000 (transceiver) from Decawave 1000 which is capable of measuring a precise time of arrival employing UWB. We utilized EVK 1000 carried by a human

to measure its range while moving in an indoor environment for LOS and hard-NLOS channels applying ch2 (4 GHz) and ch3 (4.5 GHz). It provided the accurate information we require to calculate the true distance. We evidenced that human movement does not affect the EVK 1000 measurements in the the LOS channel and up to 24 *m* in the hard-NLOS channel. We also evaluated the new NLOS identification and mitigation technique and developed two additional conditions for it to cover all NLOS and LOS probabilities. The mitigation technique measured distance with an error less than 60 *cm* in the hard-NLOS channel, which is the main goal of indoor positioning systems.

We summarize that in a hard-NLOS channel, DW 1000, EVK 1000, is dependable and useful equipment for wireless communication mechanism used to create indoor positioning systems up to 26 *m* in distance. For further distances, EVK 1000 showed difficulty precisely reading the distance of moving targets due to the ranging delay while implementing SDS-TWR. ADS-TWR minimizes the ranging delay, as we explained in the introduction section.

5. NLOS identification and mitigation method for UWB technology in indoor environment using Fuzzy logic control

A novel NLOS identification and mitigation method for UWB radio technology using the Fuzzy logic (FL) control is presented in this chapter. Most of NLOS identification for UWB methods depend on the received signal (RSL). But, usually, the estimated RSL diverges from its true value after (above) -85 dBm. To overcome this problem, Fuzzy logic is a confident algorithm to be used as we implemented it in this work. The Fuzzy logic is an approach to computing based on "degrees of truth" rather than the usual "true or false" (1 or 0) Boolean logic on which the modern computer is based. In this work, we used the DW 1000 (EVK 1000). We extract three important parameters to be used as the input set for the FL and we range these parameters for different ranges. As typical, we used the IF-THEN rule to apply then the center of gravity (CoG) method for defuzzification process for obtaining a confident output to be used to identify the propagation channels which the UWB signal travels through. For the mitigation process, we create a database includes information about the input parameters, propagation channels, and error values in the measured distance.

5.1 Introduction

Nowadays, Indoor positioning sensing systems (IPS) are very popular and important in different places such as hospitals, airports, malls, factories, and etc. IPS determine

the position of an object in a physical space continuously and in a real-time. Five major quality metrics of IPS are exist: (1) precision and accuracy of the system ; (2) coverage and its resolution; (3) latency in making location updates; (4) buildings infrastructure impact; and (5) random errors impacts on the system such as errors caused by signal interference and reflection [80]. To achieve the quality metrics, we should obtain a technology with a highly accepted ranging accuracy for indoor positioning applications. Different technologies in the market try to provide an accepted ranging accuracy. The accepted ranging accuracy depends on the indoor positioning application type. Some applications acquire centimeter positioning accuracy, and others may need for one-meter level accuracy.

Indoor localization is an emerging technology that demands a theoretical and analytic background. The authors of [81] realize the necessity for the essential study of the characterization of indoor radio propagation and its effect on the accuracy of such systems. System design and performance evaluation require a framework for the success and the growth of this technology. Four areas of challenges in position location in a mobile environment which are performance, cost and complexity, security, and application requirements are identified by [82].

For location-based applications, wireless systems in an indoor environment often operate under non-line-of-sight (NLOS) conditions that may cause ranging errors. A promising technology for location-aware sensor networks is an Ultra-wide bandwidth (UWB) transmission due to its robust operation in harsh environments, fine delay resolution, and power efficiency. However, the existence of walls and other obstacles causes a notable challenge in terms of localization, as they can result in positively biased distance estimates.

In this chapter, we are interested in the performance challenge because it is corresponding to the positioning accuracy, and we briefly explain it in the text below.

The most important performance metric is the accuracy of the position information. Normally, This is reported as an error distance between the estimated location and the actual mobile location. The report of accuracy should include the confidence interval or percentage of successful location detection which is called the location precision.

Indoor environments could be distributed as structured or known, semi-structured and unstructured or unknown depending on the control that the IPS possesses over them [83], [84].

Of the aforementioned forms of RF technology, UWB is considered one of the most precise approaches because it can provide location estimates with centimeter-level accuracy [85]. It is widely used for ranging estimation and creating an indoor positioning system. In the indoor environment, the propagation channels could be divided into a line of sight (LOS) and non-line of sight (NLOS). Also, the NLOS could be divided into soft NLOS and hard NLOS depending on the attenuation of the radio signal. In the UWB signals, it is possible to transmit and detect very short pulses permitting for high accuracy of positioning because of the accurate calculation of signal delays. In an indoor environment, the propagation path length is not always a good indicator of the ranging between a sender and receiver. Thus, these systems are predominately bounded to the LOS conditions [25]. It precisely measures the distance in the LOS channel but suffers in the NLOS channel, and the error in distance measurements is significantly high [86] [27] which impacts the positioning accuracy.

The main contributions of this chapter follow:

- To overcome the main problem in the most UWB commercial devices when estimating the value of the RSL because it diverges from its true value after (above) -85 dBm as shown in figure 5.1.
- To identify the NLOS propagation channels when using UWB technology in in-

door environment and divide them into hard and soft to facilitate the mitigation method for obtaining a precise distance measurement.

- To create a database contains information corresponding to the UWB signal traveling through LOS and NLOS (hard and soft). So, with this database, we can enhance the estimated distance without the need for any maps related to the indoor environment.

The rest of this chapter is organized as follows: Section 5.2 represents the problem formulation related to the IPS. In Section 5.3, the proposed framework (NLOS and LOS identification and mitigation method) is presented. Section 5.4 presents the experimental activities implemented in this work. Section 5.5 offered result and discussion. Finally, a conclusion is presented in section 5.6.

5.2 Problem formulation

As we mentioned in the literature survey section about the main drawback of the created systems aforementioned above, we overcome this drawback using the FL and therefore, the accuracy of the NLOS identification method is highly increased comparing with the other methods. Also, The created databases (Tables 5.2 and 5.4) help us to implement the mitigation process without the need for extra information about the environment such us maps and enhance the estimated distance achieving a distance accuracy of less than 20 *cm* error which is much better than the accuracy achieved by the other studies.

In this section, we address the problem of the NLOS identification and mitigation method solved using the proposed method.

We installed two UWB sensors (transmitter and receiver) in three different scenarios as depicted in figure 5.2. The first scenario presents the LOS channel when the signal travels between the sensors with a direct path in free space without any obstruction. The second scenario presents the soft NLOS channel when the signal travels between

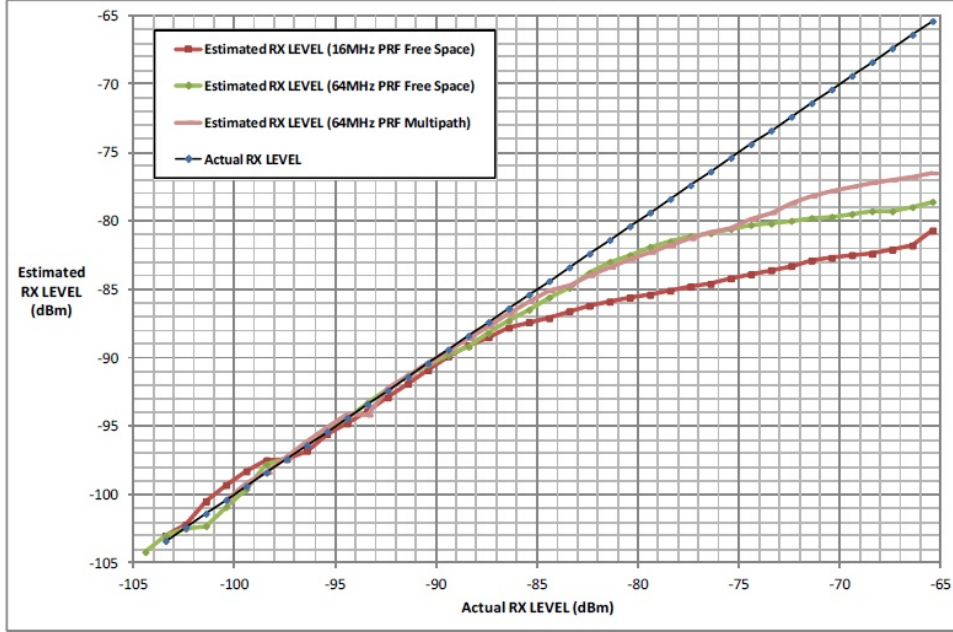


Figure 5.1: Estimated RX level versus true RX level [73].

the sensors with a direct path obstructed by one wall of 30 *cm* thickness. The last scenario presents the hard NLOS when the signal travels between the sensors with a direct path obstructed by two walls of 30 *cm* thickness of each wall.

In this chapter, first, we identify the propagation channel as LOS, hard NLOS, and soft NLOS using the Fuzzy logic (FL) method. The input parameters used in the FL are RSL, FSL, and SNR extracted from the UWB sensor and therefore, the last step of the proposed method is the mitigation process (distance enhancement) implementing the databases shown in tables 5.4 and 5.2 to compute the enhanced distance using equation 5.3 as shown in the proposed framework section.

5.3 Proposed work

In this section, we present briefly the steps of the proposed algorithm which consists of the NLOS identification and mitigation process of different propagation channels in an indoor environment.

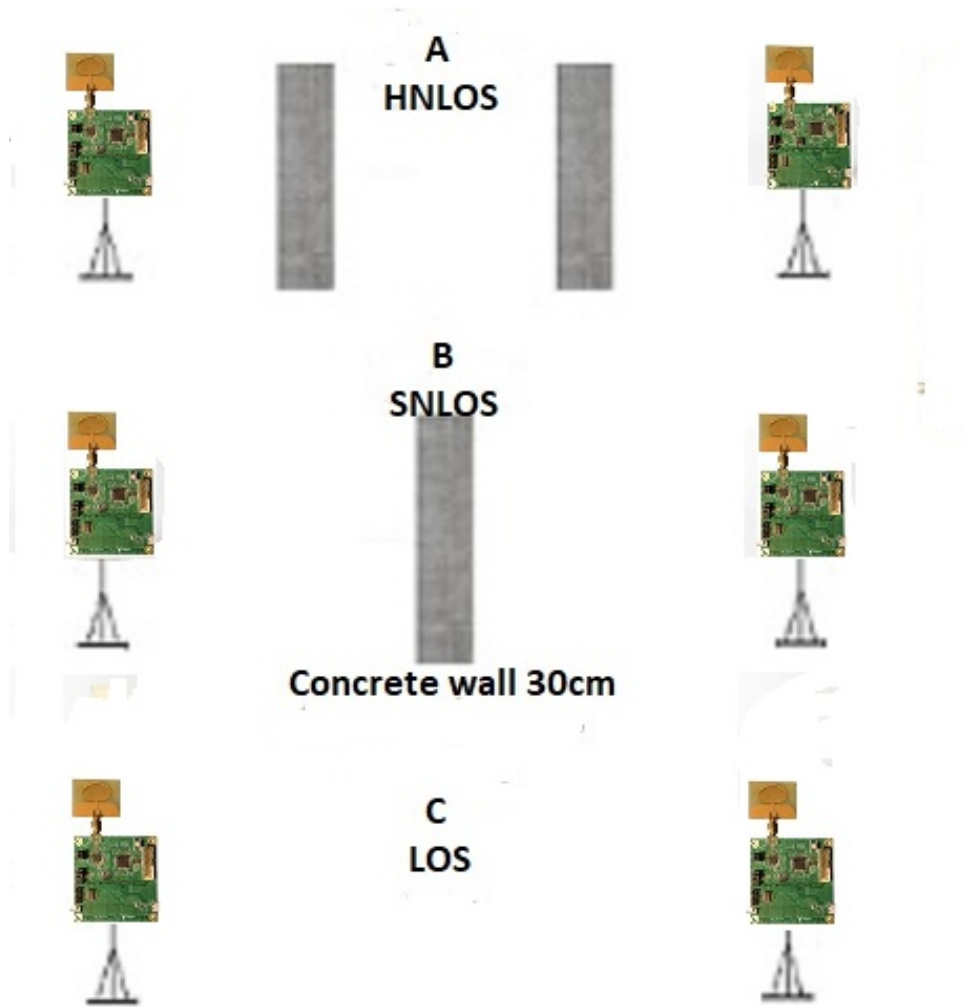


Figure 5.2: The proposed scenario.

5.3.1 NLOS identification method

a. The main parameters

The NLOS identification method depends on three parameters; i) estimated power for just the first path signal (the signal power in the first path FSL), ii) estimated receive power figure (the received signal power RSL), and iii) signal to noise ratio (SNR), and they are explained below. These parameters are extracted in this work from the implemented UWB device (DW 1000 - EVK 1000).

- a. The signal power in the first path FSL is computed using the equation 5.1 ac-

according to [73].

$$FSL(dBm) = 10 \times \log_{10}\left(\frac{F1^2 + F2^2 + F3^2}{N^2}\right) - A \quad (5.1)$$

Where, $F1$, $F2$, and $F3$ denote the First Path Amplitude (point 1), the First Path Amplitude (point 2), and the First Path Amplitude (point 3) respectively. All points mentioned above are measured by the DW 1000.

- b. The receive signal power RSL is computed using equation 5.2 according to [73].

$$RSL(dBm) = 10 \times \log_{10}\left(\frac{2^{17} \times C}{N^2}\right) - A \quad (5.2)$$

Where, C , A , and N denote the Channel Impulse Response Power value (CIR), constant value 113.77 for a PRF (Pulse repetition frequency) of 16 MHz , or, the constant value 121.74 for a PRF of 64 MHz , and the Preamble Accumulation Count value respectively.

- c. Signal to noise ratio (SNR (dB)) is computed by the DW 1000-EVK 1000 device.

All parameters mentioned in the items a, b, and c above implemented in this work are extracted from the UWB device (DW 1000 - EVK 1000) used in this work.

b. Fuzzy logic control

In the NLOS identification method and after obtaining the main parameters explained above, the main step in the NLOS identification method is the Fuzzy logic control technique. So, first, we present below an overview of the concept of the Fuzzy logic control.

Fuzzy logic is a logic process method based on several-valued logic rather than binary logic (two-valued logic). Two-valued logic overwhelmingly, considers 0 to be false and 1 to be true. However, fuzzy logic transacts with truth values between 0 and

1, and these values will be considered as intensity (degrees) of truth. To utilize fuzzy logic in a real application, we apply the following three steps [87]:

1. **Fuzzification:** Convert classical data or crisp data into fuzzy data or Membership Functions (MFs).
2. **Fuzzy Inference Process:** combine membership functions with the control rules to derive the fuzzy output.
3. **Defuzzification:** implement different methods to compute each corresponding output and put them into a table: the lookup table. Pick up the output from the lookup table according to the current input during an application.

In the following paragraph, we explain briefly the three steps aforementioned above.

Fuzzification: It is the first step in the fuzzy inferencing process. This includes a domain transformation where crisp inputs are transformed into fuzzy inputs. Crisp inputs are exact inputs computed by sensors and passed into the control system for processing, such as pressure, temperature, etc. Each crisp input will be processed by the Fuzzy inference unit (FIU) get its own group of membership functions or sets to which they are transformed. within a universe of discourse that holds all relevant values that the crisp input can possess, this group of membership functions exists. The next presents the structure of membership functions within a universe of discourse for a crisp input.

- **Degree of membership:** The degree to which a crisp value is compatible with a membership function, the value from 0 to 1, also known as truth value or fuzzy input.
- **Membership function(MF):** Defines a fuzzy set by mapping crisp values from its domain to the sets associated degree of membership.
- **Crisp inputs:** Distinct or exact inputs to a certain system variable, usually measured parameters external from the control system, e.g. 6 Volts.

- **Label:** A descriptive name used to identify a membership function.
- **Scope:** Domain, the width of the membership function, the range of concepts, usually numbers, over which a membership function is mapped.
- **Universe of discourse:** Range of all possible values, or concepts, applicable to a system variable.

The fuzzification process maps each crisp input on the universe of discourse, and its intersection with each membership function is transposed onto the μ axis as illustrated in the previous figure. These μ values are the degrees of truth for each crisp input and are associated with each label as fuzzy inputs. These fuzzy inputs are then passed on to the next step, Rule Evaluation. If-Then rule statements are implemented to create conditional statements that comprise fuzzy logic. A single fuzzy If-Then rule assumes the form

$$\text{IF } \mathbf{x} \text{ is } A_1 \text{ Then } \mathbf{y} \text{ is } B_1$$

where A_1 and B_1 are linguistic variables defined by fuzzy sets on the ranges (i.e. universe of discourse) \mathbf{x} and \mathbf{y} respectively. The If-part of the rule ' \mathbf{x} is A_1 ' is called the antecedent or premise and the Then-part of the rule ' \mathbf{y} is B_2 ' is called the consequent.

Defuzzification: Defuzzification includes the operation of transposing the fuzzy outputs to crisp outputs. There are several methods to obtain this, however, this explanation is limited to the process implemented in this thesis design.

A method of averaging is implemented here which is known as the Center of Gravity method (CoG), which it is a method of calculating centroids of sets. The output membership functions to which the fuzzy outputs are transposed are obligated to being singletons. This is so to limit the degree of calculation intensity in the microcontroller. The fuzzy outputs are transposed to their membership functions similarly as in fuzzification. With CoG the singleton values of outputs are calculated using a weighted

average, illustrated in the next figure. The crisp output is the result and is passed out of the fuzzy inference system for processing elsewhere.

5.3.2 NLOS mitigation (ranging enhancement)

After identifying the appropriate propagation channel from the NLOS identification method, the ranging enhancement technique to obtain the best possible ranging accuracy is implemented using equation 5.3 below. More details regarding the distance enhancement method are explained in the experimental activities section.

$$d = \hat{d} - Bias_{avr} \quad (5.3)$$

Where, d , \hat{d} , and $Bias_{avr}$ denote the enhanced distance after the NLOS identification method, distance extracted from the DW 1000 - EVK 1000, and the average of the Bias distance computed as explained in the experimental activities section respectively. We should mention that the device implemented in this experiment has a positive Bias in the LOS channel [88], and therefore the Bias is also positive in the NLOS channel.

All steps of the proposed framework are explained in algorithm 1.

Algorithm 1 NLOS identification and mitigation method

-
- 1: **procedure** EXTRACT INFORMATION
 - 2: FSL, RSL, SNR ▷ Extracted from the EVK 1000
 - 3: **end procedure**
 - 1: **procedure** NLOS IDENTIFICATION METHOD
 - 2: implement Fuzzy logic control
 - 3: range of Fuzzy input set
 - 4: Fuzzy control rule
 - 5: range of the Fuzzy output set
 - 6: defuzzyfication method ▷ Center of Gravity (CoG)

$$P = \frac{\sum_{i=1}^n A_i \times c_i}{\sum_{i=1}^n A_i}$$

- 7: **end procedure**
- 1: **procedure** NLOS MITIGATION ▷ Distance enhancement
- 2: create a database of the average of the extracted information
- 3: create a database of the average Bias for every propagation channel
- 4: Find the enhanced distance

$$d = \hat{d} - Bias_{avr}$$

- 5: **end procedure**
-

5.4 Fuzzy Logic-based NLOS identification and mitigation

In this work, we experimented three different propagation channels as shown in figure 5.2 and explained below:

- We placed Two EVK 1000 as follows:
 - i) LOS channel: The traveling signal (UWB signal) passes between two wireless sensors (DW 1000-EVK 1000) through a direct path without any restriction.
 - ii) Soft NLOS channel: The signal travels through a 30 *cm* thickness wall.
 - iii) Hard NLOS channel: The signal travels through two 30 *cm* thickness walls.
- Propagation distances range between 2 *m* and 22 *m*. The first Fresnel zone in the vicinity of TX and RX is not blocked.
- Measuring the estimated distance, the RSL, FSL, and SNR for 1000 times to

create the database depicted in table 5.4.

Next, we introduce the Fuzzy Logic (FL) based strategy to find out a distance correction $Bias_{avr}$ from the input data RSL, FSL and SNR.

5.4.1 NLOS identification

The goal in our Fuzzy Logic approach is to output a score of P that helps in identifying the type of channel as depicted in Table 5.2. We consider three input values: SNR, RSL and $dif = FSL - RSL$.

The first step in our Fuzzy Logic is the input fuzzification. The range of each tuple as follows:-

- i) RSL = [-98 dBm -78 dBm],
- ii) SNR = [-18 dB 1 dB], and
- iii) dif = [-25 dB 1 dB].

The input fuzzy sets for dif , SNR and RSL are depicted in figures 5.3, 5.4, and 5.5, respectively. After the input fuzzification, the fuzzy rules applied to each input parameter are explained in the Fuzzy IF-THEN rules as shown in table 5.1. The fuzzy rule applied in this approach is the IF-THEN rule. All rules fire to some extent in a fuzzy system or in other words, they fire partially. If the antecedent is true to some degree of membership, then the consequent is also true to that same degree. A fuzzy rule can have multiple antecedents, for example from table 5.1:

IF SNR has a value of high (for example between -5 dB and 1 dB), the RSL has a value of low, and FSL has a low value, Then the output of the FL (P) will be Rather Low which means close to the NLOS channel. The Fuzzy Logic rules were explained as in table 5.1.

The output set of FL is divided into different ranges of the propagation channel types as shown in figure 5.6.

The last step of the FL is the defuzzification process. The output of the Fuzzy

Table 5.1: Fuzzy IF-THEN rule

Rule	RSL	dif	SNR	P
1	Low	Low	Low	Very Low
2	Low	Low	Medium	Low
3	Low	Low	High	Rather Low
4	Low	Medium	Low	Rather Medium
5	Low	Medium	Medium	Medium
6	Low	Medium	High	Very medium
7	Low	High	Low	Rather Medium
8	Low	High	Medium	Medium
9	Low	High	High	Very Medium
10	Medium	Low	Low	Rather Low
11	Medium	Low	Medium	Low Medium
12	Medium	Low	High	Rather Medium
13	Medium	Medium	Low	Rather Medium
14	Medium	Medium	Medium	Medium
15	Medium	Medium	High	Very Medium
16	Medium	High	Low	Medium
17	Medium	High	Medium	Very Medium
18	Medium	High	High	High
19	High	Low	Low	Rather Medium
20	High	Low	Medium	Medium
21	High	Low	High	Rather High
22	High	Medium	Low	Medium
23	High	Medium	Medium	Very Medium
24	High	Medium	High	High
25	High	High	Low	Rather High
26	High	High	Medium	High
27	High	High	High	Very High

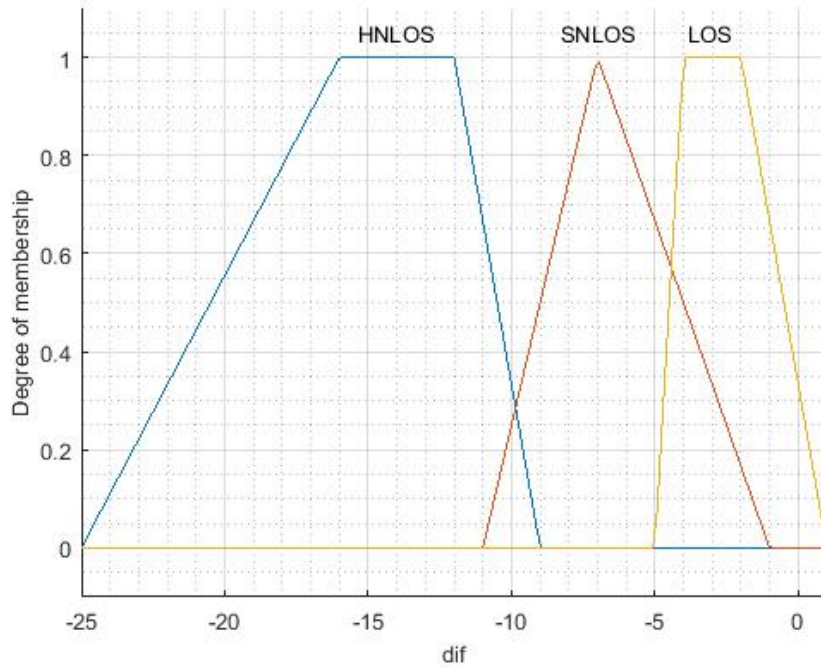


Figure 5.3: The degree of the membership function of the *dif* (input) parameter.

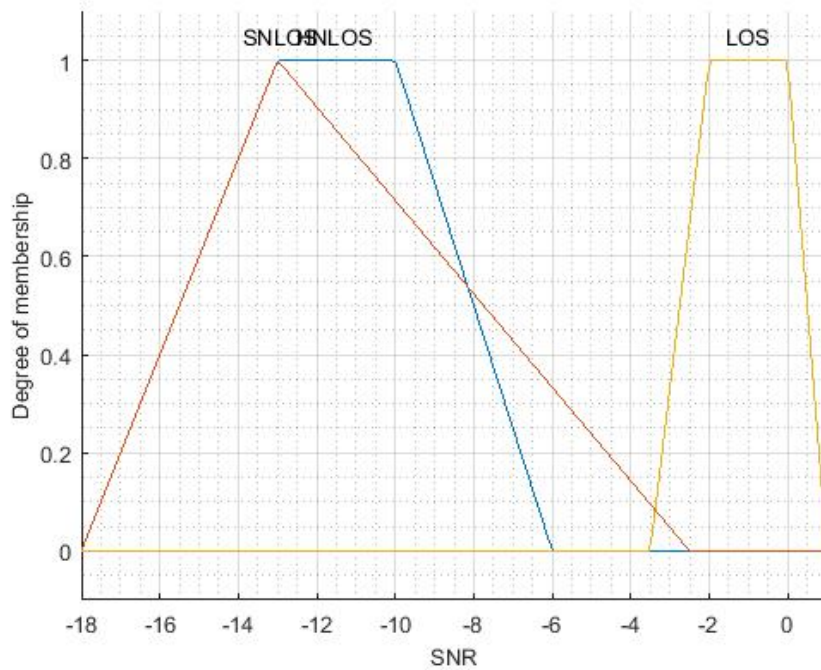


Figure 5.4: The degree of the membership function of the SNR (input) parameter.

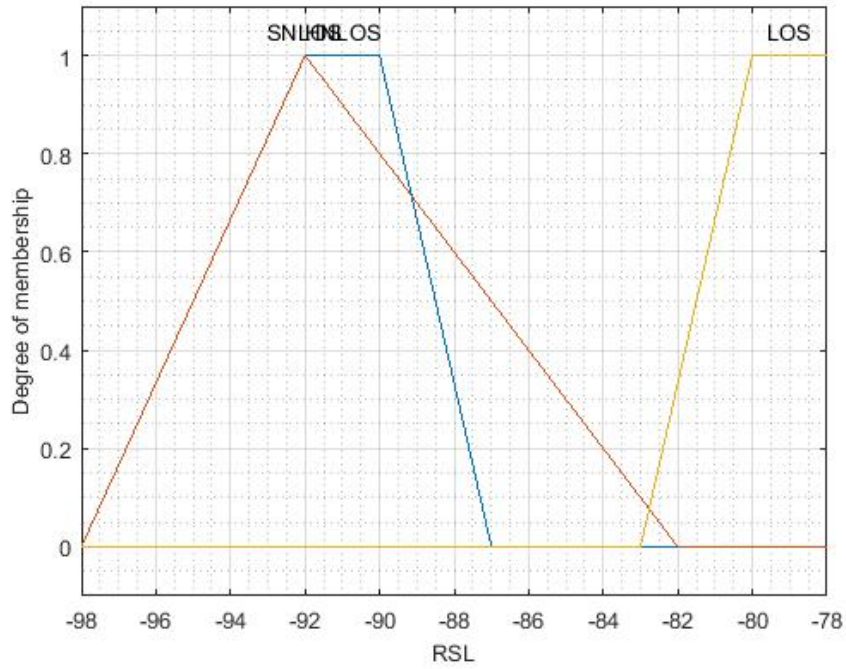


Figure 5.5: The degree of the membership function of the RSL (input) parameter.

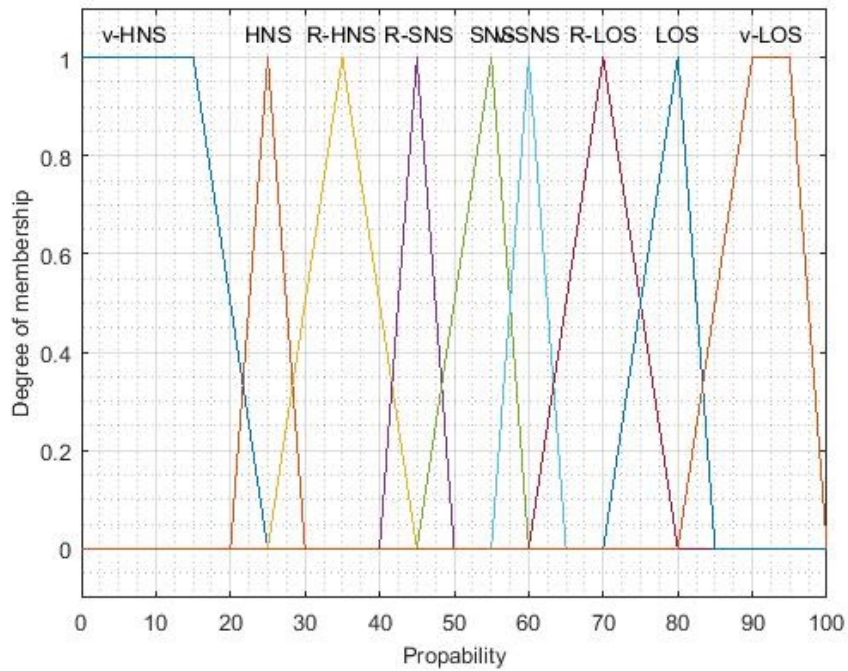


Figure 5.6: The degree of the membership of the output sets.

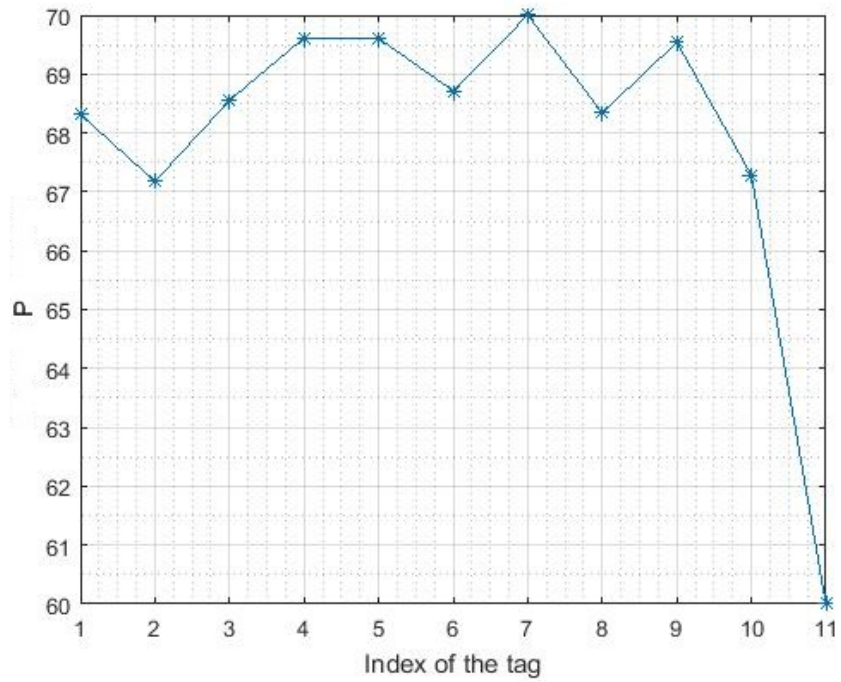


Figure 5.7: The output of the Fuzzy system (P) for LOS channel.

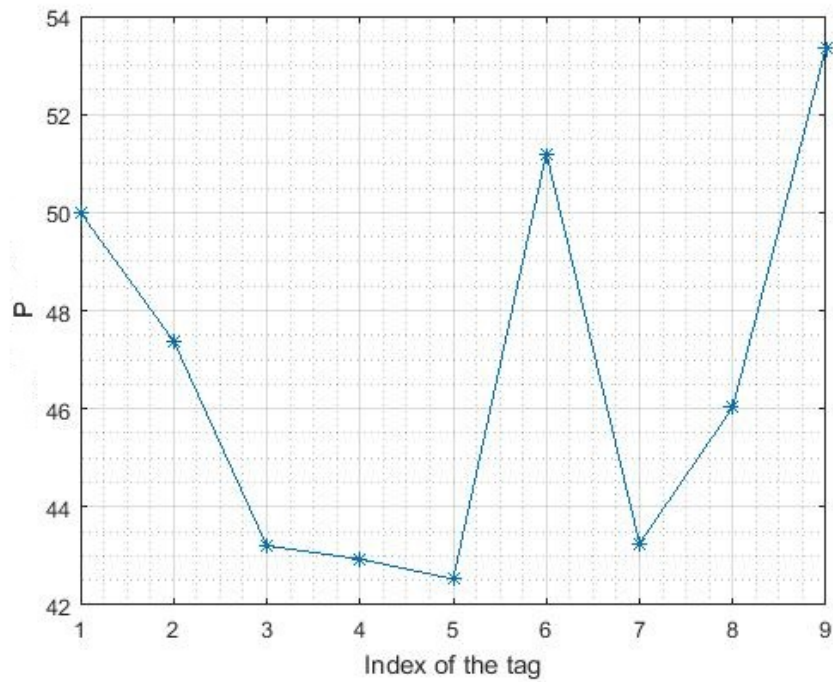


Figure 5.8: The output of the Fuzzy system (P) for soft NLOS channel.

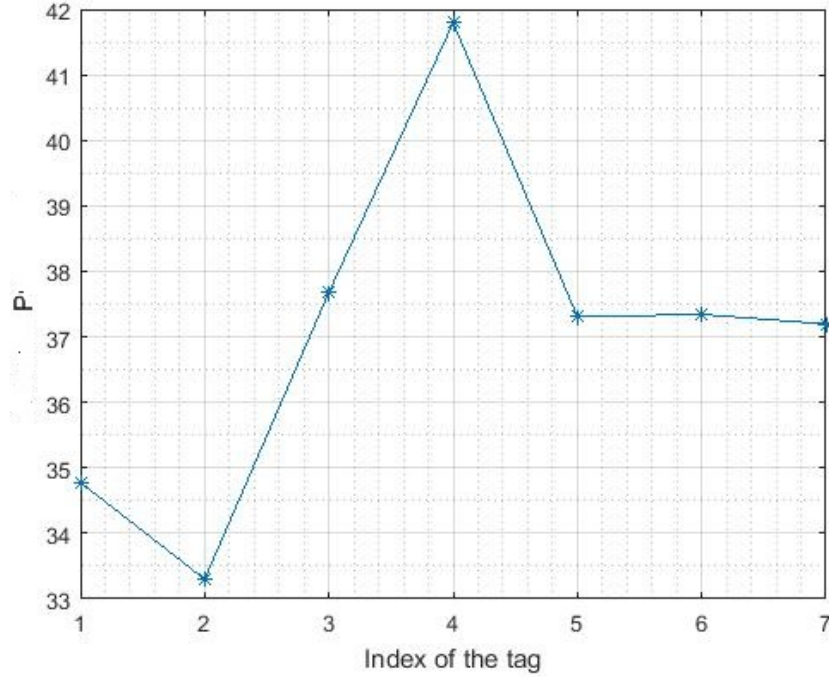


Figure 5.9: The output of the Fuzzy system (P) for hard NLOS channel.

system (P) is defuzzified implementing the CoG defuzzification method as expressed in equation 5.4. P are unit-less value, and we created a metric of its range. This metric is as follows:

LOS: $P > 56$, hard NLOS: $P = [30 - 41]$, and soft NLOS: $P = [42 - 57]$. Figures 5.7, 5.8, and 5.9 depict the output of the Fuzzy system (P) as shown below. According to the P (equation 5.4) metric, we will be able to identify the propagation channel into LOS or hard and soft NLOS. The horizontal coordinate in the figures aforementioned above presents the number of the points (index of the receiver) ranged between $2m$ and $22m$ tested in this experiment, and the vertical coordinate presents the output of the Fuzzy system (P).

$$P = \frac{\sum_{i=1}^n A_i \times c_i}{\sum_{i=1}^n A_i} \quad (5.4)$$

Where, P , A , c , and $n = 27$ denote the Fuzzy system output, the subarea of the input system, and the centroid of the subarea, and the total number of the subareas respectively. After the determination of the type of the propagation channel, the NLOS mitigation method (distance enhancement) is implemented as explained below.

Table 5.2: Type of the propagation channel corresponding to the range of P and Bias value

Range of P	channel type	Bias value m
25-35	Very hard NLOS	1.3
36-39	hard NLOS	0.8
40-42	Rather hard NLOS	0.5
43-44	Very soft NLOS	0.5
45-51	Soft NLOS	0.3
52-55	Rather soft NLOS	0.15
≥ 56	LOS	0

5.4.2 NLOS mitigation

The idea of distance enhancement is to obtain the best possible ranging accuracy. To reach this goal, we experimentally created a database of the measured distance in different types of propagation channels (LOS, soft NLOS, and hard NLOS). This database also includes the average Bias, RSL, FSL, and SNR of the measured distance computed for every channel as shown in table 5.4, and therefore, we divide the aforementioned channels into three probabilities, rather (low), medium, and very(high) as shown in table 5.2. Then, applying equation 5.3 is to obtain the final result of the enhanced measured distance.

5.5 Result and discussion

In this section, we present the results of the proposed NLOS identification and mitigation method of the UWB signal in an indoor environment obtained experimentally

Table 5.3: Accuracy of NLOS identification algorithm compared to the methods crated by [86] and [56]

Channel mode	distances (m)	TPR	TNR	ACC	Note
2	4-20	0.897	0.983	0.929	[59] algorithm
2	4-20	0.761	0.891	0.826	[90] algorithm
2	4-20	0.989	0.998	0.990	Proposed algorithm

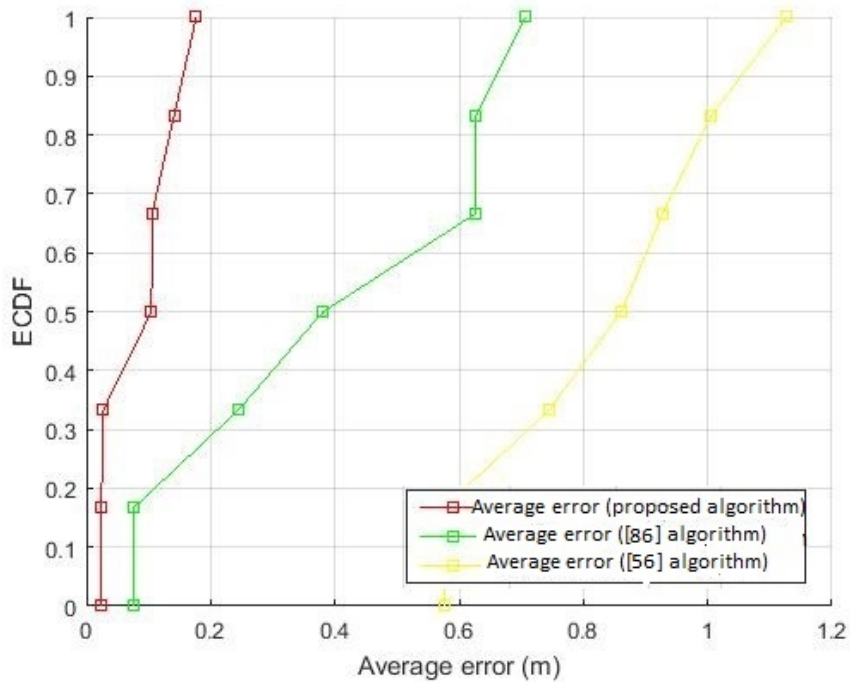


Figure 5.10: The average of ranging error in a hard NLOS channel for the proposed method (Red curve) and the methods created by [86] (Green curve) and by [56] (yellow curve).

using the FL. After obtaining the result of the NLOS identification method, we tested the sensitivity and specificity metrics to assess the accuracy of the proposed NLOS identification method. Table 5.3 shows the identification accuracy of the proposed method and the method created by [86] and [56]. The two equations, 5.5 and 5.6, below express the true positive rate (TPR), sensitivity, recall, and true negative rate (TNR), specificity, respectively.

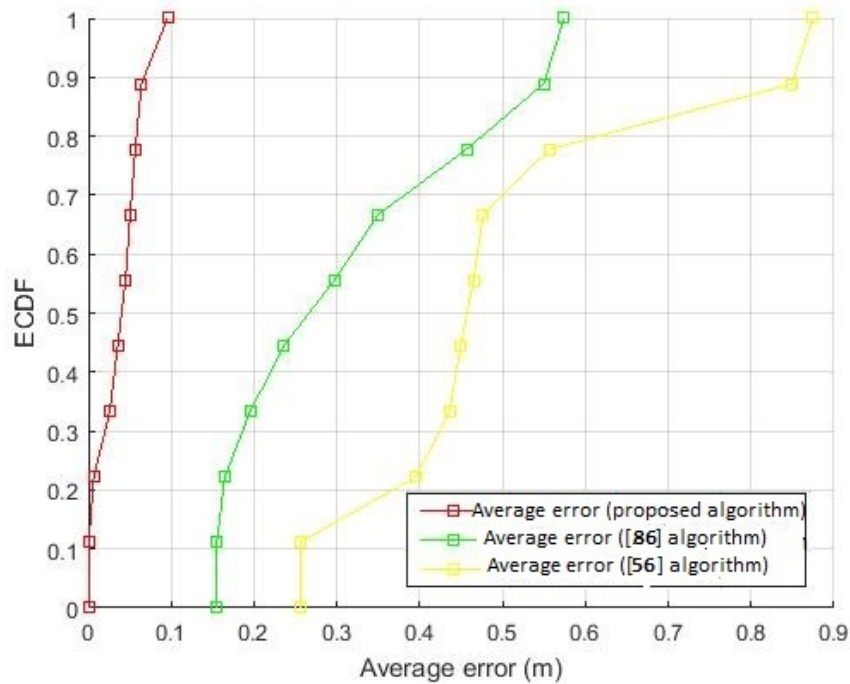


Figure 5.11: The average of ranging error in a soft NLOS channel for the proposed method (Red curve) and the methods created by [86] (Green curve) and by [56] (yellow curve).

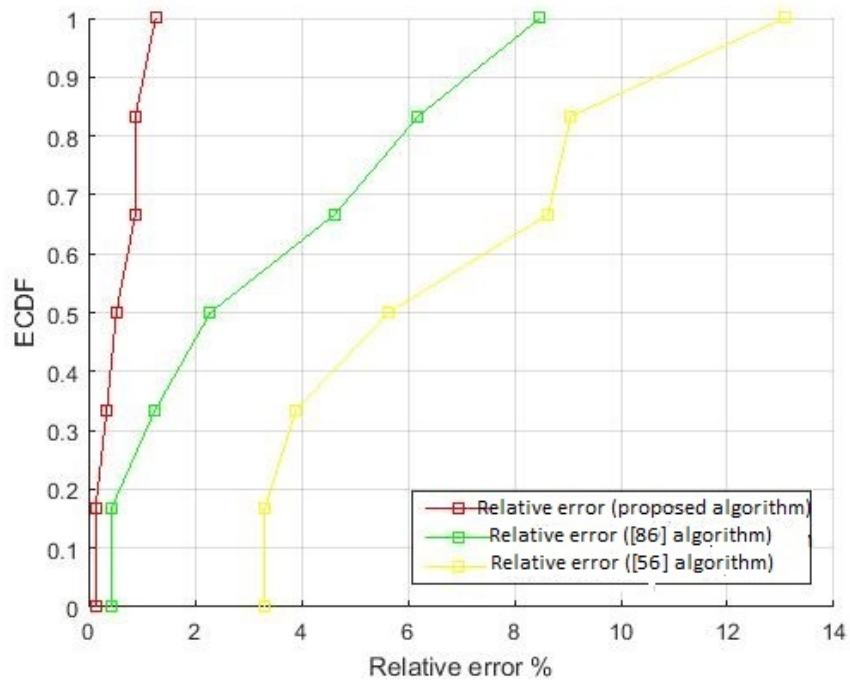


Figure 5.12: The relative error of the enhanced distance and real distance in a hard NLOS channel for the proposed method (Red curve) and the methods created by [86] (Green curve) and by [56] (yellow curve).

Table 5.4: Distance measurement where, d , and Av denote the real distance and the average of the distance Bias respectively

d (m)	LOS				SNLOS				HNLOS			
	RSL (dBm)	dif (dB)	SNR (dB)	Bias (m)	RSL (dBm)	dif (dB)	SNR (dB)	Bias (m)	RSL (dBm)	dif (dB)	SNR (dB)	Bias (m)
2	-78.97	-2.17	0.6	0.09	-	-	-	-	-	-	-	-
4	-79.22	-4.23	0.3	0.08	-79.8	-4.24	-5.3	0.19	-	-	-	-
6	-79.81	-4.85	-0.3	0.02	-85.85	-3.25	-6.5	0.26	-	-	-	-
8	-79.83	-3.27	0.28	0.05	-90.66	-5.41	-11	0.27	-87.3	-17.89	-7.3	1.33
10	-79.39	-2.46	0.2	0.05	-94.76	-7.84	-15	0.11	-86.83	-21.98	-11	0.74
12	-79.72	-1.36	-0.3	0.01	-96.60	-8.23	-17	0.10	-91.38	-17.29	-11.8	0.58
14	-79.75	-1.38	-0.2	-0.01	-93.18	-4.24	-13	0.50	-92.54	-9.11	-13.1	1.00
16	-79	-2.33	0.00	0.08	-91.07	-6.01	-11.6	0.35	-89.42	-12.56	-9.6	0.94
18	-80.53	-0.88	-1.00	0.02	-90.24	-4.72	-11	0.24	-89.2	-17.19	-9.5	0.48
20	-80.78	-2.70	-1.3	0.70	-88.81	-5.18	-9	0.50	-89.70	-16.49	-9.3	0.69
22	-81.37	-1.37	-1.9	0.11	-	-	-	-	-	-	-	-
Av Bias	-	-	-	0.05	-	-	-	0.3	-	-	-	0.82

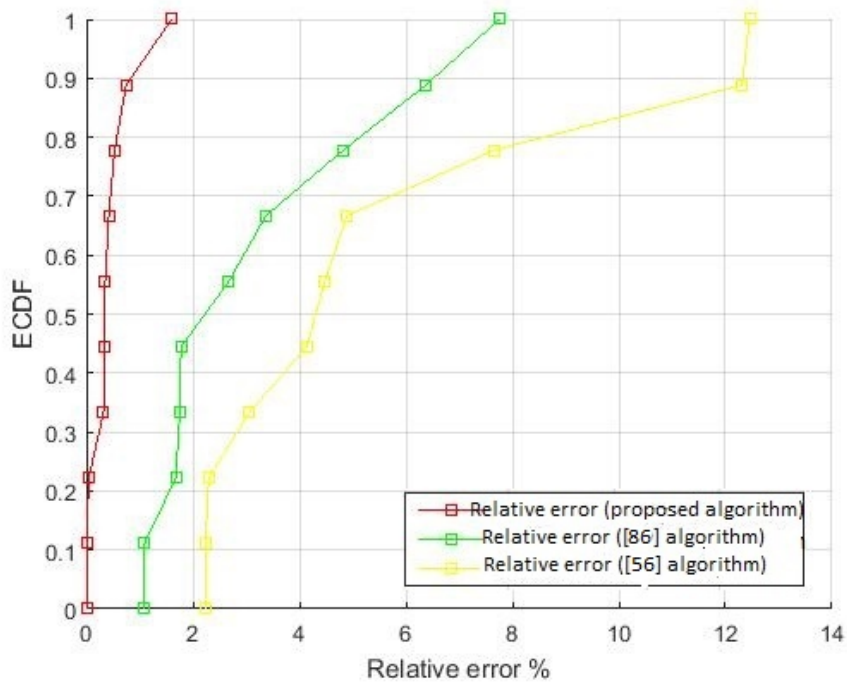


Figure 5.13: The relative error of the enhanced distance and real distance in a soft NLOS channel for the proposed method (Red curve) and the methods created by [86] (Green curve) and by [56] (yellow curve).

$$TPR = \frac{\sum TP}{\sum CP} \quad (5.5)$$

Where, TP and CP denote true positive and condition positive values respectively.

$$TNR = \frac{\sum TN}{\sum CN} \quad (5.6)$$

Where, TN and CN denote true negative and condition negative values respectively.

And the accuracy equation (ACC) shown in equation 5.7 is

$$ACC = \frac{\sum TP + TN}{\sum ToTP} \quad (5.7)$$

Where, $ToTP$ denotes the total population. Then, we implemented the relative error (average of 1000 times) expressed in equation 5.8 and the average error of the enhanced distance to assess the ranging accuracy.

$$E_r = \frac{d_{i(n)} - r}{r} \times 100\% \quad (5.8)$$

Where, r , d , and n denote the real distance, enhanced distance, and the total number of the enhanced distance respectively.

For the NLOS mitigation process, we compute the average and relative error of the enhanced distance in hard and soft NLOS channels, and then compared the Empirical cumulative distributed function (ECDF) of the results with the ECDF of the results of the NLOS mitigation methods created by [86] and [56] as shown in figures 10, 11, 12, and 13. Figures 10 and 12 present the average of ranging error in a hard NLOS channel and it is clear from these figures that the distance error for the proposed algorithm is around 20 *cm*. Figures 11 and 13 present the rational error of the enhanced distance and it is clear from these figures for the proposed algorithm is between 1 and 2 %.

It is clear from the result of the proposed method that the proposed algorithm

has 99 % of an accuracy of NLOS identification approach and a relative error of the enhanced estimated distance approximately below 1.3 % in 99 % of the cases whereas the methods in [86] and [56] have 92 % and 82 % of an accuracy of NLOS identification approach and relative error of the enhanced estimated distance around 8 % and 14 % respectively in 99 % of the cases.

5.6 Conclusion

In this chapter, a novel method is implemented to overcome the main limitation of UWB signal in a harsh indoor environment which is the ranging accuracy and to solve the main drawback that effects the ranging accuracy in the previous work aforementioned in the literature Survey section. The identification and mitigation algorithm using Fuzzy logic control decision and the information extracted from the UWB commercial device is a confident method that provides a very high acceptable NLOS identification method about 99 % and ranging accuracy with less than 20 *cm* of average error of the distance. In average, The NLOS identification method and the ranging accuracy obtained in this work is higher among other identification and mitigation techniques in the market.

6. Anchor selection for UWB indoor positioning

In this chapter, we extend the study of the NLOS identification and mitigation methods to study the IPS comprehensively. To build an accurate IP system that can be suitable for different indoor environments and situations including emergency is a challenging task. But, in this chapter, we present a novel IP system called anchor selection (AS) that we can confidently advise it to be used for different indoor applications. Also, The AS system implements the UWB technology in an indoor environment having a harsh condition in part of it.

6.1 Introduction

On the positioning accuracy, the geometric distribution of anchor nodes in wireless sensor networks (WSN) has notable impacts. To select the optimum node combination, conventional methods that depend on geometric dilution of precision (GDOP) demand to spend time on calculating every possible combination of nodes. In military urban and emergency response operations, the time is a crucial issue, and a precise positioning system with a clear indoor covering is a highly prerequisite tool to enhance safety. It should be seamless, low, frugal, power efficacious, low cost and supply less meter-level accuracy.

Localization in radio frequency (RF) communication network could be divided into range-free and range-based techniques [89]. The most common range-free method is a radio signal strength indication (RSSI). The theoretical or experimental model of the signal propagation in this method is translated into position or distance estimations

[6], [7]. The range based methods are according to distances measurements between transceivers utilizing the time of arrival (TOA), time difference of arrival (TDOA) or tow way ranging time of flight (TWR-TOF) [8].

Of the aforementioned forms of RF technology, ultra wideband (UWB) signal is considered one of the most precise approaches because it can provide location estimates with centimeter-level accuracy [89]. It is widely used for ranging estimation and creating an indoor positioning system. In the indoor environment, the propagation channels could be divided into a line of sight (LOS) and nonline of sight (NLOS). Also, the NLOS could be divided into soft NLOS and hard NLOS depending on the attenuation of the radio signal. In the UWB signals, it is possible to transmit and detect very short pulses permitting for high accuracy of positioning because of the accurate calculation of signal delays. In an indoor environment, the propagation path length is not always a good indicator of the ranging between a sender and receiver. Thus, these systems are predominately bounded to the LOS conditions [25]. It precisely measures the distance in the LOS channel but suffers in the NLOS channel, and the error in distance measurements is significantly high [27] [86] which impacts the positioning accuracy.

In this chapter, we address the UWB indoor positioning in different environments and scenarios such as an emergency scenario using the AS algorithm.

Our approach helps to avoid installing all anchors in a proper way and just distribute them randomly to reduce the installation time, and the cost of using a high number of sensors and could be used to precisely locate a mobile station with an error ranges from 10 *cm* to 50 *cm* in any environments. It is implemented experimentally using UWB technology.

In this chapter, the contributions are as follow

- Obtaining of the MSE of the IPS when linearized LS is adopted as the trilateration solution.
- Development of an anchor selection (AS) strategy to mitigate the positioning error induced by the least accurate distance measurements.
- For using the MSE to evaluate the positioning accuracy of the two anchor group, addition of a virtual node to employ the linearized LS in the case where ambiguity is resolved by additional information.

In Section 6.2, the system model is presented. MSE computation in linearized LS is presented in section 6.3. Section 6.4 presents AS algorithm. Experimental and evaluation activities are presented in section 6.5. Section 6.6 presents results and discussion related to the experimental activities. Finally, section 6.7 offers a conclusion.

6.2 System model

In this chapter, some problems of UWB technology in indoor environments aforementioned in the introduction section likely solved. We create an IP system using MSE to online evaluate the accuracy of the positioning system of a mobile station created using different anchor groups (\hat{n} groups) installed in the environment then selecting the anchor group having better positioning accuracy to relocate the mobile station.

The proposed system consists of a number of wireless sensors created using UWB technology. It consists of n anchor nodes installed randomly and one mobile station moving around. Figure 6.1 depicts the proposed model when n anchor nodes in the network and only $\hat{n} < n$ optimum anchor node is selected to compute the mobile position (see section 6.4 for details). To fit with different situations and one of them is the emergency situation, we took into consideration some constraints may exist in such scenarios, such as the anchor nodes were randomly distributed to reduce the installation time. Also, the installation area should be narrow and not very suitable to distribute the anchor nodes in a proper way, and the mobile station has been restricted

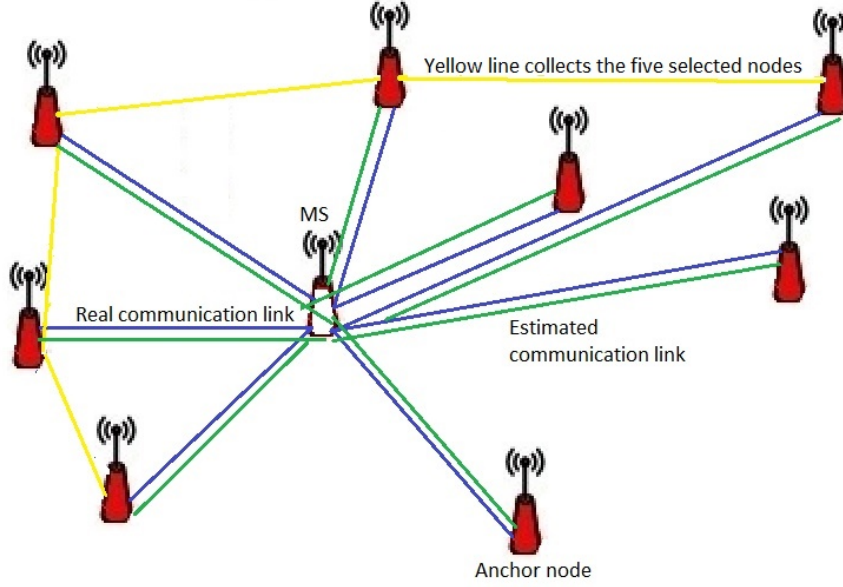


Figure 6.1: The system model that has n number of anchor nodes and one mobile station (should be in any direction in the plane). and distance measurements have different errors. The yellow line denotes the $\hat{n} = 2, 3, \dots < n$ selected anchor nodes.

to move through a harsh environment. Then, we use the linearized LS to locate the mobile station and evaluate the positioning accuracy by implementing the proposed MSE, and a proposed algorithm named AS is used to select the anchor group providing the best positioning accuracy and relocate the mobile with the selected group using the WLS method. The linearized LS and WLS are implemented to avoid the initial guess point and the iteration that should be used in the non-linear LS method, so the computation time of the mobile location is reduced. Also, the proposed MSE will be computed with less complexity in the linearized LS. Estimating a positioning node in two-dimensions acquires range information from at least three anchors. In this model and for simplicity, we provide an analysis of two dimensional localization. Let $h = [x; y]$ presents the mobile station position in Cartesian coordinates x and y . Also, $A_i = [x_i; y_i]$ denotes Anchor nodes positions. $i = 1, \dots, \hat{n}$ denotes the index of the anchor node and \hat{n} denotes the number of the entire optimum anchor nodes. Then, we can compute the Euclidean (real) distance (r) between h and A in a generic way as shown in Eq. 6.1.

$$r_i^2 = \|x_i - x\|^2 = (x_i - x)^2 + (y_i - y)^2 \quad (6.1)$$

A localization algorithm should be applied once the distances (r) to different anchor nodes are measured to calculate the position of the mobile node. The simplest and most common positioning algorithm that has been used for RSS-based localization is the hyperbolic positioning algorithm [20, 21]. As we explained above, r denotes the real distance and let denote the measured distance extracted from the sensor as \hat{r} then the error is computed as presented in Eq. 6.2.

$$\epsilon = \sum_{i=1}^n (r_i - \hat{r}_i) \quad (6.2)$$

The estimated position can be calculated as shown in Eq. 6.3. iteratively by implementing a straight gradient method for an example.

$$\hat{h} = \begin{bmatrix} \hat{x} \\ \hat{y} \end{bmatrix}_{k+1} = \begin{bmatrix} \hat{x} \\ \hat{y} \end{bmatrix}_k - \alpha \begin{bmatrix} \frac{\partial \epsilon}{\partial x} \\ \frac{\partial \epsilon}{\partial y} \end{bmatrix}_{x=\hat{x}_k, y=\hat{y}_k} \quad (6.3)$$

Where α is a scalar selected to minimize ϵ . Also, \hat{x} and \hat{y} the estimated coordinates of the MS.

In this method, an initial value of the position estimation is needed. To convert this nonlinear into a linear problem, the hyperbolic positioning algorithm is used by implementing least square method [62] as we presented in the next subsection.

6.2.1 LS linearization

To linearize the LS solution, one of the equations in the group of the equations in Eq. 6.1 is selected as a reference equation and subtract it from all other equations in the system. For simplicity, we state A_1 as a reference node having $x_1 = y_1 = 0$, so

$$r_1^2 = x^2 + y^2 \quad (6.4)$$

Then the linearization problem will be as in Eq. 6.5.

$$r_1^2 - r_i^2 = x^2 + y^2 - ((x_i - x)^2 + (y_i - y)^2) \quad (6.5)$$

Where, $i = 1, \dots, n$

By modifying Eq. 6.5, we obtain Eq. 6.6 as written below

$$x_i^2 + y_i^2 + r_1^2 - r_i^2 = 2xx_i + 2yy_i \quad (6.6)$$

Then converting Eq. 6.6 to matrix notation, we can obtain

$$A = \begin{bmatrix} 2x_2 & 2y_2 \\ 2x_3 & 2y_3 \\ \vdots & \vdots \\ 2x_n & 2y_n \end{bmatrix}$$

$$b = \begin{bmatrix} x_2^2 + y_2^2 + r_1^2 - r_2^2 \\ x_3^2 + y_3^2 + r_1^2 - r_3^2 \\ \vdots \\ x_n^2 + y_n^2 + r_1^2 - r_n^2 \end{bmatrix} = \begin{bmatrix} b_2 \\ b_3 \\ \vdots \\ b_n \end{bmatrix}$$

Where, r_1 denotes the real distance between the reference node and mobile station and r_i denotes the distance between the mobile station and all nodes except the reference.

Finally, the mobile station coordinates h will be computed as shown in Eq. 6.7.

$$h = \begin{bmatrix} x \\ y \end{bmatrix} = (A^T A)^{-1} A^T b \quad (6.7)$$

As mentioned in Eq. 6.7, at least three distance measurements will be needed to obtain a solution using the LS method. However, it is not always installing more anchor nodes in the network means that we obtain a good IP system. In some cases, we could have a better positioning system with only two anchor nodes as shown in figure 6.2. So, the

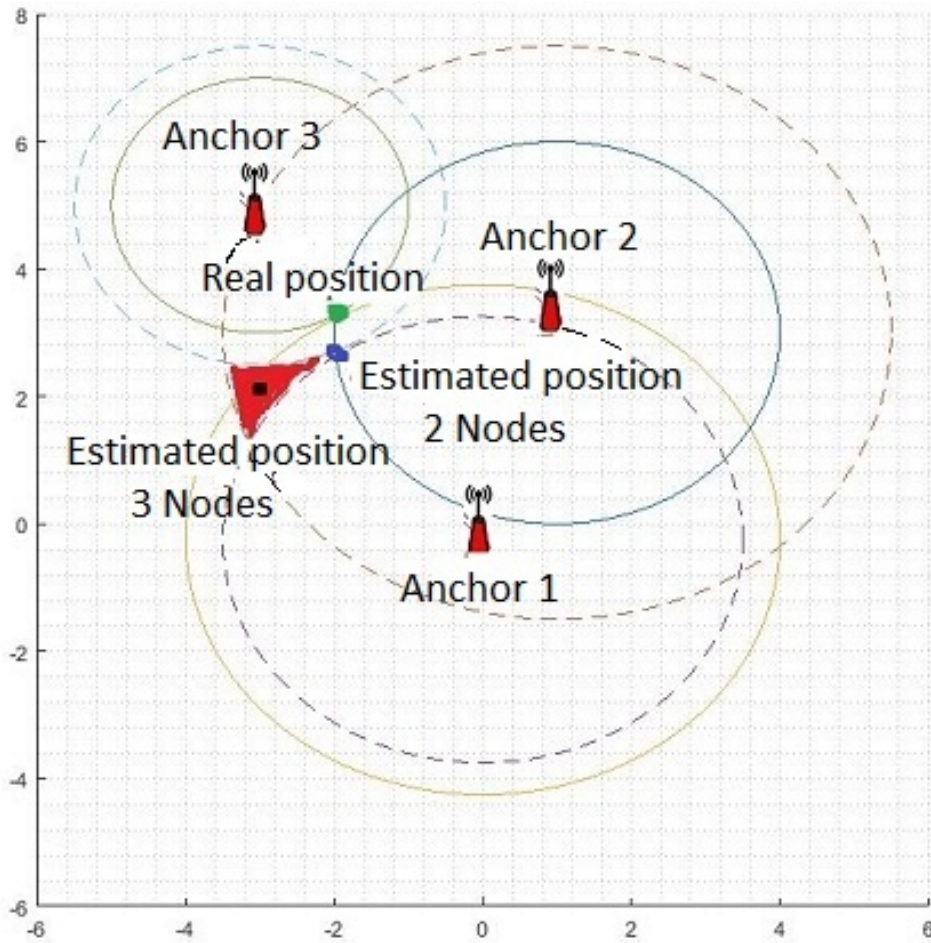


Figure 6.2: Two and three anchor nodes having different distance error to the mobile station when the localization system with two anchor nodes provides better accuracy.

solution presented in this work is to involve virtual anchor nodes in the LS method instead of the worst measured distance. With two anchor nodes, only two equations are available to guess the x and y coordinates. However, two equations provide two possible solutions and, if we know how to resolve the ambiguity by some extra information such as to locate the mobile position using three anchor nodes then replacing the node that provides worst distance estimation by the virtual distance so the LS could be used for unifying the MSE method for group two or more anchor nodes. The next subsection explains the virtual distance.

6.2.2 Virtual distance

As stated before, The two anchor nodes system could be in some states provide better positioning accuracy. Such a system also will be involved in the MSE and the AS

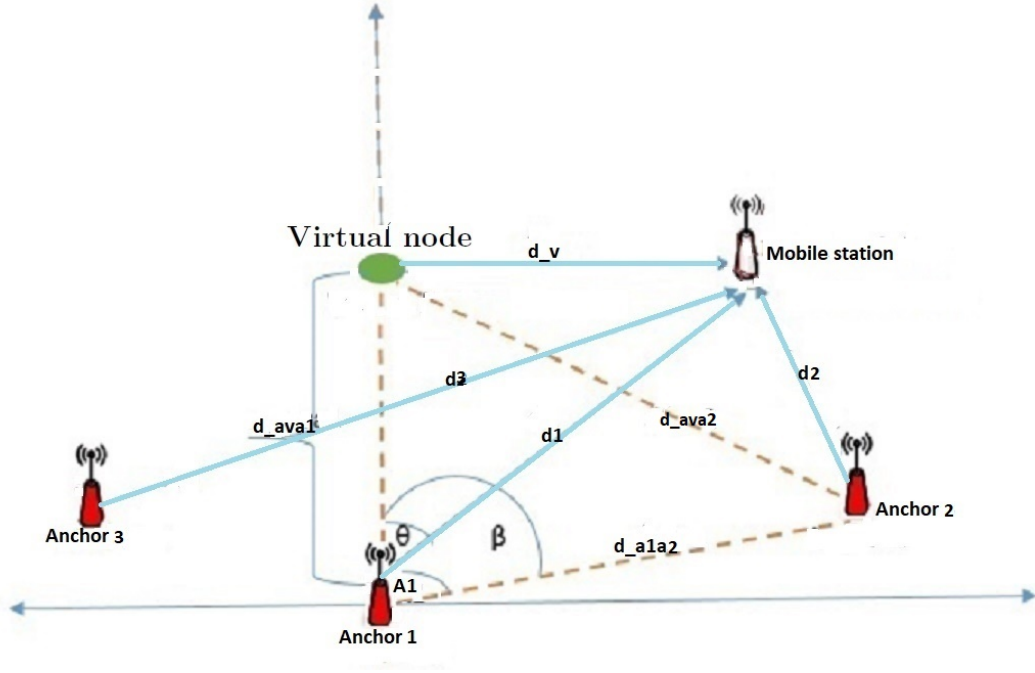


Figure 6.3: Virtual node and its distance to the mobile station.

algorithms using the virtual node. Thus, we can unify the proposed MSE to extend the selection of anchor node by also selecting two anchor nodes system. Figure. 6.3 depicts the creation of the virtual distance d_v and all variables mentioned in Eq. 6.8. The Virtual node could be fixed in any place in the space. Then, it is computed using the triangle rules as shown below.

$$d_v = \sqrt{d_1^2 + d_{ava1}^2 - 2d_1d_{ava1}\cos(\theta)} \quad (6.8)$$

Where, θ could be $\beta - A1$ or $\beta + A1$ according to the mobile station position located previously.

$$\beta = \cos^{-1}\left(\frac{d_{a1a2}^2 + d_{ava1}^2 - d_{ava2}^2}{2d_{a1a2}d_{ava1}}\right)$$

and

$$A1 = \cos^{-1}\left(\frac{d_{a1a2}^2 + d_1^2 - d_2^2}{2d_{a1a2}d_1}\right)$$

The next section presents the MSE derivation.

6.3 MSE computation in linearized LS

In this section, the MSE is achieved by the linearized LS solution explained in subsection 1 of section 6.2 when the true value of the mobile position is unknown.

In this work, the solution of LS method is considered for the best linear unbiased estimator (BLUE) when n anchor nodes distributed in an environment to locate a mobile station as aforementioned in the anchor selection section. The MSE could be written in a generic way as shown in Eq. 6.9

$$MSE = \mathbf{E} \left\{ \left\| \hat{h} - h \right\|^2 \right\} = \mathbf{E} \left\{ \hat{h}^T \hat{h} \right\} - 2\mathbf{E} \left\{ \hat{h}^T \right\} h + h^T h \quad (6.9)$$

Where h and \hat{h} denote the real and estimated position of the MS respectively. Also, Eq. 6.7 in section 6.2 can be split into two parts as shown below:

The first part of Eq. 6.7 $((A^T A)^{-1})$ is only deterministic data (the coordinates of the anchor nodes) and therefore, implementing matrix operation to it, we obtain a new matrix of 2 by 2 as shown below when we denoted it as V .

$$V = \begin{bmatrix} v_{11} & v_{12} \\ v_{21} & v_{22} \end{bmatrix}$$

where,

$$v_{11} = 0.25 \frac{(y_2^2 + y_3^2 + \dots y_n^2)}{(y_2^2 + y_3^2 + \dots y_n^2)(x_2^2 + x_3^2 + \dots x_n^2) - (x_2 y_2 + x_3 y_3 + \dots x_n y_n)^2}$$

$$v_{12} = -0.25 \frac{(x_2 y_2 + x_3 y_3 + \dots x_n y_n)}{(y_2^2 + y_3^2 + \dots y_n^2)(x_2^2 + x_3^2 + \dots x_n^2) - (x_2 y_2 + x_3 y_3 + \dots x_n y_n)^2}$$

$$v_{22} = 0.25 \frac{(x_2^2 + x_3^2 + \dots x_n^2)}{(y_2^2 + y_3^2 + \dots y_n^2)(x_2^2 + x_3^2 + \dots x_n^2) - (x_2 y_2 + x_3 y_3 + \dots x_n y_n)^2}$$

and $v_{21} = v_{12}$

Also implementing matrix operation to the second part of Eq. 6.7 ($A^T b$) will be

$$A^T b = \begin{bmatrix} \sum_{i=2}^n 2x_i b_i \\ \sum_{i=2}^n 2y_i b_i \end{bmatrix} \quad (6.10)$$

Where, $b_i = x_i^2 + y_i^2 + r_1^2 - r_i^2$

Then, the Eq. 6.7 in section 6.2 is rearranged to be

$$h = \begin{bmatrix} v_{11} \sum_{i=2}^n 2x_i b_i + v_{12} \sum_{i=2}^n 2y_i b_i \\ v_{21} \sum_{i=2}^n 2x_i b_i + v_{22} \sum_{i=2}^n 2y_i b_i \end{bmatrix} \quad (6.11)$$

To start solving Eq. 6.9, we solve each part of it individually then combine them. First and for simplicity, let us denote the first, second, and third part of it as:

$$p1 = \mathbf{E}\{\hat{h}^T \hat{h}\}$$

$$p2 = \mathbf{E}\{\hat{h}^T\} h$$

$$p3 = h^T h$$

So, Eq 6.9. could be rewritten as

$$MSE = p1 - 2p2 + p3 \quad (6.12)$$

So, we solve every part of Eq. 6.12 separately then collect them to obtain the final

mathematical expression of the derived MSE. First, we start with $p3$,

$$p3 = \left[v_{11} \sum_{i=2}^n 2x_i b_i + v_{12} \sum_{i=2}^n 2y_i b_i \right]^2 + \left[v_{21} \sum_{i=2}^n 2x_i b_i + v_{22} \sum_{i=2}^n 2y_i b_i \right]^2$$

Furthermore, only the first part of $p3$ is solved because the second part is similar and the difference is only with v values which is constant. The first and second part of it are denoted by $p3_1$ and $p3_2$ respectively and starting to solve $p3_1$

$$p3_1 = v_{11}^2 \left[\sum_{i=2}^n 2x_i b_i \right]^2 + 2v_{11}v_{12} \sum_{i=2}^n 2x_i b_i \sum_{i=2}^n 2y_i b_i + v_{12}^2 \left[\sum_{i=2}^n 2y_i b_i \right]^2$$

Second, the other parts ($p1$ and $p2$) in Eq. 6.12 are computed. So, b should be changed to \hat{b} .

$$\hat{b} = \begin{bmatrix} x_2^2 + y_2^2 + \hat{d}_1^2 - \hat{d}_2^2 \\ x_3^2 + y_3^2 + \hat{d}_1^2 - \hat{d}_3^2 \\ \vdots \\ x_n^2 + y_n^2 + \hat{d}_1^2 - \hat{d}_n^2 \end{bmatrix}$$

Where, $\hat{b}_i = x_i^2 + y_i^2 + \hat{d}_1^2 - \hat{d}_i^2$,

$$\hat{d}_1 = r_1 + e_1 \rightarrow \hat{d}_1^2 = r_1^2 + 2e_1r_1 + e_1^2$$

and, $\hat{d}_i = r_i + e_i \rightarrow \hat{d}_i^2 = r_i^2 + 2e_i r_i + e_i^2$ Then substituting \hat{d}_1^2 and \hat{d}_i^2 in \hat{b} , to

obtain

$$\hat{b} = \begin{bmatrix} x_2^2 + y_2^2 + r_1^2 + 2e_1r_1 + e_1^2 - r_2^2 + 2e_2r_2 - e_2^2 \\ x_3^2 + y_3^2 + r_1^2 + 2e_1r_1 + e_1^2 - r_3^2 + 2e_3r_3 - e_3^2 \\ \vdots \\ x_n^2 + y_n^2 + r_1^2 + 2e_1r_1 + e_1^2 - r_n^2 + 2e_nr_n + e_n^2 \end{bmatrix}$$

Now, let denote

$\bar{\mathbf{b}}_i = e_1^2 - e_i^2 + 2r_1e_1 + 2r_ie_i$. Then, the expectation value of $\hat{\mathbf{b}}$ is written as

$$\mathbf{E}\{\hat{\mathbf{b}}\} = \mathbf{E}\left\{\begin{bmatrix} b_2 + \bar{\mathbf{b}}_2 \\ b_3 + \bar{\mathbf{b}}_3 \\ \vdots \\ b_n + \bar{\mathbf{b}}_n \end{bmatrix}\right\}$$

In Eq. 6.12, the difference between $p1$ and $p3$ is only the notation of the expectation value which is expressed in $p1$. Thus, solving $p1$ will be in the same way of solving $p3$ with taking into account the expectation notation. Also, we denote the first part of $p1$ as $p1_1$ and the second part $p1_2$. For the similarity in $p1_1$ and $p1_2$, we solve only $p1_1$.

$$\begin{aligned} p1_1 &= v_{11}^2 \mathbf{E}\left\{\left[\sum_{i=2}^n 2x_i(b_i + \bar{\mathbf{b}}_i)\right]^2\right\} \\ &+ 2v_{11}v_{12} \mathbf{E}\left\{\sum_{i=2}^n 2x_i(b_i + \bar{\mathbf{b}}_i) \sum_{i=2}^n 2y_i(b_i + \bar{\mathbf{b}}_i)\right\} \\ &+ v_{12}^2 \mathbf{E}\left\{\left[\sum_{i=2}^n 2y_i(b_i + \bar{\mathbf{b}}_i)\right]^2\right\} \end{aligned}$$

Now, we analyze

$$v_{11}^2 \mathbf{E}\left\{\left[\sum_{i=2}^n 2x_i(b_i + \bar{\mathbf{b}}_i)\right]^2\right\}$$

to obtain

$$\begin{aligned} v_{11}^2 \mathbf{E}\left\{\left[\sum_{i=2}^n 2x_i(b_i + \bar{\mathbf{b}}_i)\right]^2\right\} &= v_{11}^2 \left[\sum_{i=2}^n 2x_i b_i\right]^2 \\ &+ 2v_{11}^2 \sum_{i=2}^n x_i b_i \mathbf{E}\left\{\sum_{i=2}^n 2x_i \bar{\mathbf{b}}_i\right\} \\ &+ v_{11}^2 \mathbf{E}\left\{\left[\sum_{i=2}^n 2x_i \bar{\mathbf{b}}_i\right]^2\right\} \end{aligned}$$

Also, by the same way, we obtain

$$\begin{aligned} v_{12}^2 \mathbf{E} \left\{ \left[\sum_{i=2}^n 2y_i(b_i + \bar{\mathbf{b}}_i) \right]^2 \right\} &= v_{12}^2 \left[\sum_{i=2}^n 2y_i b_i \right]^2 \\ &+ 2v_{12}^2 \sum_{i=2}^n 2y_i b_i \mathbf{E} \left\{ \sum_{i=2}^n 2y_i \bar{\mathbf{b}}_i \right\} \\ &+ V_{12}^2 \mathbf{E} \left\{ \left[\sum_{i=2}^n 2y_i \bar{\mathbf{b}}_i \right]^2 \right\} \end{aligned}$$

The last part needed to analyze is

$$\begin{aligned} &2v_{11}v_{12} \mathbf{E} \left\{ \sum_{i=2}^n 2x_i(b_i + \bar{\mathbf{b}}_i) \sum_{i=2}^n 2y_i(b_i + \bar{\mathbf{b}}_i) \right\} = \\ &2v_{11}v_{12} \sum_{i=2}^n 2x_i b_i \sum_{i=2}^n 2y_i b_i + 2v_{11}v_{12} \mathbf{E} \left\{ \sum_{i=2}^n 2x_i b_i \sum_{i=2}^n 2y_i \bar{\mathbf{b}}_i \right\} \\ &+ 2v_{11}v_{12} \mathbf{E} \left\{ \sum_{i=2}^n 2y_i b_i \sum_{i=2}^n 2x_i \bar{\mathbf{b}}_i \right\} \\ &+ 2v_{11}v_{12} \mathbf{E} \left\{ \sum_{i=2}^n 2x_i \bar{\mathbf{b}}_i \sum_{i=2}^n 2y_i \bar{\mathbf{b}}_i \right\} \end{aligned}$$

Then using the same way, we can find p_{32} and p_{12} and compute

$$p_{32} + p_{31} = p_3$$

$$p_{12} + p_{11} = p_1$$

Finally, compute the last part of Eq. 6.12, p_2 and split it into two parts which will be denoted p_{21} and p_{22} respectively, also, we can compute one of them. We are

computing $p2_1$.

$$\begin{aligned}
p2_1 = & v_{11}^2 \left[\sum_{i=2}^n 2x_i b_i \right]^2 + v_{11}^2 \mathbf{E} \left\{ \sum_{i=2}^n 2x_i b_i \sum_{i=2}^n 2x_i \bar{b}_i \right\} \\
& + 2v_{11}v_{12} \sum_{i=2}^n 2x_i b_i \sum_{i=2}^n 2y_i b_i \\
& + v_{11}v_{12} \mathbf{E} \left\{ \sum_{i=2}^n 2y_i b_i \sum_{i=2}^n 2x_i \bar{b}_i \right\} \\
& + v_{11}v_{12} \mathbf{E} \left\{ \sum_{i=2}^n 2x_i \bar{b}_i \sum_{i=2}^n 2y_i \bar{b}_i \right\} \\
& + v_{12}^2 \left[\sum_{i=2}^n 2y_i b_i \right]^2 + v_{12}^2 \mathbf{E} \left\{ \sum_{i=2}^n 2y_i b_i \sum_{i=2}^n 2y_i \bar{b}_i \right\}
\end{aligned}$$

After solving the $p2_2$, we will have

$$p2_2 + p2_1 = p2$$

Then, The performance in terms of MSE achieved (Eq. 6.13) is

$$MSE = \begin{bmatrix} v_{11}^2 + v_{21}^2 \\ v_{12}^2 + v_{22}^2 \\ 2v_{11}v_{12} + 2v_{21}v_{22} \end{bmatrix}^T \begin{bmatrix} \mathbf{E} \left\{ \left[\sum_{i=2}^n 2x_i \bar{b}_i \right]^2 \right\} \\ \mathbf{E} \left\{ \left[\sum_{i=2}^n 2y_i \bar{b}_i \right]^2 \right\} \\ \mathbf{E} \left\{ \sum_{i=2}^n 2x_i \bar{b}_i \sum_{i=2}^n 2y_i \bar{b}_i \right\} \end{bmatrix} \quad (6.13)$$

To implement the proposed MSE method, we should clarify that the only input variable of the MSE function is the real distance (r). But, in a real experiment when we don't have it, we implement a proper NLOS identification and mitigation method created by [86]. In addition to the aforementioned method of NLOS identification, we created a database as shown in table 6.1 to estimate the average distance error in hard and soft NLOS and LOS propagation channels to enhance the measured distance as

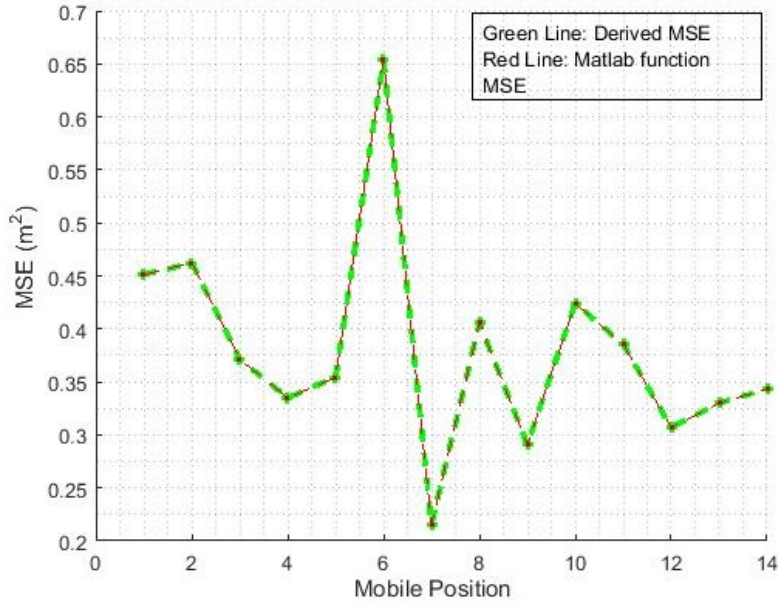


Figure 6.4: Values of the proposed MSE and matlab functions.

shown in Eq. 6.14 below.

$$\acute{r} = \hat{r} - \varepsilon(e) \simeq r \quad (6.14)$$

Where, \acute{r} , \hat{r} , $\varepsilon(e)$, and r denote the approximated real distance, measured distance, the average distance error, and the real distance respectively. So, the approximated real distance (\acute{r}) is used in the MSE method instead of the real distance (r) and also used in all positioning methods used in this work.

6.4 Anchor selection (AS)

The proposed IP system which is an online selection of a group of two anchor nodes or more up to \hat{n} anchor nodes using MSE evaluation method is explained below.

For a generic scenario of IP system dealing with UWB signal, we may install n nodes in the WSN and we could select $\hat{n} < n$ using the RSL. In this work, we consider a real environment with 6 UWB sensors covering an area of 9 m^2 : one sensor as a tag and the remaining five sensors installed as anchor nodes. According to our experience, positioning accuracy is not significantly improved when a large number of anchor nodes

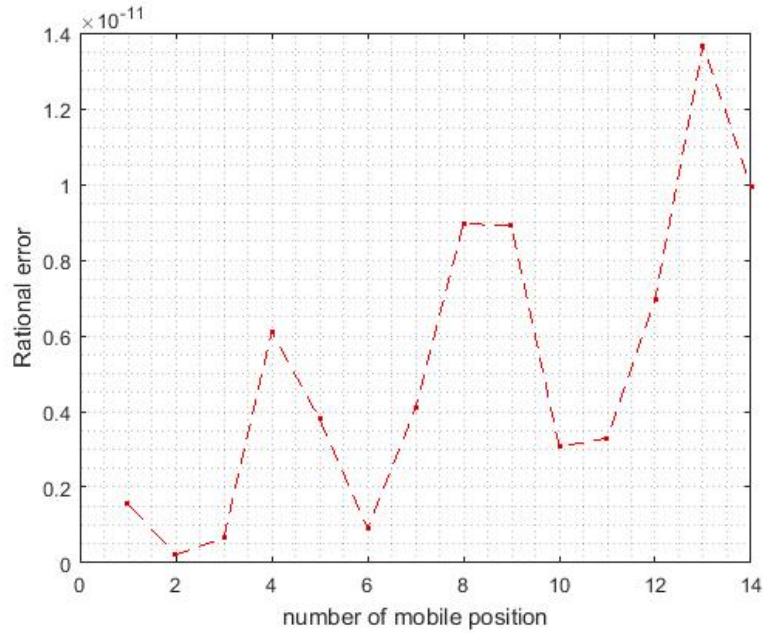


Figure 6.5: Rational error between the derived and matlab MSE functions.

is available and usually 4 to 6 anchor nodes provides a good compromise. Then, the 5 nodes are clustered into different groups according to the combination algorithm. So the total number of groups $= \binom{\hat{n}}{2} + \binom{\hat{n}}{3} + \dots + \binom{\hat{n}}{\hat{n}}$.

Where, n and \hat{n} are the total number of the anchor nodes installed in the entire network and the total number of selected anchors (in this work $\hat{n} = 5$) installed to build the positioning system.

The RSL is extracted from the UWB device (DW 1000 - EVK 1000) used in this work. It indicates the level of the received signal power provided by an anchor node [30]. It is chosen in this work as criteria to select the optimum anchor nodes (\hat{n}) selected for the combination process. The total number of the anchor nodes used in this work (5 anchor nodes) is not large, and it is not so important, and therefore it does not depend on how large the network (n anchor nodes).

Also, every group should have a reference node. We locate the mobile station using the conventional LS method then evaluate the positioning accuracy of each group of anchor nodes using the derived MSE and select the group having less MSE and remov-

ing all other anchor groups from the positioning system to relocate the mobile station using WLS algorithm. The algorithm 1 depicts the steps of the proposed algorithm.

The next section provides the experimental results of the LS, WLS, and MLSI (before anchor selection), and AS localization algorithms.

Algorithm 2 Anchor Selection (AS)

```

1: procedure ANCHOR GROUP ▷ Create different anchor node groups
2:    $\hat{n} \leftarrow n$  ▷ The total anchor nodes
3:   for  $i = 2$  to  $\hat{n}$  do
4:     Anchor group =  $\binom{\hat{n}}{i}$ 
5:      $m = \sum_i \binom{\hat{n}}{i}$  ▷ the total anchor groups
6:   end for
7: end procedure
1: procedure LS ▷ Locate the mobile station

```

$$\hat{h} = (A^T A)^{-1} A^T \hat{b}$$

```

2: end procedure
1: procedure MSE ▷ Compute MSE for each group
2:   for  $i = 1$  to  $m$  do

```

$$MSE = \mathbf{E} \left\{ \left\| h(\hat{i}) - h(i) \right\|^2 \right\}$$

```

3:   end for
4: end procedure
1: procedure AS ▷ Select the group having minimum MSE
2:   for  $i = 1$  to  $m$  do

```

$$MSE = \mathbf{min} \left\{ MSE(i) \right\}$$

```

3:   end for
4: end procedure
1: procedure WLS
  ▷ Compute the variance of the estimated distance
  ▷ Relocate the Mobile station

```

$$\hat{h} = (A^T W^{-1} A)^{-1} A^T W^{-1} \hat{b}$$

```

2: end procedure

```

6.5 Experimental and evaluation activities

In this section, we provide experimental results obtained with a commercial UWB device (DW 1000 - EVK 1000). The DW 1000 is a fully integrated low-power, multi-channel single-chip CMOS radio transceiver that meets the IEEE 802.15.4-2011 UWB standard [73].

Before starting with the experimental activities, we start with the evaluation process of the derived MSE and an overview of the WLS and MLSI methods as explained in the next items.

6.5.1 Evaluation of the derived MSE and an overview of WLS, MLSI, and GDOP

The items below explain the process of the evaluation method used for evaluating the derived MSE and provides an overview of the WLS and MSLI methods used to be compared with the proposed IP system (AS).

- ***Evaluation of the derived MSE***

After computing the MSE, it is compared with MSE Matlab function using a rational error as shown in Eq. 6.15 to ensure the accuracy of the mathematical derivation. Figures 6.4 and 6.5 show the value of the derived MSE compared to MSE Matlab function of a mobile positioning for 14 different mobile positions and the rational error between them respectively.

$$E = \frac{MSE_{dir} - MSE}{MSE} 100\% \quad (6.15)$$

Where, E , MSE_{dir} , and MSE denote the rational error, proposed MSE, and MSE of matlab function respectively.

- ***Weighted least square (WLS).***

To validate the anchor selection system model, it is compared to the conventional LS and also, to the WLS and MLSI algorithms created by [62] and [58] respectively. A short overview of the WLS and MLSI algorithms is presented below.

The liner equation in Eq. 6.7 could be solved implementing a weighted least-square estimator as shown in Eq.16 below. The weights implemented in the WLS algorithm is adjusted taking into account the inverse of the variance of the corresponding distance measurements [62]. The DW 1000 (EVK 1000) device provides 8 distance measurements per second and therefore, we calculate and update the variance every one second and calculate the matrix of it (W) which is the covariance matrix of vector \hat{b} as aforementioned below, then using the inverse of it in the final equation of the WLS as shown in Eq. 6.16.

$$W = \begin{bmatrix} var(\hat{r}_1^2) + var(r_2^2) & var(\hat{r}_1^2)... & var(r_1^2) \\ var(\hat{r}_1^2) & var(\hat{r}_1^2) + var(r_3^2)... & var(r_1^2) \\ \vdots & \vdots & \vdots \\ var(\hat{r}_1^2) & var(\hat{r}_1^2)... & var(r_1^2) + var(r_n^2) \end{bmatrix}$$

Where, $var(\hat{r}_1^2)$ denotes the variance of a squared estimated distance between the reference node and mobile station, and $var(\hat{r}_i^2)$ denotes variance of a squared estimated distance between all other nodes and the mobile station.

$$\hat{b} = \begin{bmatrix} x_2^2 + y_2^2 + r_1^2 - r_2^2 \\ x_3^2 + y_3^2 + r_1^2 - r_3^2 \\ \vdots \\ x_n^2 + y_n^2 + r_1^2 - r_n^2 \end{bmatrix}$$

$$\hat{h} = \begin{bmatrix} \hat{x} \\ \hat{y} \end{bmatrix} = (A^T W^{-1} A)^{-1} A^T W^{-1} \hat{b} \quad (6.16)$$

Presuming that the distance measurements \hat{b}_i to different nodes are independent and x_i and y_i are constant.

- **Modified least square iteration (MLSI) method.**

The MLSI method has the same mathematical expression of the conventional LS (Eq. 6.7) with modifying the distance vector (\hat{b}) by involving the average distance error to it as shown below.

First, let $\varepsilon(e_1)$ and $\varepsilon(e_i)$ denote the average distance error between the MS and the reference node and the average distance error between the MS and the rest of the entire anchor nodes respectively where $i = 2, \dots, n =$ Then:

$$\hat{b}_i = x_i^2 + y_i^2 + r_1'^2 - r_i'^2 + \varepsilon(e_1) - \varepsilon(e_i)$$

Or

$$\hat{b} = \begin{bmatrix} x_2^2 + y_2^2 + r_1'^2 - r_2'^2 + \varepsilon(e_1) - \varepsilon(e_2) \\ x_3^2 + y_3^2 + r_1'^2 - r_3'^2 + \varepsilon(e_1) - \varepsilon(e_3) \\ \vdots \\ x_n^2 + y_n^2 + r_1'^2 - r_n'^2 + \varepsilon(e_1) - \varepsilon(e_n) \end{bmatrix}$$

- **Geometric dilution of precision(GDOP)**

Geometric dilution of precision (GDOP) has been widely implemented as an accuracy metric for tracking and navigation systems. while high accuracy in a localization system needs both precise measurement of the range and a good geometric relationship between the mobile device and the measuring points (anchor nodes), the analysis of GDOP is an essential feature in determining the performance of a positioning system. due to our interest in IPS, we should address



Figure 6.6: The real environment.

some drawbacks that impact the indoor positioning accuracy. First, we should address that IPS usually have irregular propagation models and barriers that complicate deployment, making it defy to specify a metric to readily compare anchor configuration. GDOP is a unit-less quantity which is a function of the geometry between the target and the beacons, often utilized to estimate the expected accuracy of GPS due to the location of satellites [90]. GDOP has three main drawbacks when utilized as a metric for assessing indoor accuracy.

First, Some circumstances cause the standard GDOP metric to expand towards infinity which makes it difficult to normalize over multiple competing configurations [95].

Second, For a terrestrial system, if the location and number of base stations in the desired coverage area are not neatly planned, the GDOP effect can become the dominant factor in limiting the performance of a system [91].

Third, theoretically, the more the nodes involved in the calculation, the lower the GDOP value of the combination will be, which represents a higher positioning accuracy. Also, In the traditional GDOP-based nodes selection algorithm, n nodes will be selected from m anchor nodes, and therefore in order to select a subset which has the smallest GDOP, matrix multiplication and inversion should

be executed for a combination of m to n times [60].

In this chapter, we present an example of GDOP which is presented in [61], where it is assumed that there is no mobile target but all anchor nodes will act as mobile units. In that work, 36 nodes are considered and a positioning accuracy around a half meter is obtained. Also, we compared our algorithm to [61] algorithm as explained in the result and discussion section. below, we present the mathematical expression of the algorithm created by [61].

$$GDOP_{total} = \frac{2}{\sqrt{N_R}} \frac{\sigma_{\Delta_r, total}}{\sigma_r}$$

Where, N_R , Δ_r , and $\sigma_{r, total}$ denote total number of the anchor nodes, ranging error, and variance of the range respectively.

$$\sigma_{r, total} = \sqrt{1 + \left(\frac{2}{N_R} + \frac{6}{N_R^2} \right) \times (\sigma_r^2 + \sigma_B^2)}$$

$$\sigma_B = \frac{\lambda}{R_{max}} \sqrt{\frac{N_R \times (N_R + 3)}{N_R^2 + 2 \times N_R + 6}}$$

Where, σ_B is the quasi-STD associated with the range bias error.

Table 6.1 presents the values of the parameters aforementioned above used by [61].

6.5.2 Experimental activities

In this part of the work, different scenarios are created to examine the proposed method used for a moving target in different directions and distances to the installed anchor nodes. We randomly installed the anchor nodes as shown in figure 6.7 inside a narrow squared area of 9 m side within the total moving area of 16 m width and 25 m length. Figure 6.8 presents scenario 1 for a trajectory of the mobile station created using the AS, MLSI, and WLS algorithms. Figure 6.10 presents scenario 2 for a different trajectory created by the AS, WLS, and LS. The AS algorithm with a suitable anchor

Table 6.1: Example of Computed Values Based on Theoretical Expressions [61]

Parameter	Value	Comments
σ_r	2 m	Random STD, typical for indoor system
λ	0.1	Bias parameter, typical for indoor system
R_{max}	30 m	Assumed maximum radio range
N_R	12	Expected nodes in range
σ_B	0.72 m	Effective bias error STD

group for every point in the trajectory. The MLSI with the four and five anchor nodes group. The WLS and LS algorithms with the group of five anchor nodes for the entire trajectory. The coordinates of the anchor nodes in the two different scenarios as follows:

Scenario 1 : $A_1 = (0; 0)$, $A_2 = (1;7.8)$, $A_3 = (2;7.8)$, $A_4 = (2.6; 1.4)$, and $A_5 = (3;1.6)$ as shown in figure 6.8.

Scenario 2 : $A_1 = (0; 0)$, $A_2 = (2;4.8)$, $A_3 = (4;4.8)$, $A_4 = (7.6; 4.4)$, and $A_5 = (3;1.6)$. as shown in figure 6.10.

Where A_i denotes the anchor node in the network.

The estimated distances between anchor nodes and the mobile station are extracted from the EVK 1000 device. To build the proposed IP system by implementing the AS method, we implemented a proper NLOS identification method [86] and created table 6.1 to estimate the average distance bias. Then, Eq. 6.14 is used to obtain the approximated real distance for the proposed MSE to evaluate the positioning accuracy of different groups of anchor nodes (including the virtual nodes group), and select the group having the less MSE, then relocated the mobile station with the selected group using the WLS method. In this work, the distance measurement is extracted from the EVK 1000. It is a transceiver sensor uses two-way time of flight to compute the distance between two transceivers, and it is a Bias estimator in a LOS environment

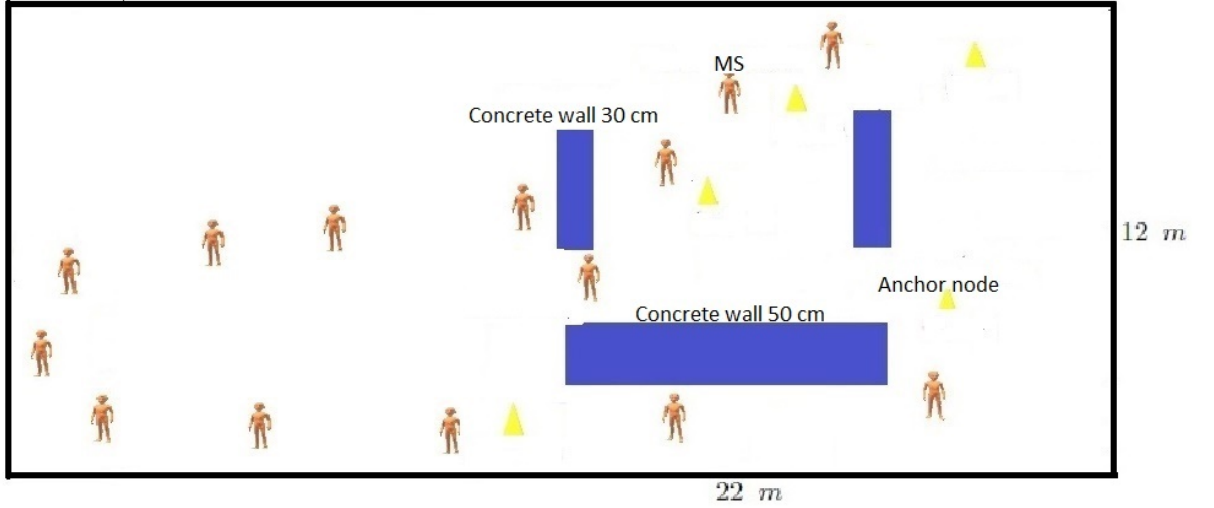


Figure 6.7: Simulation of the moving target in real environment (one of different scenarios) that will be located using different distance measurement affect by different walls.

according to [88, 92, 93] so we should overcome this issue to cope with the proposed linear MSE method. So, we applied an algorithm presented by [94] to modify the EVK 1000 having the BLUE specifications in a LOS environment. This algorithm is to place two EVKs 1000 with 8 m apart in between inside a LOS environment and take at least 400 times of distance measurements then compute the average error between the true and estimated values then apply Eq. 6.17 below to obtain a new estimated distance by reprogramming EVK 1000, and Table I shows that modified EVK 1000 is a BLUE estimator.

$$e_{av} = d_{real} - d_{est}$$

$$d_{new} = d_{est} + e_{av} \quad (6.17)$$

Where, the d_{real} , d_{new} , d_{est} , e_{av} , are the real distance, new estimated distance, average of old estimated distance, and the average of the computed error experimentally for 8 m distance. The transceivers were randomly distributed in the environment presented in fig. 6.6 as shown in fig. 6.7.

In [86], we estimated the error of a measured distance of a walking human in an indoor environment having different channel types (LOS, soft NLO, and hard NLOS)

using UWB technology (DW1000, EVK 1000). The estimated error of the distance from 2 m to 26 m ranges between 0.3 m to 1.8 m depends on the traveled distance and number of walls that may affect the measured distance.

In the work presented in this chapter, we restricted the mobile station to move through one and two concert walls 30 cm width each (soft and hard NLOS channels) and through LOS channel using channel 2 mode 2 of DW 1000 (EVK 1000) [74, 86]. Also, in [86], the ch 2 mode 2 of EVK 1000 was experimentally validated for obtaining ranging measurements.

To place a wireless sensor in a network, an area should be taken into consideration called a Fresnel zone (FZ) around the visual line of sight that radio waves spread out into after they leave the antenna [27]. The FZ must be clear to avoid the weak in the signal strength level.

Then, we measured the distances and computed the related average error to eliminate the bias in the distance and compute the approximated real distance used in the MSE evaluation method.

The ranging measurements are used in different environments (LOS, soft NLOS, and hard NLOS) for distance ranges from 2 m to 20 m. Table I presents the information used for the AS algorithm extracted from the modified EVK 1000.

6.6 Results and discussion

In the experimental activity, Different Mobile station trajectories have been created to measure the estimated distance having different distance errors then the average and variance of it used for the AS and WLS algorithms are computed.

As mentioned before, we assume a proper NLOS identification method is used to

Table 6.2: Distance measurement where, r, \hat{r} , and Var denote the real, estimated, and variance of distance respectively for LOS, soft NLOS, and hard NLOS channels and Av denotes the average of the distance Bias

$r(m)$	LOS			HNLOS			SNLOS		
	$\hat{r}(m)$	Bias (m)	Var (m^2)	$\hat{r}(m)$	Bias (m)	Var (m^2)	$\hat{r}(m)$	Bias (m)	Var (m^2)
2	2.09	0.09	0.00	—	—	—	—	—	—
4	4.09	0.09	0.00	—	—	—	4.20	0.16	0.06
6	6.02	0.02	0.01	—	—	—	6.3	0.26	0.10
8	8.05	0.05	0.08	9.33	1.33	0.01	8.28	0.27	0.07
10	10.06	0.06	0.00	10.74	0.74	0.08	10.12	0.12	0.11
12	12.000	0.00	0.01	12.59	0.59	0.07	12.10	0.10	0.04
14	14.00	-0.06	0.00	15.00	1.00	0.09	14.505	0.51	0.07
16	16.05	0.05	0.00	16.95	0.95	0.05	16.36	0.36	0.06
18	18.02	0.02	0.00	18.47	0.47	0.12	18.24	0.244	0.10
20	20.07	0.07	0.00	20.70	0.70	0.14	20.50	0.50	0.12
Av Bias	—	0.052	—	—	0.822	—	—	0.279	—

extract the average distance bias as shown in Table I used to enhance the approximated distance computed in Eq. 6.14 to compute the proposed MSE to evaluate the LS method. For special cases in the NLOS propagation channels, It is observed; when placing a transceiver opposite to a wall with distance less than 1.3 m , the distance error increased abnormally to approximately 1 m . This abnormal increment in distance error is due to the high attenuation of the UWB signal when placing or moving the sensors close to a wall. This problem should be taken into consideration when using an NLOS identification and mitigation method.

In this chapter, the results plot trajectories of the mobile node but, at every point in the trajectory, the position is computed without taking into account node dynamics. Only, the last known position is used to obtain the estimated distances to the anchors in order to feed the anchor selection algorithm. The AS is compared to the LS, WLS, MLSI, and GDOP methods as shown in figure 6.9 which presents the empirical cumulative distribution function (ECDF) of the trajectory presented in scenario 1 (figure 6.8), and figure 6.11 presents the same information provided in figure 6.9 but for the

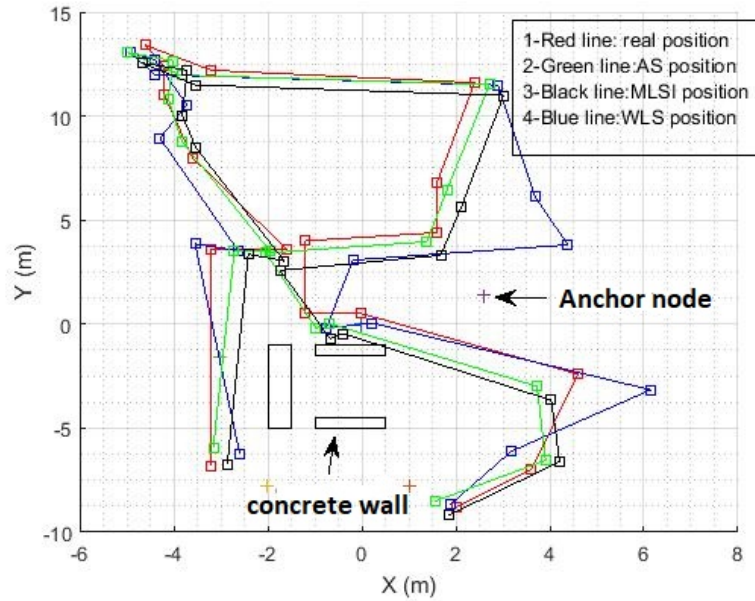


Figure 6.8: Scenario 1: simulation of the moving target in real environment (one of different scenarios) affected by different walls and will be located using AS, MLSI, and WLS localization algorithm.

scenario 2 (figure 6.10). As we mentioned in the title of figure 6.7, The AS is implemented for different groups of anchor nodes according to the proposed MSE method and therefore, the points may be located by 2,3,... \hat{n} anchor nodes. But, the WLS and LS methods are implanted with \hat{n} anchor nodes. Also, the MLSI and GDOP methods are implemented with \hat{n} anchor nodes (in this work $\hat{n} = 5$ nodes).

Finally, some accuracy results are provided to have a reference about performance obtained with GDOP. For instance, the best positioning accuracy obtained in [60] is around 1 m when 10 anchor nodes are involved in the system. Another example of GDOP is presented in [61], where it is assumed that there is no mobile target but all anchor nodes will act as mobile units. In that work, 36 nodes are considered and a positioning accuracy around a half meter is obtained. For the sake of comparison, we also include results corresponding to the GDOP strategy proposed in [61] in Fig. 6.9. In particular, this figure presents the ECDF of MSE of MLSI, WLS, AS, and GDOP and shows how the technique derived in this work outperforms the other methods.

The result of figures 6.9 and 6.11 experimentally show that the proposed method

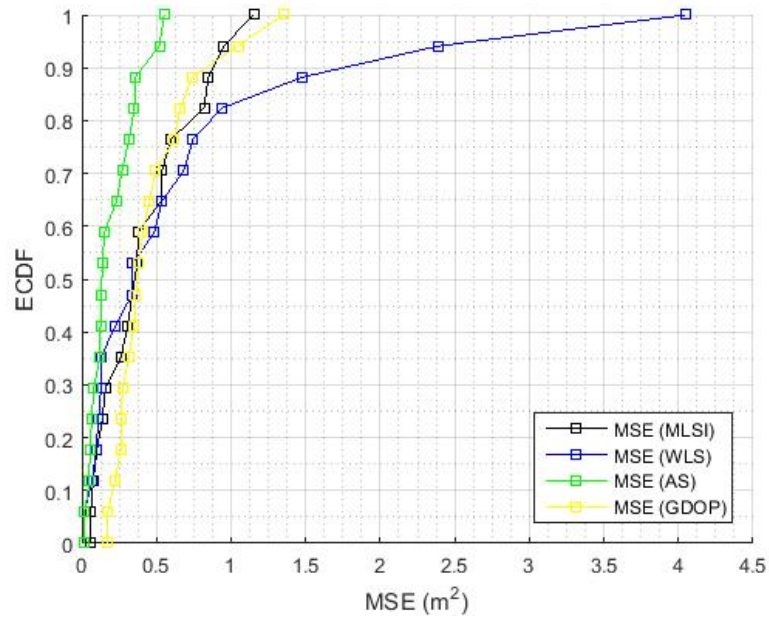


Figure 6.9: Empirical distributed function (ECDF) of AS, MLSI, WLS, and GDOP methods in scenario 1.

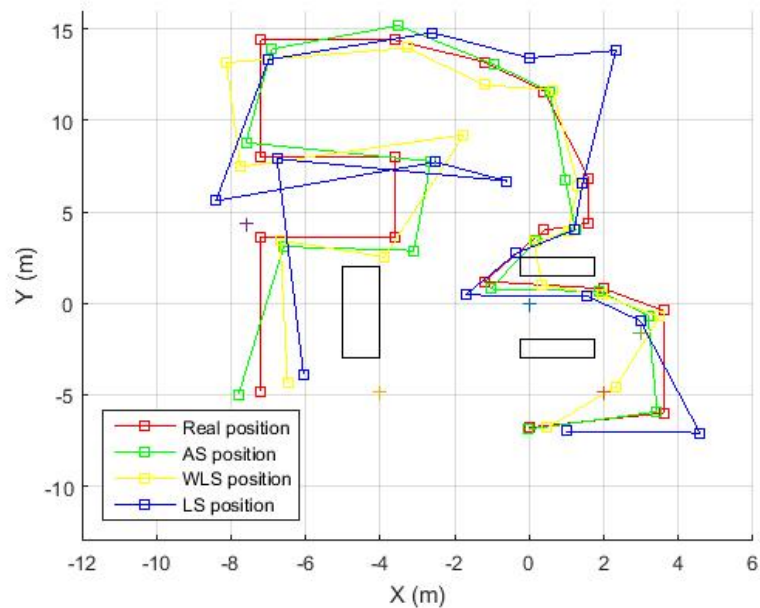


Figure 6.10: Scenario 2: simulation of the moving target in real environment (one of different scenarios) affected by different walls and will be located using AS, WLS, and LS localization algorithm.

significantly improves the localization accuracy, reducing the estimation error between 60 % and 95 % on average, compared with the existing approaches. The results presented in this section clearly show how the AS method is confident in different indoor scenarios including emergency.

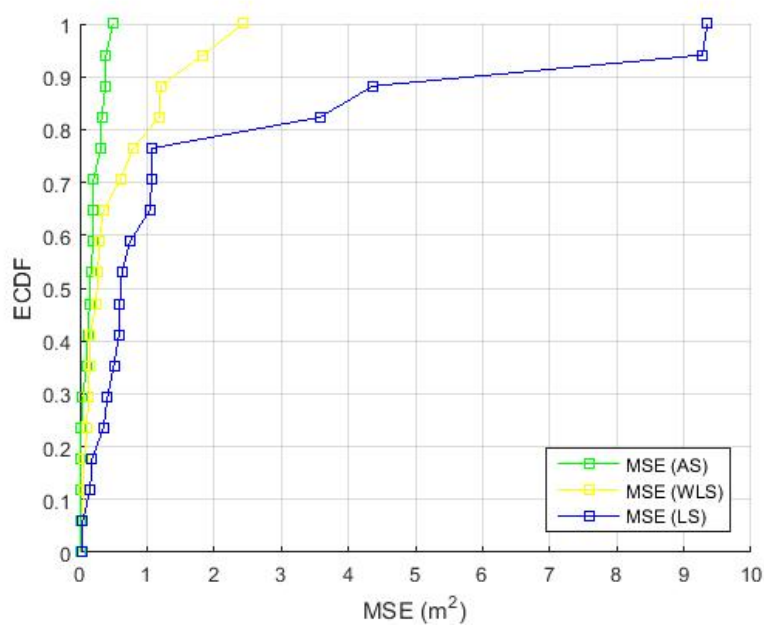


Figure 6.11: Empirical distributed function (ECDF) of AS, WLS, and LS methods in scenario 2.

6.7 Conclusion

The cost in term of installation time and the number of wireless sensors in an indoor environment and precisely locate a moving target are the goals in this chapter. To obtain this goal, we present a novel algorithm of three steps: i- create online an MSE using the linearized LS to dynamically evaluate the positioning accuracy of the IP system created by different groups of anchor nodes. ii- Select the group having the best accuracy (AS) and relocate the mobile station using the WLS. iii- Involve the virtual node to enable the LS working with only two anchor nodes when needed for the MSE. The work done with the experiment phase presents evidence using the AS can reach an accurate IP system with less than $0.5 m^2$ of MSE of a positioning and less installation time and number of wireless sensors in a harsh environment while the WLS, MLSI, GDOP, and LS algorithms reach more than $3.5 m^2$, $1.2 m^2$, $1.4 m^2$, and $9 m^2$ of MSE respectively. The proposed method provides a highly accepted localization accuracy for different scenarios including emergency.

7. Conclusion and future work

This PhD. dissertation has explored the design of indoor positioning systems from an experimental perspective by studying IPS that can be implemented with the current commercial technologies. Moreover, we have focused on the design of IPS that can be easily scaled to mass market applications by employing network based positioning systems and widely used wireless networks like the wireless sensor networks, which play a key role in the context of the internet of the things and its applications to smart cities and smart buildings.

First, we have considered evaluation and validation for a commercial device of UWB radio technology to be used for creating an appropriate IP system that could be suitable to be implemented in different indoor environment and situations especially emergencies.

Second, we have considered designs of NLOS and LOS identification and mitigation methods for UWB radio signal. When using UWB radio technology for building an IP system, the NLOS and LOS identification and mitigation methods play the main role due to the main impact of the UWB signal when traveling through obstructions such as walls and human. The main impact of the UWB radio signal is the potential error in the estimated distance. Two different novel methods to identify the propagation channels and to mitigate the NLOS channels have been implemented in this thesis.

Finally, we have created a novel IP system called AS to be optimum for different indoor environments and situations especially emergencies.

7.1 Conclusions

After motivating this PhD thesis and presenting an overview of the state of the art, in Chapter 3 we have presented some of the key topics that have been implemented throughout this dissertation. Specifically, we have revisited the concepts of UWB radio technology with special attention to the analytic solution provided by the commercial UWB device called DW 1000 and especially the sub-optimal solution provided by this device which has been used in every indoor positioning system designed in this work.

Chapter 4 has been devoted to the study of NLOS identification and mitigation method using UWB radio technology in an indoor environment. Before starting with the NLOS identification method, we have studied and evaluated the UWB device (DW 1000 - EVK 1000). More precisely, we have focused our attention on the different ranging protocols implemented for UWB technology, and therefore we have deeply studied the ranging protocol used in this device. We have evaluated this device with two channel modes (ch2 and ch3).

Also, we have studied the information extracted from this device (FSL and RSL) to be used as main parameters to identify the propagation channels that the UWB signal travels through. The NLOS identification method created in this chapter is an extension of the method created by [74] to overcome the gap of this method. For the mitigation of NLOS channels and enhance the estimated distance, we have collected information about the building that the experiment implemented in it such as the map of this building and types of the wall.

The NLOS identification and mitigation method has been experimentally validated in two different types of propagation channels (LOS and NLOS) and for a walking human moving through these channels where the NLOS channel has different types and number of the walls. In this work the accuracy of the NLOS identification method has

been increased to about 93 % for ch2 and 92 % for ch3. Also, the estimated distance has been improved to reduce the error to less than 60 *cm* in the hard-NLOS channel.

In chapter 5, we have extended and improved the chapter's 4 work based on the UWB radio technology. As we mentioned in chapter 5/section 5.2 about the main impact of the UWB device which the estimated RSL diverges from its true value when reaching above than -85 dBm. In this chapter, we have overcome the problem aforementioned above using Fuzzy logic control technique. For the NLOS identification method, we have extracted 3 parameters (RSL, FSL, and SNR) to be used as an input set of the Fuzzification process.

Also, we have created IF- THEN Fuzzy rule table and give specific ranges for output sets divided into different types of propagation channels. In the defuzzification step, we have used a center of gravity method to extract the Fuzzy output used to identify the propagation channels. For mitigation method to improve the estimated distance, we have created a database that includes information about a distance bias corresponding to the extracted parameters from the UWB device (RSL, FSL, SNR).

This work has been implemented and validated experimentally in the lobby of the engineering school of UAB university having different propagation channels(LOS, hard NLOS, and soft NLOS). In this work, the main drawback of the UWB device has been eliminated, and the accuracy of the NLOS identification method reaches to about 99 %. Also, the error of the estimated distance has been reduced to about 20 *cm* in a harsh indoor environment.

Chapter 6 has been devoted to the study of indoor positioning systems using UWB radio technology and to design a novel IP system based on a commercial UWB radio technology convenient to different indoor environments and situations. In this chapter, we have created an IP system called anchor selection (AS) based on an evalu-

ation method used for evaluating the positioning accuracy of different groups of anchor nodes installed in a narrow area of $9 m^2$. These groups consist of 2 anchor nodes to 5 anchor nodes used to locate a mobile station. The evaluation method used in the AS system is called a mean square error (MSE).

The conventional MSE needs for the true value of the mobile station to be compared with its estimated value. But, in a real experiment, we unable to obtain the true value and only the estimated value is available. So and for online evaluation of the positioning accuracy, we have derived mathematically a novel MSE which doesn't need for the true value. Then, we have selected the anchor nodes group having the lower MSE and relocate the mobile station using a WLS algorithm.

Also, The conventional MSE needs for at least 3 anchor nodes to compute the positioning accuracy, but in this work, we have extended the MSE to have also 2 anchor nodes by adding a virtual node instead of the anchor node that has more distance error than other anchor nodes in the group of 3 anchor nodes.

The IP system has been experimentally validated in the lobby of the engineering school of the UAB university which has a soft and harsh environment. The positioning accuracy obtained in this work has a position error with less than $0.5 m^2$ of MSE for a harsh indoor environment. We have proofed experimentally that the AS system could be confident for different indoor environments having different situations including emergency.

7.2 Future work

The work presented in this PhD dissertation can be extended as follows:

- To extend the indoor positioning problem to the cooperative problem where different users cooperate between them to increase the localization accuracy.
- To extend the indoor positioning problem to a hybrid technique using integrated UWB and the Wi-Fi measurements.

As for the specific problems addressed in each chapter, chapters 4 and 5, some of possibilities are:

- To improve the ranging accuracy of the UWB device (DW 1000) implementing the (ADS-TWR) ranging protocol instead of SDS ranging protocol.
- To extend the NLOS identification and mitigation methods combining the Fuzzy logic technique and map information about the building used for an experiment.

In Chapter 6, we have considered the following extension:

- To extend the indoor positioning problem to different assessment methods where we can online evaluate the positioning accuracy created by UWB technology using MSE and GDOP.

Bibliography

1. Andre G. Ferreira, Duarte Fernandes, Andre P. Catarino, and Joao L. Monteiro, "Localization and Positioning Systems for Emergency Responders: a Survey", 2017, DOI 10.1109/ COMST, 2703620, IEEE, 2017.
2. C. Fuchs, N. Aschenbruck, P. Martini, and M. Wieneke, "Indoor tracking for mission critical scenarios: A survey," *Pervasive Mob. Comput.*, vol. 7, no. 1, pp. 1-15, Feb. 2011.
3. Indoor location in retail: Where is the money?," *ABI Research: Location Technologies Market Research*", 2015.
4. Matteo Ridol, Stef Vandermeeren, Jense Defraye,"Experimental Evaluation of UWB Indoor Positioning for Sport Postures", *Sensors*, 2018.
5. T., Huang, C., Blum, B.M., Stankovic, J.A. and Abdelzaher, T. (2003) "Range free location schemes for large scale sensor networks", *MobiCom 03*, September, 2003.
6. Lourenco P, Batista P, Oliveira P, Silvestre C, Chen P,"A received signal strength indication-based localization system", *21st Mediterranean Conference on Control Automation,(MED)*, pp. 1242-1247, 2013.
7. Wu L, Meng MQ-H, Lin Z, He W, Peng C, Liang H, "practical evaluation of radio signal strength for mobile robot localization" *International Conference on Robotics and Biomimetics (ROBIO)*, pp. 516-522, 2009.
8. Farid Z, Nordin R, Ismail M, "Recent advances in wireless indoor localization techniques and system", *J Comput Netw Commun*, 2013.
9. Tian He, Chengdu Huang, BrianM. Blum, John A. Stankovic, Tarek Abdelzaher,"Range-Free Localization Schemes for Large Scale Sensor Networks1", *MobiCom 03*, pp. 81-95, 2003.

10. N. Bulusu, J. Heidemann and D. Estrin, "GPS-less Low Cost Outdoor Localization for Very Small Devices", *IEEE Personal Communications Magazine*, 7(5): pp. 28-34, October 2000.
11. N. Bulusu, J. Heidemann and D. Estrin, "Density Adaptive Algorithms for Beacon Placement in Wireless Sensor Networks", In *IEEE ICDCS 01*, Phoenix, AZ, April 2001.
12. D. Nicosescu and B. Nath, "Ad-Hoc Positioning Systems (APS)", In *Proceedings of IEEE GLOBECOM 01*, November 2001.
13. Tian He, Chengdu Huang, Brian M. Blum, John A. Stankovic, Tarek Abdelzaher, "Range-Free Localization and Its Impact on Large Scale Sensor Networks", *ACM Transactions on Embedded Computing Systems*, Vol. 4, No. 4, PP. 877-906, 2005.
14. Amin Gholoobi, Stavros Stavrou, "Accelerating TOA/TDOA packet based localization methods", *IEEE Conference on Wireless Sensors (ICWiSE)*, pp. 1-5, 2014.
15. Moustafa Youssef, Adel Yosuf, Chuck Rieger, and Ashok Agrawala, "An Asynchronous Time-Based An Asynchronous Time-Based", In *Proceedings of the 4th international conference on Mobile systems, application, and services*, IEEE, pp. 165-176, 2006.
16. Ciurana M. Barcelo, F. Izquierdo, A Ranging Method with IEEE 802.11 Data Frames for Indoor Localization. In: *Proc. of Wireless Communications and Networking Conference*, pp. 2092-2096, 2007.
17. X. Cheng, A. Thaler, G. Xue, and D. Chen. TPS: "A Time-Based Positioning Scheme For Outdoor Sensor Networks". In *Proceedings of IEEE Infocom*, volume 4, pp. 2685-2696, 2004.
18. M. Mah, N. Gupta, and A. Agrawala, "Pinpoint Time Difference of Arrival for Unsynchronized 802.11 Wireless Cards", in *Proc. of the 29th IEEE Conference on Computer communication (INFOCOM 10)*, USA, 2010.

19. Christian Hoene and Jorg Willmann, "Four-way TOA and software based trilateration of IEEE 802.11 devices", IEEE PIMRC, Cannes, September 2008.
20. A. G.A onther and Christian Hoene, "Measuring round trip times to determine the distance between WLAN nodes", Waterloo, Canada, May 2005.
21. Bahillo, A, Fernandez, P, Prieto, J, Mazuelas, S, Lorenzo, R. M, and Abril, E. J," Distance Estimation Based on 802.11 RTS/CTS Mechanism for Indoor Localization", In: Almei-da M. (ed.) Advances in Vehicular Networking Technologies. Rijeka, pp. 217-236, 2011.
22. Gholoobi, A Stavrou, S. "A hybrid TDoA-ToA localization method," Telecommunications (ICT), 2013 20th International Conference on., pp. 1-4, May 2013.
23. M. Ciurana, F. Barcelo-Arroyo, and F. Izquierdo, "A ranging system with IEEE 802.11 data frames," in IEEE Radio and Wireless Symposium, p. 133, 2007.
24. Matteo Ridol, Stef Vandermeeren, Jense Defraye,"Experimental Evaluation of UWB Indoor Positioning for Sport Postures", Sensors, 2018.
25. Ali Yassin, Youssef Nasser, Mariette Awad,"Recent Advances in Indoor Localization: A Survey on Theoretical Approaches and Applications", University of New South Wales, IEEE, 2016.
26. Kai Wen, Kegen Yu and Yingbing Li," NLOS Identification and Compensation for UWB Ranging Based on Obstruction Classification", EUSIPCO, pp 2704-2708, IEEE, 2017.
27. Decawave LTD. APS 006 application notes,"Channel effects on communications range and time stamp accuracy in DW 1000 based systems", Version 1.02, pp. 12-16, 2014.
28. N. Patwari, J.N. Ash, S. Kyperountas, III Hero, A.O., R.L. Moses, and N.S. Correal, "Locating the nodes cooperative localization in wireless sensor networks," , Signal Processing Magazine, IEEE, vol. 22, no. 4, pp. 54-69, July 2005.

29. B.D. Van Veen and K.M. Buckley, "Beamforming: A versatile approach to spatial filtering", *IEEE ASSP Mag*, vol. 5, no. 2, pp. 4-24, 1988.
30. B. Ottersten, M. Viberg, P. Stoica, and A. Nehorai, "Exact and large sample ML techniques for parameter estimation and detection in array processing", in *Radar Array Processing*, S.S. Haykin, J. Litva, and T. Shepherd, Eds. New York: Springer Verlag, pp 99-151, 1993.
31. Neal Patwari, Joshua N. Ash, Spyros Kyperountas, Alfred O. Hero III, Randolph L. Moses, and Neiyer S. Correal, "Locating the Nodes" (Cooperative localization in wireless sensor networks), *IEEE SIGNAL PROCESSING MAGAZINE*, pp. 54-89, 2005.
32. N. Patwari, "Location Estimation in Sensor Networks", Thesis of Neal Patwari at University of Michigan, *IEEE Transactions on Vehicular Technology*, pp. 1-14, 2005.
33. T. S. Rappaport, "Wireless Communications: Principles and Practice.", Prentice-Hall, 1996.
34. B. BAejar and S. Zazo, "A Practical Approach for Outdoor Distributed Target Localization in Wireless Sensor Networks", *EURASIP Journal on Advances in Signal Processing*, vol. 2012, no. 95, May 2012.
35. M. L. Sichitiu and V. Ramadurai, "Localization of Wireless Sensor Networks with a Mobile Beacon", in *Proc. of IEEE MASS*, pp. 174-183, Oct. 2004.
36. N. Patwari, R. J. O Dea, and Y. Wang, "Relative Location in Wireless Networks" in *Proc. of IEEE VTC*, pp. 1149-1153, May 2001.
37. R. W. Ouyang, A. K. S. Wong, and C. T. Lea, "Received Signal Strength-based Wireless Localization via Semidefinite Programming : Noncooperative and Cooperative Schemes", *IEEE Trans. Veh. Technol.*, vol. 59, no. 3, pp. 1307-1318, Mar. 2010.

38. G.Wang and K. Yang, "A New Approach to Sensor Node Localization Using RSS Measurements in Wireless Sensor Networks", *IEEE Trans. Wireless Commun.*, vol. 10, no. 5, pp. 1389-1395, May 2011.
39. Slavisa Tomic, Marko Beko, and Rui Dinis, "RSS-based Localization in Wireless Sensor Networks Using Convex Relaxation: Noncooperative and Cooperative Schemes" *IEEE Transactions on Vehicular Technology*, pp 1-14, 2013.
40. J. Yang and Y. Chen, "Indoor localization using improved rss-based lateration methods", *IEEE Global Telecommunications Conference*, pp. 1-6, 2009.
41. A. Bahillo, S. Mazuelas, R. M. Lorenzo, P. Fernandez, J. Prieto, R. J. Duran, and E. J. Abril, "Hybrid RSS-RTT Localization Scheme for Indoor Wireless Networks", *EURASIP Journal on Advances in Signal Processing*, no. 1, Mar. 2010.
42. N. Alam and A. G. Dempster, "Cooperative Positioning for Vehicular Networks: Facts and Future", *IEEE Transaction on Intelligent Transportation Systems*, vol. 14, no. 9, Dec. 2013.
43. Mohammed Yavari and Bradford G. Nickerson. Ultra-Wideband Wireless Positioning Systems: Technical Report TR 14-230.2014.
44. (2013, December) University of Maryland-Ranger NBV.[Online]. <http://www.ssl.umd.edu/projects/RangerNBV/thesis/2-4-1.htm>.
45. D. H. Titterton and J. L. Weston, *Strapdown inertial navigation technology -2nd ed.:* the Institution of Electrical Engineers, London, United Kingdom, 2004.
46. X. Niu, Y. Li, Q. Zhang, Y. Cheng, and C. Shi, "Observability Analysis of Non-Holonomic Constraints for Land-Vehicle Navigation Systems", *Journal of Global Positioning Systems*, vol. 11, pp. 80-88, 2012.
47. M. H. Afzal, V. Renaudin, and G. Lachapelle, "Use of earth's magnetic

- eld for mitigating gyroscope errors regardless of magnetic perturbation”, *Sensors*, vol. 11, pp. 11390-11414, 2011.
48. InterSense. (2014, July 7). NavShoe Pedestrian Navigation System. Available: <http://www.abs-tech.com/admin/modulos/produtos/upload/mais-informacoes/987/1590.pdf>.
 49. TrustedPositioning. (2014, July 7). Trusted Portable Navigator (T-PN). Available: <http://www.trustedpositioning.com/uploads/1/6/4/6/16469144/t-pn.pdf>.
 50. Seungwoo Lee, Byounggeun Kim, Hoon Kim, Rhan Ha, and Hojung Cha, ”Inertial Sensor-Based Indoor Pedestrian Localization with Minimum 802.15.4a Configuration”, *IEEE, transaction on industrial informatic*, VOL. 7, NO. 3, pp. 455-466, AUGUST 2011.
 51. M. Mladenov and M. Mock, ”A step counters service for java-enabled devices using a built-in accelerometer”, in *Proc. 1st Int. Workshop on Context-Aware. Middleware and Services, CAMS 09*, New York, pp. 1-5, ACM, 2009.
 52. I. Constandache, X. Bao, M. Azizyan, and R. R. Choudhury, ”Did you see Bob?: Human localization using mobile phones”, in *Proc. 16th Annu. Int. Conf. Mobile Comput. Networking*, pp. 149-160, 2010.
 53. Dae Ho Kim, Goo Rak Kwon, and Jae Young Pyun, ”NLOS Identification in UWB channel for Indoor Positioning”, *IEEE Annual Consumer Communications and Networking Conference (CCNC)*, pp. 1-4, 2018.
 54. Zhuoling Xiao, Hongkai Wen, Andrew Markham, ”Non-Line-of-Sight Identification and Mitigation Using Received Signal Strength”, *IEEE transaction on wireless communications*, VOL. 14, NO. 3, MARCH, pp 1689-1702, 2015.
 55. Stefano Marano, Wesley M, Henk Wymeersch, Moe Z. Win, ”NLOS Identification and Mitigation for Localization Based on UWB Experimental Data”, *IEEE journal ON selected areas in communication*, VOL. 28, NO. 7, 1026-1035, September 2010.

56. Bo You, Xueen Li, Xudong Zhao, Yijun Gao, "A Novel Robust Algorithm Attenuating Non-Line-of-Sight Errors in Indoor Localization", IEEE (ICCSN). PP. 1-6, 2015.
57. Imane Horiya Brahmi, Giovanni Abbruzzo, Michae Walsh, Hichem Sedjelmaci, and Brendan O Flynn, "A Fuzzy Logic Approach for Improving the Tracking Accuracy in Indoor Localisation Applications", IEEE -Wireless Days (WD), pp 137-144, 2018.
58. Kuang-Hao Lin, Chi-Chang Lu, Hou-Ming Chen, Hsu- Feng Li, and Cheung-Fu Chuang, "A Modified Least Squares Iteration for Indoor Positioning System", IEEE International Conference on Consumer Electronics, Taiwan.,2017,
59. Mathias Pelka, Grigori Goronzy, and Horst Hellbruck, "Iterative approach for anchor configuration of positioning systems", ScienceDirect, 2016.
60. Yunzhou Zhang, Dongfei Wei, Wenyan Fu, and Bing Yang, "Target Positioning with GDOP Assisted Nodes Selection Algorithm in Wireless Sensor Networks", International Journal of Distributed Sensor Networks, pp 1-10, 2014.
61. Ian Sharp, Kegen Yu, and Mark Hedley, "On the GDOP and Accuracy for Indoor Positioning", IEEE transaction on aerospace and electronic system VOL. 48, NO. 3, pp 2032-2051, 2012.
62. Paula Tarrío, Ana M. Bernardos and Jose R. Casar, "Weighted Least Squares Techniques for Improved Received Signal Strength Based Localization", Sensors, pp 8570-8592, 2011.
63. FCC, Office of Engineering and Technology, Revision of Part 15 of the Commission's Rules Regarding Ultra-Wideband Transmission System", ET Docket, no. 98-153, 2002.
64. CEPT ECC document, ECC decision of 24 march 2006 on the harmonized conditions for devices using ultra-wideband (UWB) technology in bands below 10.6 ghz" Tech. Rep. Doc. ECC/DEC/(06)04.

65. Jun-ichi Takada, Shinobu Ishigami, Juichi Nakada, "Measurement Techniques of Emissions from UltraWideband Devices", IEICE TRANS. Fundamentals, VOL.E88-A, NO.9, pp 2252-2263, 2005.
66. Zhuo Li, Qilian Liang, "Capacity Optimization of IR Ultrawide Band System Under the Coexistence with IEEE 802.11n", Adhoc and Sensor Wireless Networks, Vol. 21 Issue 1, p 59-75, 2014.
67. Kamran Ayub¹, Valerijs Zagurskis,"Technology Implications of UWB on Wireless Sensor Network-A detailed Survey", International Journal of Communication Networks and Information Security (IJCNIS), Vol. 7, No. 3,pp 147-159, December 2015.
68. Xuemin Shen, Mohsen Guizani, Robert Caiming Qiu, Tho Le Ngoc, "UltraWideband Wireless Communications and Networks", Publisher John Wiley and Sons, ISBN 0470028513, pp. 8-9, 2007.
69. Syan Bingbing, Ren Wenbo, Yin Bolin, Li yang, "An indoor positioning algorithm and its experiment research based on RFID", International Journal of Smart Sensing and Intelligent Systems, Vol. 7 Issue 2, pp 879-897, Jun. 2014.
70. Marco Chiani, "Coexistence between UWB and Narrowband Wireless Communication Systems", Proceeding of IEEE Vol. 97, No. 2, Feb. 2009.
71. M.G. diBenedetto, T. Kaiser, A.F. Molish, I. Oppermann, C Plitano, and D. Porcino (eds). UWB Communication systems: A Comprehension Overview. EURASIP Publishing, 2005.
72. IEEE Working Group 802.15.4a.Draft Specification for IEEE 802.15.4a Standard
73. Decawave Ltd.DW 1000 USER MANUAL, 2015.
74. Decawave Ltd.EVK 1000 USER MANUAL, 2015.
75. Decawave Ltd.APS 011 Application Note: Source of error in DW Based Tow-Way Ranging (TWR) schemes, 2014.

76. Yi Jiang* and C.M. Victor Leung. An Asymmetric Double Sided Two-Way Ranging for Crystal Offset, 2007.
77. Y. Tingcong, M.I Walsh, P. Haigh, J. Barton, A. Mathewson, and B. OFlynn. Experimental Impulse Radio IEEE 802.15.4A UWB, Based Wireless. Sensor Localization Technology: Characterization, Reliability and Ranging.2011.
78. Decawave Ltd.APS 006 Part 2 Application Note: Non Line of Sight Operation and Optimization to improve performance in DW 1000 Based Systems 2014.
79. H. GU01, M. URADZLNSKI, H. YIN, and M. YU. Indoor positioning based on foot-mounted IMU. bullet in of the polish academy of sciences, 2015.
80. Hui Liu, T. Kaiser,"Survey of Wireless Indoor Positioning techniques and Systems", IEEE transaction on systems, man, and cybernetics, pp. 1067-1080, 2007.
81. K. Pahlavan, X. Li, and J. P. Makela, "Indoor geolocation science and technology," IEEE Commun. Mag., vol. 40, no. 2, pp. 112-118, 2002.
82. P. Krishnamurthy, "Position location in mobile environments," in Proc. NSF Workshop on Context-Aware Mobile Database Management (CAMM), Providence, RI, Jan. 2002.
83. J. Callmer, "Autonomous localization in unknown environments", Linkoping University Electronic Press, 2013.
84. M. Algabri, H. Mathkour, H. Ramdane, and M. Alsulaiman, "Comparative study of soft computing techniques for mobile robot navigation in an unknown environment", Comput. Human Behav., vol. 50, pp. 42-56, 2015.
85. Matteo Ridolfi, Stef Vandermeeren, Jense Defraye,"Experimental Evaluation of UWB Indoor Positioning for Sport Postures", Sensors, 2018.
86. Abbas Albaidhani, Antoni Morell, Jose Lopez Vicario," Ranging in UWB using commercial radio modules: experimental validation and NLOS mitigation", IEEE, IPIN conference, pp. 1-7, 2016.

87. Ying Bai and Dali Wang, "Fundamentals of Fuzzy Logic Control-Fuzzy Sets, Fuzzy Rules and Defuzzifications", *Advanced Fuzzy Logic Technologies in Industrial Applications*, pp. 1-20.
88. Valent in Barral, Pedro Suarez Casal, Carlos J. Escudero, Jose A. Garcia Naya, "Assessment of UWB Ranging Bias in Multipath Environments" *IEEE*, pp 1-4, IPIN 2016.
89. He T, Huang C, Blum BM, Stankovic A, Abdelzaher T, "Range free localization schemes for large scale sensor networks", *Proceedings of the 9th annual international conference on Mobile computing and networking*, pp 81-95, 2003.
90. Pratap Misra and Per Enge. "Global Positioning System: Signals, Measurements and Performance Second Edition.", Lincoln, MA: Ganga- Jamuna Press, 2006. (ICCE-TW), 2017.
91. Ian Sharp, Kegen Yu, Y. Jay Guo, "GDOP Analysis for Positioning System Design", *IEEE transaction on vehicular technology*, VOL. 58, NO. 7, SEPTEMBER 2009.
92. Decawave, "Sources of error in DW 1000 based two-way ranging (TWR) schemes, Decawave, 2014.
93. D. B. Jourdan, J. J. Deyst, M. Z. Win, and N. Roy, "Monte carlo localization in dense multipath environments using UWB ranging", *IEEE International Conference on Ultra-Wideband*, pp 314-319, Sept 2005.
94. Decawave LTD. "Upgrading EVB 1000 to latest software:software: Offset Compensation", [http/ www.decawave.com](http://www.decawave.com), 2015.
95. Niranjini Rajagopal, Sindhura Chayapathy, Bruno Sinopoli, Anthony Rowe, "Beacon Placement for Range- Based Indoor Localization", *IEEE*, pp 1-8, IPIN 2016.